

AD-A111 209

TECHNION RESEARCH AND DEVELOPMENT FOUNDATION LTD. HAI--ETC F/8 11/1
DURABILITY OF STRUCTURAL ADHESIVELY BONDED SYSTEM.(U)

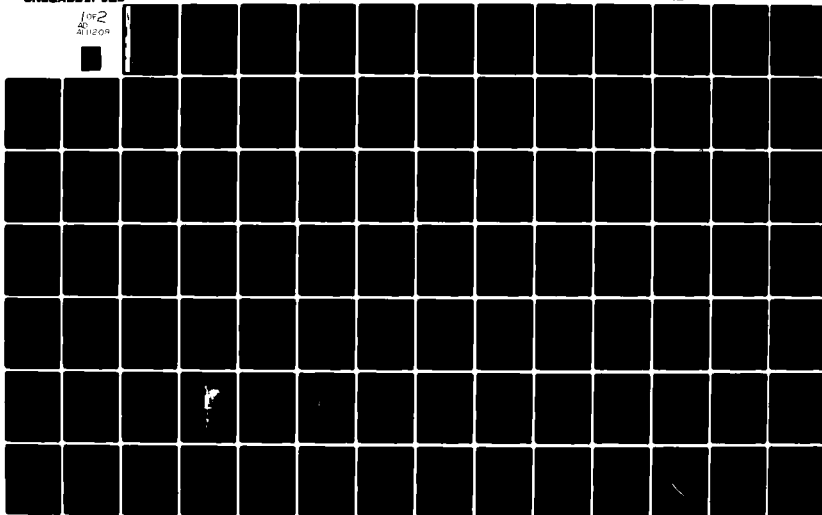
JUN 81 O ISHAI, S GALI, S YANIV

DAJA37-80-C-0303

NL

UNCLASSIFIED

for 2
AD
A11209



(12)

AD A111209

DURABILITY OF STRUCTURAL ADHESIVELY BONDED SYSTEM

by

O. Ishai, S. Gali and G. Yaniv

July 1981

United States Army

European Research Office of the U. S. Army

London England

DEC 22 1982
H

DTIC FILE COPY

Contract Number DAJA 37-80-C-0303

Technion Research & Development Foundation Ltd.

Technion-Israel Institute of Technology, Haifa, Israel

Approved for Public Release; Distribution Unlimited

82 02 22 010

UNCLASSIFIED

R&D 2615-MS

SECURITY CLASSIFICATION OF THIS PAGE (When Data Entered)

| REPORT DOCUMENTATION PAGE | | READ INSTRUCTIONS BEFORE COMPLETING FORM |
|---|-----------------------|---|
| 1. REPORT NUMBER | 2. GOVT ACCESSION NO. | 3. RECIPIENT'S CATALOG NUMBER |
| | | AD A111 207 |
| 4. TITLE (and Subtitle) Durability of Structural Adhesively Bonded System | | 5. TYPE OF REPORT & PERIOD COVERED First Annual Report |
| | | 6. PERFORMING ORG. REPORT NUMBER |
| 7. AUTHOR(s) O.Ishai, S. Gali and G. Yaniv | | 8. CONTRACT OR GRANT NUMBER(s) DAJA37-80-C-0303 |
| 9. PERFORMING ORGANIZATION NAME AND ADDRESS Technion Research & Development Foundation Ltd Haifa, Israel | | 10. PROGRAM ELEMENT, PROJECT, TASK AREA & WORK UNIT NUMBERS T161102BH57-01 |
| 11. CONTROLLING OFFICE NAME AND ADDRESS USARDCG-UK, Box 65 FPO NY 09510 | | 12. REPORT DATE June 1981 |
| | | 13. NUMBER OF PAGES 111 |
| 14. MONITORING AGENCY NAME & ADDRESS (If different from Controlling Office) | | 15. SECURITY CLASS. (of this report) Unclassified |
| | | 15a. DECLASSIFICATION/DOWNGRADING SCHEDULE |
| 16. DISTRIBUTION STATEMENT (of this Report) | | |
| <div style="border: 1px solid black; padding: 5px; text-align: center;"> DISTRIBUTION STATEMENT Approved for Public Release Distribution Unlimited </div> | | |
| 17. DISTRIBUTION STATEMENT (of the abstract entered in Block 20, if different from Report) | | |
| Approved for Public Release - Distribution Unlimited | | |
| 18. SUPPLEMENTARY NOTES | | |
| 19. KEY WORDS (Continue on reverse side if necessary and identify by block number) Adhesive, Bonding, Interlaminar adhesive layer, Adherend, Hygrothermal, Environment, Durability, Fiber Reinforced Plastics (FRP), Carbon Fiber, Reinforced Plastics (CFRP), Thermoelastic, Hygroelastic, Time-dependent, Relaxation, Viscoelastic, Viscoplastic, Stress-strain, Composites, Finite, Element Method | | |
| 20. ABSTRACT (Continue on reverse side if necessary and identify by block number) A comprehensive literature survey is made and the findings of investigations conducted by the authors during the past few years in this field are summarized. Basic assumptions for the present work are outlined, based on the conclusions of the above survey. An analytical study, supported by empirical data, was conducted on the effects of the state of stress on the adhesive mechanical behavior of a bonded interlaminar layer phase in the non-linear range and the time-dependency | | |

DD FORM 1473

JAN 73

EDITION OF 1 NOV 65 IS OBSOLETE

UNCLASSIFIED

SECURITY CLASSIFICATION OF THIS PAGE (When Data Entered)

UNCLASSIFIED

SECURITY CLASSIFICATION OF THIS PAGE(When Data Entered)

20.

of that behavior.

Tests were conducted for the derivation of viscoelastic characteristics of the adhesive phase and of the thermoelastic and hygroelastic parameters of the representative adhesives and of CFRP adherends. The effects of temperature and humidity with exposure time on the above characteristics were investigated.

The major objective of the experimental work was two-fold:

- a) To provide the basic data to serve as inputs for the analysis of the hygrothermomechanical behavior of the bonded system;
- b) To develop a methodology for the reduction of the vast experimental work involved in the derivation and evaluation of such data, which are essential for predicting the durability of bonded systems during real service life.

UNCLASSIFIED

SECURITY CLASSIFICATION OF THIS PAGE(When Data Entered)

DURABILITY OF STRUCTURAL ADHESIVELY BONDED SYSTEMSO. Ishai*, S. Gal¹** and G. Yaniv***ABSTRACT

The subject is approached on three levels:

A comprehensive literature survey is made and the findings of investigations conducted by the authors during the past few years in this field are summarized. Basic assumptions for the present work are outlined, based on the conclusions of the above survey.

An analytical study, supported by empirical data, was conducted on the effects of the state of stress on the adhesive mechanical behavior of a bonded interlaminar layer phase in the non-linear range and the time-dependency of that behavior.

Tests were conducted for the derivation of viscoelastic characteristics of the adhesive phase and of the thermoelastic and hygroelastic parameters of the representative adhesives and of CFRP adherends. The effects of temperature and humidity with exposure time on the above characteristics were investigated.

The major objective of the experimental work was two-fold:

- a) To provide the basic data to serve as inputs for the analysis of the hygrothermomechanical behavior of the bonded system;
- b) To develop a methodology for the reduction of the vast experimental work involved in the derivation and evaluation of such data, which are essential for predicting the durability of bonded systems during real service life.

*) Professor, Faculty of Mechanical Engineering
Technion - Israel Institute of Technology, Haifa, Israel

**) Research Assistant, Faculty of Mechanical Engineering, Technion
At present, Post-doctorate position, Department of Mechanical Engineering
Imperial College, London, England

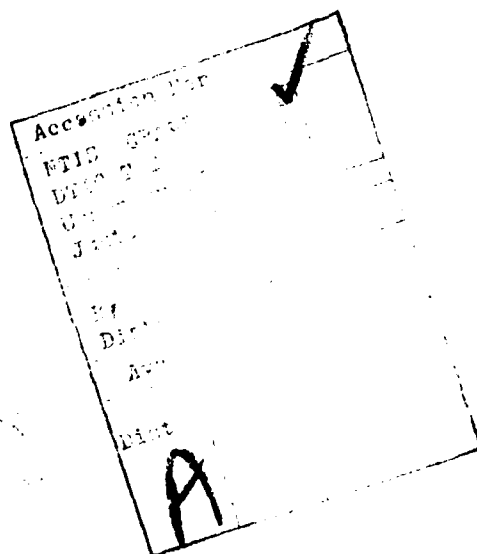
***) Instructor, D.Sc. Candidate, Faculty of Mechanical Engineering, Technion,
Haifa, Israel

List of Key Words

Adhesive, Bonding, Interlaminar adhesive layer, Adherend, Hygrothermal, Environment, Durability, Fiber Reinforced Plastics (FRP), Carbon Fiber Reinforced Plastics (CFRP), Thermoelastic, Hygroelastic, Time-dependent, Relaxation, Viscoelastic, Viscoplastic, Stress-strain, Composites, Finite Element Method.

DURABILITY OF STRUCTURAL ADHESIVELY BONDED SYSTEMSTABLE OF CONTENTS

| | | |
|-----|--|-----|
| 1. | Introduction..... | 1 |
| 2. | Summary of Relevant Previous Investigations..... | 3 |
| 3. | Literature Survey..... | 10 |
| 4. | Objectives and Procedures for Present Research..... | 22 |
| 5. | Mechanical Behavior of Adhesive Materials under a Combined State of Stress..... | 24 |
| 6. | Hygrothermal Effects on Time-dependent Characteristics of Adhesive Materials..... | 30 |
| 7. | The Time-dependent Mechanical Behavior of an Interlaminar Adhesive Layer within a Loaded Bonded System..... | 34 |
| 8. | Thermoelastic and Hygroelastic Characteristics of Adhesives and FRP Adherends, Constituents of the Bonded System..... | 37 |
| 9. | Summary and Conclusions..... | 44 |
| 10. | Future Research..... | 45 |
| 11. | Literature Cited..... | 46 |
| | Glossary..... | 55 |
| | Figures..... | 57 |
| | Tables..... | 109 |
| | Appendices..... | 113 |



III

LIST OF ILLUSTRATIONS

- Fig. 1.1 Stress and failure analysis procedure for the structural design of bonded systems.
- Fig. 1.2 Flow chart for research program on the effect of moisture on failure of bonded joint.
- Fig. 1.3 Relevance of previous investigations to present research.
- Fig. 2.1 Proposed procedure for mechanical characterization of structural adhesives.
- Fig. 4.1 Flow chart of present research objectives and procedure.
- Fig. 5.1 Shear stress-strain relationship based on torsional test of tubular specimen compared with ring specimen of the adhesive in-situ.
- Fig. 5.2 Illustration of device for combined uniaxial and shear loading of tubular specimens.
- Fig. 5.3 Effective stress-strain relationship for epoxy resin derived from different loading mode combinations.
- Fig. 5.4 Shear stress-strain relationship at different levels of normal stresses.
- Fig. 5.5 Basic stress-strain curves under uniaxial loading in tension and compression of bulk FM73 adhesive vs. shear stress-strain curve.
- Fig. 5.6 Effective stress-strain relationship for FM73 adhesive based on uniaxial tensile test, as examined by shear test.
- Fig. 5.7 Failure envelope for bulk and bonded epoxy adhesive derived from different loading mode combinations.
- Fig. 5.8 Failure envelopes for structural adhesive FM73 at different temperature levels.
- Fig. 6.1 Weight changes with time of bulk FM73 specimens immersed in RT water. (23°C)
- Fig. 6.2 Temperature dependence of shear modulus - for the determination of glass-transition temperature (T_g) of different adhesives.
- Fig. 6.3 Typical tensile stress-strain relationship of FM73 wet and dry adhesive specimens at different temperatures.
- Fig. 6.4 Compressive stress-strain curves of wet and dry FM73 specimens under different strain rate and temperature conditions. ($T = 40^\circ\text{C}, 60^\circ\text{C}$).

IV

- Fig. 6.5 Compressive stress-strain curves of wet and dry FM73 specimens under different strain rate and temperature conditions. ($T = 23^{\circ}\text{C}, 78^{\circ}\text{C}$).
- Fig. 6.6 Master curve for tensile yield stress of FM73 and FM 300 K adhesive specimens.
- Fig. 6.7 Shift factor vs. temperature for tensile yield stress master curve of FM73 and FM 300 K adhesive specimens.
- Fig. 6.8 Tensile stress relaxation curves of FM73 specimens at different strain and temperature levels.
- Fig. 6.9 Compressive stress relaxation curves of FM73 specimens at different strains at RT, as compared to tensile stress relaxation.
- Fig. 6.10 Stress-relaxation curves vs. time of FM73 specimens at different temperature levels on log-log scale.
- Fig. 6.11 Stress relaxation master curve of FM73 and FM 300 K adhesive specimens. ($T_{\text{ref}} = 23^{\circ}\text{C}$).
- Fig. 6.12 Shift factor vs. temperature for stress relaxation master curve of FM73 and FM 300 K adhesive specimens.
- Fig. 6.13 Tensile stress relaxation curves for FM 300 K adhesive specimens at different temperature levels.
- Fig. 7.1 Symmetrical doubler model.
- Fig. 7.2 Illustration of FEM scheme for different IAL Thicknesses.
- Fig. 7.3 Effective stress-strain curves of epoxy resin at different strain rates and relevant work curves in different external loading conditions $\epsilon_c / \dot{\epsilon}_c$
- Fig. 7.4 Shear stress (τ_{xzo}) distribution within the IAL boundary zone - non-linear solution with strain rate effect (i.e. linear solution).
- Fig. 7.5 Lateral normal stress (σ_{zo}) distribution within the IAL boundary zone - non-linear solution with strain-rate effect (i.e. linear solution).
- Fig. 7.6 The effect of IAL thickness on the shear stress (τ_{xzo}) distribution (non-linear solution with strain-rate effect).
- Fig. 7.7 The effect of IAL thickness on the lateral normal stress (σ_{zo}) distribution (non-linear solution with strain-rate effect).
- Fig. 7.8 Stress relaxation curves as functions of time at different strain (ϵ_o) levels.
- Fig. 7.9 Effective stress-strain relationships for different time intervals (Δt).

- Fig. 7.10 Shear stress (τ_{xz0}) distribution within the IAL boundary zone at a time interval of $\Delta t = 60$ minutes (i.e. non-linear with strain rate effect solution).
- Fig. 7.11 Lateral normal stress (σ_{z0}) distribution within the IAL boundary zone at a time interval of $\Delta t = 60$ minutes (i.e. non-linear with strain rate effect solution).
- Fig. 8.1 Sequence of environmental history cycle No.I, for investigation of hygrothermal behavior of CFRP and adhesive specimens, representing the material constituents of a bonded system.
- Fig. 8.2 Sequence of environmental history cycle Nos. II and III, for investigation of hygrothermal behavior of CFRP and adhesive specimens, representing the material constituents of a bonded system.
- Fig. 8.3 Device for measuring the thermoelastic and the hygroelastic deformations of adhesive and FRP specimens under exposure to different hygrothermal (HT) conditions.
- Fig. 8.4 Deformation and weight changes (absorption) vs. time curves for longitudinal and transverse U.D. CFRP specimens exposed to HT conditions during cycle I.
- Fig. 8.5 Deformation and weight changes (absorption) vs. time curves for adhesive specimens exposed to HT conditions during cycle I.
- Fig. 8.6 Deformation and absorption vs. time curves for U.D. transverse CFRP and FM73 adhesive specimens exposed to warm water (36°) during cycle II.
- Fig. 8.7 Deformation and absorption vs. time curves for cross-ply and angle-ply CFRP specimens exposed to warm water during cycle II.
- Fig. 8.8 Deformation and absorption vs. time curves for U.D. transverse CFRP and FM73 adhesive specimens exposed to hot-water (70°C) during cycle III.
- Fig. 8.9 Deformation and absorption vs. time curves for cross-ply and angle-ply CFRP specimens exposed to hot-water during cycle III.
- Fig. 8.10 Thermoelastic strain vs. temperature change for determination of CTE of dry and wet transverse CFRP specimens.
- Fig. 8.11 Hygroelastic strains vs. moisture content for the determination of HEC of transverse U.D. CFRP specimens under water exposure at different temperature levels.
- Fig. 8.12 Thermoelastic strain vs. temperature change for the determination of CTE of dry and wet cross-ply CFRP specimens (as compared to U.D. transverse reference).

- Fig. 8.13 **Hygroelastic strains vs. moisture content for the determination of HEC of cross-ply and angle-ply CFRP specimens under water exposure at different temperature levels.**
- Fig. 8.14 **Thermoelastic strain vs. temperature change for the determination of CTE of dry and wet FM73 and FM 300 K adhesive specimens.**
- Fig. 8.15 **Hygroelastic strains vs. moisture content for the determination of HEC of FM73 and FM 300 K adhesive specimens under water exposure at different temperature levels.**

List of Tables

- Table 1.1: **Parametric effects on structural performance of adhesively bonded joints.**
- Table 2.1: **Modes of behavior during different stages of hygrothermal exposure of FRP laminates.**
- Table 3.1: **Data of coefficient of thermal expansion (CTE) for different U.D. FRP materials, from literature sources.**
- Table 8.1: **Coefficient of thermal expansion (CTE) and hygroelastic coefficients (HEC) for FRP and adhesive specimens exposed to different hygrothermal conditions.**

List of Appendices

- Appendix 1: **Hygrothermal data evaluation for transverse U.D. CFRP specimen exposed to hot water during cycle III.**
- Appendix 2: **Hygrothermal data evaluation for cross-ply CFRP specimens exposed to hot-water during cycle III.**
- Appendix 3: **Hygrothermal data evaluation for FM73 adhesive specimens exposed to hot-water during cycle III.**

1. INTRODUCTION

1.1 PREFACE

The present project is in part a continuation of a previous research conducted under the sponsorship of the U.S. Army European Research Office in the years 1974-77. The present investigation was effectively started at the beginning of 1980, following informal approval of the research proposal by U.S. Army officials in London.

Thus the report here submitted covers more than a year's research activity. It constitutes a cooperative effort led by the Principal Investigator, with contributions by a post-doctoral research worker, S. Gali, and two graduate students - G. Yaniv (D.Sc. Candidate) and G. Dolev (M.Sc. Graduate).

The report comprises three main parts:

- a) A survey of the international literature on the subject and a summary of the results and conclusions of previous relevant investigations carried out by the authors.
- b) An investigation of the thermo-mechanical and hygromechanical behavior of the constituents of a bonded system, namely adhesives and FRP.
- c) An analysis of the stresses and the deformational behavior of the bonded system as functions of time and of hygrothermal conditions.

1.2 BACKGROUND - PREVIOUS WORK

The present investigation is a continuation of extensive research work carried out under the supervision of the principal investigator at the Material Mechanics Laboratory of Technion - Israel Institute of Technology during the last decade.

Part of the work was based on previous research activity, shared in by the principal investigator, which was conducted in the U.S.A. under the sponsorship of Monsanto/Washington Univ.Assoc. ONR, ARPA, Department of Defence in 1967-69.

That investigation was mainly devoted to the temperature effects in time on the mechanical behavior of fiber-reinforced plastic (FRP) composites and their "ductile" epoxy matrix (which in its mechanical behavior is qualitatively similar to modern structural adhesives). Most of the results have been reported in the literature [1-5].

At the Technion the relevant research activity began in 1970 on a wider front, also covering the effects of the environmental-loading history on the mechanical performance of similar FRP composites (which may serve as adherends in structural bonded systems). That investigation thus included in its scope the effects, in time, of moisture and temperature on both loaded and unloaded FRP composites and their matrices. The research was sponsored by the U.S. National Bureau of Standards in 1970-73 and by the Israel Council for Research and Development in 1973-76. The results were reported in the literature [6-12].

The Research on adhesively bonded systems was divided into two stages. The first stage was concerned mainly with the stress analysis of the bonded system under loading in the elastic and inelastic ranges, without, however, considering either the time-dependence of the behavior or hygrothermal effects. It was sponsored by the European Research Office of the U.S. Army during 1974-1977, and was reported in [13-18]. The second stage of the research effort here referred to dealt with the mechanical characterization of structural adhesives, under different loading modes and hygrothermal conditions. That investigation has been sponsored by the Israel Ministry of Defence since 1978 and will be carried on until 1981. It has so far been reported in [19-23].

The scope, and the goal, of the present research project, entitled "Durability of Adhesively Bonded Systems", are wider and more complex than any of the foregoing investigations. It embraces, in combination, all the subjects reviewed above, as demonstrated by its title:

Durability - refers to the environmental effects with time, the effects comprising temperature, moisture, and loading.

Adhesive - is meant to refer to the viscoelasto-plastic phase, the mechanical characteristics of which are non-linear and strongly influenced by hygrothermal factors in time, and, finally, Bonded-systems: These include two additional major phases: The composite FRP adherends and the adhesive-adherend interfaces, which are both strongly dependent on the different variables of the environmental-loading history and on current conditions.

The complexity of the stress and failure analysis when dealing with the adhesive alone (considering metal adherends, and cohesive failure) is demonstrated in Fig.1.1 while the problems encountered in the study of the effect of moisture when interfacial behavior must be considered, is shown in Fig.1.2

Even a qualitative evaluation of parametric effects on a bonded joint, when all three phases must be considered, is indecisive, as can be seen from Table 1.1.

It follows that in order successfully to tackle the complex problems involved in the present research, all available information on the different phases and aspects of the subject must be collated and evaluated.

Fortunately, as previously pointed out, most of the preceding investigations are relevant, covering as they do different but complementary parts of the subject, as illustrated in Fig.1.3.

The first part of the research effort in the first year was accordingly organised as shown by the following sequence of activities:

1. Compilation and summing up of information available from previous investigations relevant to the subject.
2. A survey of the international literature.

determining the steps to be taken in order to attain the research objectives, determining the preferred research approach, and setting priorities, based on assessment of existing knowledge and the availability of information.

c) completion of studies initiated in the course of the investigation already reported on and essential for the future progress of the present research.

2. SUMMARY OF RELEVANT PREVIOUS INVESTIGATION

In this section, previous research conducted by the principal investigator has dealt with three major and related topics in the following order: (Fig. 1.1)

Environmental effects on mechanical behavior of FRP laminates.

- Mechanical characterizations of structural adhesives.
- Mechanical performance of adhesively bonded models.

These topics will be briefly summarized in the following pages:

2.1 ENVIRONMENTAL EFFECTS ON FRP LAMINATES (Refs.1-12)

2.1.1 Research objectives

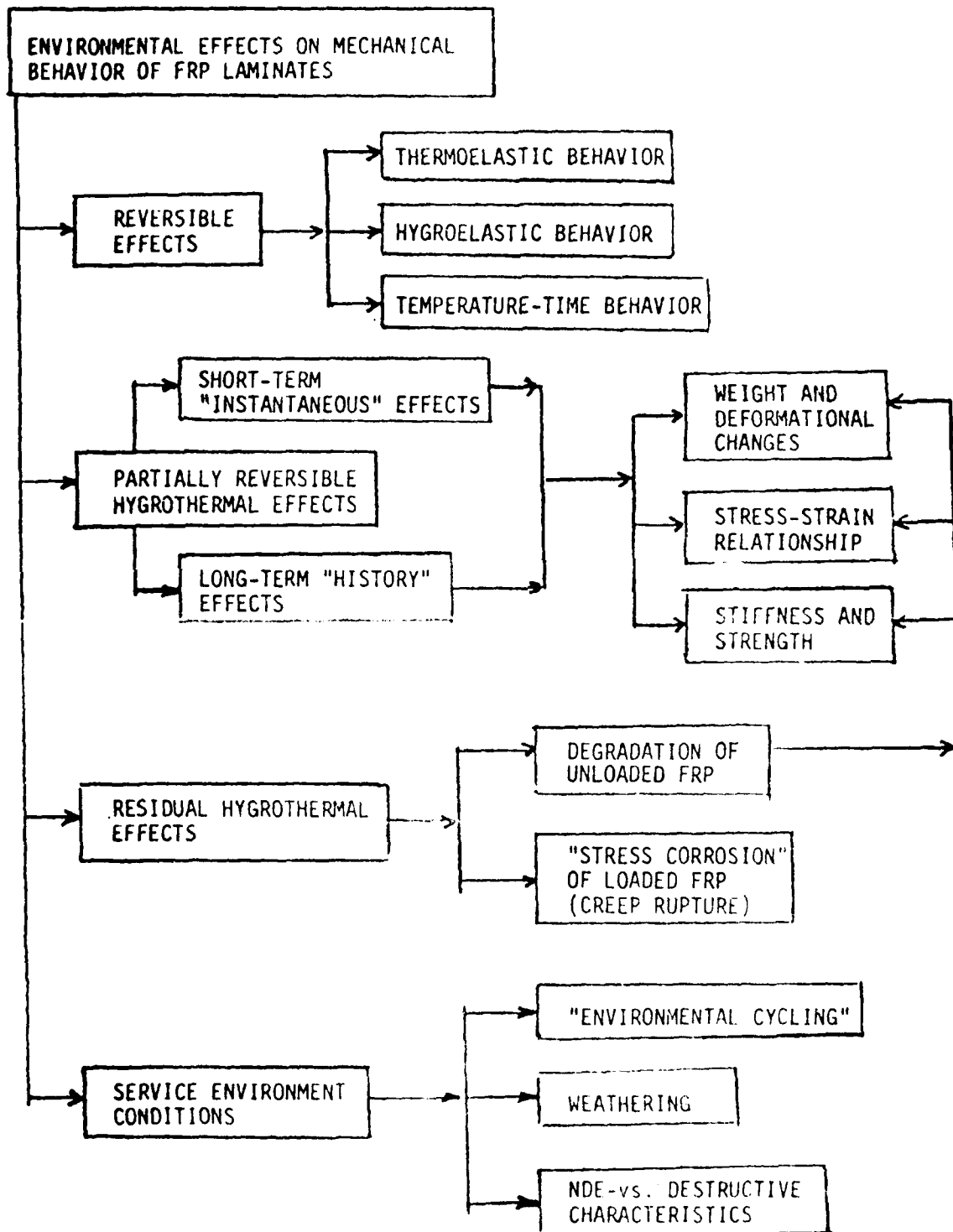
Investigation of separate and combined effects of moisture, temperature and loading on FRP with time.

Assessment of the response and contribution of each composite phase: fibers, matrix, and interfaces, to the FRP durability.

- Distinction between reversible and residual effects.
- Distinction between current and history effects.
- Study of out-door weathering effects as compared with in-door controlled laboratory conditions.
- Correlation between macro-behavior and interstructural micromechanisms responsible for the composite durability, in order to develop a non-destructive methodology for following-up FRP in service life.

The scope of this research is illustrated in Section 2.1.2 and major findings are given in Table 2.1.

2.1.2 Scope of research

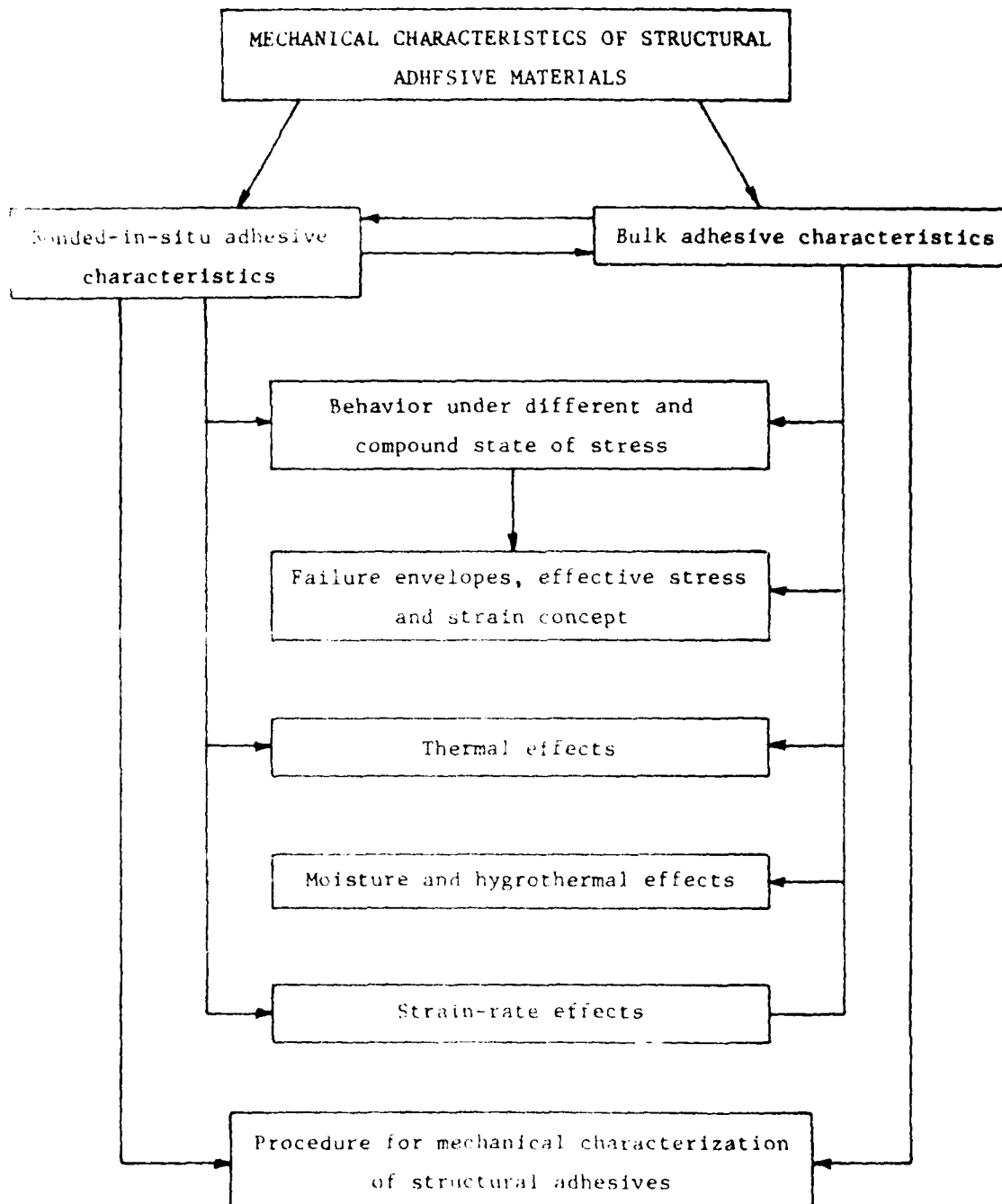


2.1.3 Research Conclusions

- Thermoelastic and hygroelastic behavior have similar effects on internal stresses and deformation behavior.
- Time-dependent thermal effects on FRP matrix-dominated properties obey same law as for the unfilled matrix and are not affected by the mode of loading.
- Moisture penetration mainly reduces matrix-dominated FRP properties, at elevated temperatures. This effect is reversible by drying
- Fiber and interfacial degradation process in GRP composites is activated above a critical hygrothermal level. This effect is non-reversible and is accompanied by weight loss.
- Stress corrosion of fibers is activated above a critical loading level and accelerated by hygrothermal conditions.

2.2 MECHANICAL CHARACTERISTICS OF ADHESIVE MATERIALS (Refs. 19-23)

2.2.1 Scope of research



2.2.2 Problems involved in the mechanical characterization of the adhesive layer

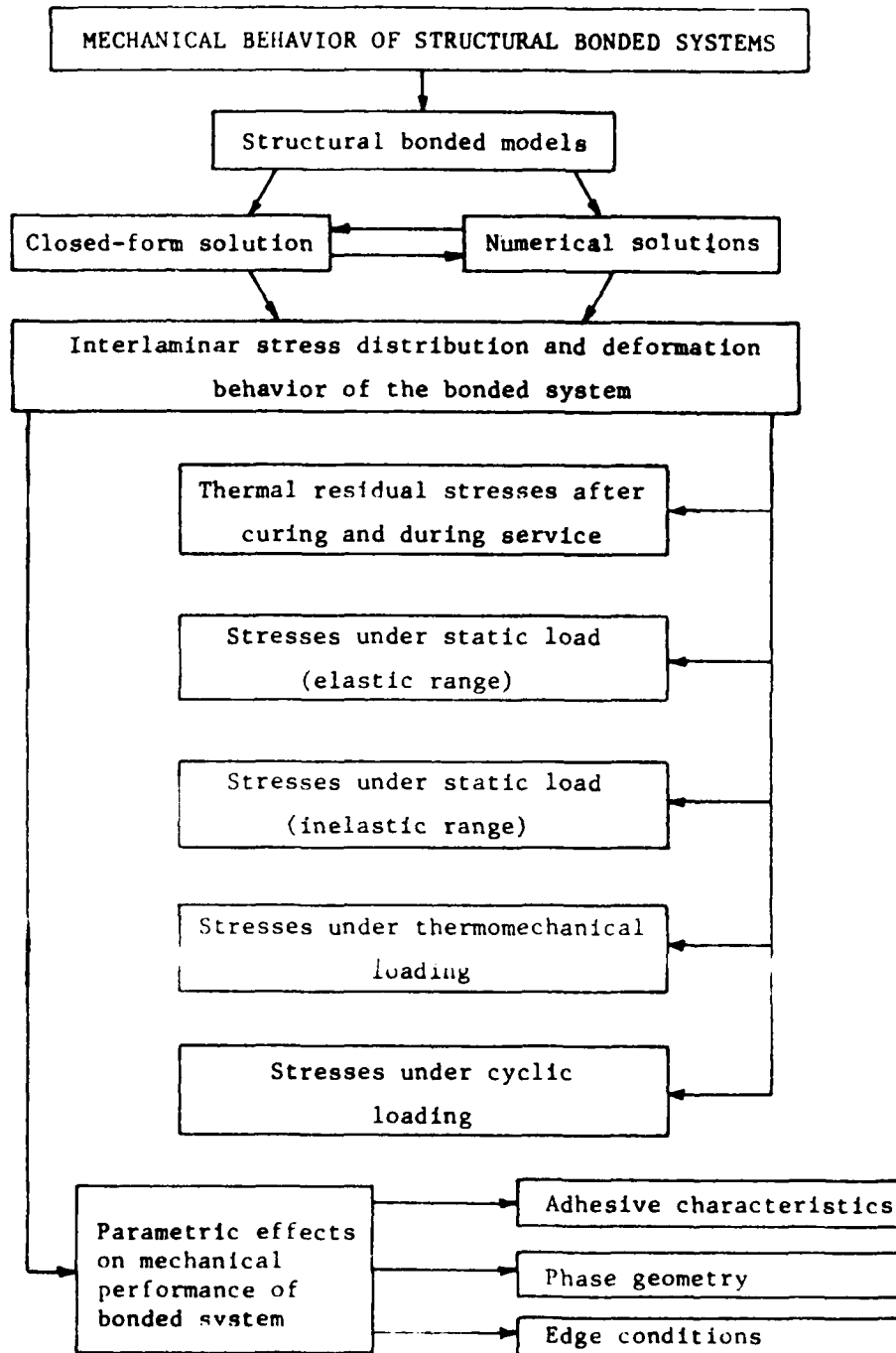
- A weak and flexible polymeric layer - the adhesive - is assigned the task of transferring a load between strong and stiff elements - the adherends.
- Measuring the mechanical properties of the thin and confined adhesive layer is a highly sophisticated operation.
- There is poor correlation between the characteristics obtained by testing bonded specimens in the laboratory and those exhibited by a bonded structural element in service.
- The mechanical behavior of - usually polymeric - adhesives is of a visco-elasto-plastic nature, which is characterized by non-linearity, time-dependence, and sensitivity to hygrothermal conditions even at low stress levels.

2.2.3 Proposed procedure for the mechanical characterization of a bonded adhesive layer. (See the flow chart in Fig.2.1)

- The mechanical characterization of bulk adhesive specimens by standard methods as used for the characterization of a lamina in a multilayer laminate.
- Simple uniaxial loading tests will be conducted by conventional methods in order to obtain stress-strain relationships in tension and compression.
- The elastic behavior and the failure envelope of the bonded adhesive will be determined from the available elastic relationships between moduli and failure criteria respectively.
- The stress-strain relationship for the bonded adhesive up to failure under compound stresses will be determined by applying an effective stress-strain methodology.
- The time-dependent bonded adhesive behavior in different environmental conditions will be assessed using the known stress-strain-hygrothermal-time relationships of the adhesive material's bulk behavior.

2.3 MECHANICAL BEHAVIOR OF BONDED SYSTEMS (Refs. 13-18)

2.3.1 Scope of research



2.3.2 Problems involved in the stress analysis and the failure evaluation of bonded systems.

- Three-dimensional non-linear analytical and numerical methods are required for the prediction of the mechanical behavior under compound stresses.
- The bonded structure (the joint) is characterized by material heterogeneity and geometrical discontinuity. Both induce a complex stress concentration, which is located inside a very narrow zone close to the adhesive boundaries.
- Residual stresses are induced during the fabrication process and, in service, fluctuate with hygrothermal conditions.
- Due to the joints' multiphase structure, several failure modes may be activated in the different phases of the bonded system, all difficult to predict, detect, and track, especially during exposure in service.

2.3.3 Conclusions:

The following conclusions are based on the finite-element numerical solution of an axially loaded symmetrical doubler model composed of aluminum adherends and thick adhesive epoxy layer (IAL).

- The distribution of shear and lateral normal stresses through the IAL thickness and length are uniform within the "middle zone", which comprises about 98% of its total length.
- Maximum values of all stresses and their principal counterparts were attained in the "boundary zone", which constitutes only 2% of the IAL length close to the central adherend interfaces.
- The average interlaminar stress levels were significantly lower than their actual individual extreme levels; they could thus not be used for the prediction of the doubler strength.
- Due to the narrowness of the boundary zone, its stress behavior is not reflected in the overall deformation behavior of the bonded structure, nor could this behavior be directly measured experimentally. It is, however, of a decisive influence on the ultimate IAL behavior and must be considered when failure and strength characteristics are discussed.
- A non-linear FEM procedure can be applied to the determination of the two-dimensional stress distribution within the double IAL through the linear and non-linear ranges of the stress-strain relationship of the adhesive material.
- The FEM results can be used for predicting the visco-plastic ductile failure mode within the IAL, provided its effective inelastic stress-strain relationship is available.
- A significant difference in stress distribution was found to exist between the linear and the non-linear solutions in the critical "boundary zones". The assumption of plane stress led to higher effective stress levels compared with plane-strain state.
- A simplified elasto-plastic stress-strain relationship input leads to an IAL stress distribution similar to that obtained with the more realistic non-linear stress-strain curve.

2.4 BASIC ASSUMPTION FOR THE PRESENT AND FUTURE STUDY

Conclusions drawn from previous investigations led to several assumption, for the present research, as follows:

- The fundamental mechanical behavior of a thin adhesively bonded layer in situ is similar to that of the bulk adhesive material.
- The bonded adhesive layer between adherends can be treated as a lamina within a multilayer multimaterial laminate.
- The adhesive layer can be defined as a visco-elasto-plastic material, the behavior of which is time-dependent and affected by environmental conditions in accordance with laws dictating the behavior of "ductile" polymers.
- In a bonded system which has been given proper surface treatment, the failure is cohesive, i.e. it initiates within the adhesive layer.
- Failure initiation within the adhesive layer can be related to two critical points:
 - a. The onset of elastoplastic behavior - or, in other words, the exceeding of the elastic limit. Beyond this limit residual stresses and strains accumulate during cyclic loading, possibly leading eventually to failure.
 - b. The yield point - or the plastic limit.

3. LITERATURE SURVEY

Material for the survey was mainly collected from the following sources:

Current Journals and Conference Proceedings

International Journal of Adhesion and Adhesives

Journal of Composite Materials

Fiber Science and Technology

Composites Journal

Polymer Engineering and Science

Journal of Applied Polymer Science

ASTM Journal of Materials and Evaluation

Journal of Material Science

SAMPE Quarterly-SAMPE Journal

SAMPE Conference Proceedings

SPI Conference proceedings

Information Sources

U.S. National Technical Information Service (NTIS)

Engineering Index (Compendex)

Current Research Reports (SSIE)

Conference Papers Index

Scientific Technical Aerospace Reports (STAR)

International Aerospace Abstracts (IAA)

Applied Mechanics Review (AMR)

In the past decade extensive research was devoted to the hygrothermal effects on the durability of composite polymeric materials and their matrix and of structural adhesives.

The vast information available on this subject, which is of major importance to the technological development of high-performance materials for mainly aircraft and spacecraft structures, may be classified as follows:

- Hygrothermal effects on polymeric matrices and adhesives
- Hygrothermal effects on fiber-reinforced plastics (FRP) (adherends)
- Thermoelastic and hygroelastic characteristics
- Hygrothermal effects on bonded systems
- Durability considerations in the design and applications of bonded systems

3.1 HYGROTHERMAL EFFECTS ON POLYMERIC MATRICES AND ADHESIVES MATERIALS

3.1.1 The absorption process

The subject of moisture absorption into, and desorption from, polymers, polymeric matrices, and FRP composites, is being widely investigated.

This topic was briefly surveyed in ref. [24]. There are two mechanisms for water penetration into a polymer, polymeric composites, and bonded systems:

a) Diffusion through the matrix bulk, and b) Absorption through the fiber-matrix, or the adhesive-adherend, interface.

It was found that bulk diffusion into polymeric materials, adhesives, or composite matrices, approximately follows Fick's diffusion law until close to the equilibrium absorption state.

In bonded systems and composite materials, however, the situation is much more complex, and the absorption laws are correspondingly so [25]. This is due to the fact that the matrix is not free to swell during exposure. If a matrix or thin adhesive layer is under stress due to adherend or fiber-restraints, absorption will not follow Fick's law, as was demonstrated by Shen and Springer [26] and Loos et al. [27]. The moisture profile through the material thickness as a function of time is of interest for the stress analysis of laminated composites and bonded systems.

Althof [28] succeeded in measuring the moisture profile along a bonded adhesive layer as a function of time, and his experimental findings conform well with the analytical prediction. Data of diffusion parameters for epoxy composites and neat resins can be found in ref. [29]. Recently the determination of moisture distribution in composite laminates as a function of time and relative humidity was discussed by Sandorff and Tajima [30,31].

The difficulty in the analytical determination and the measurement of the moisture distribution in in-situ bonded adhesives is above all due to the obscuring and restraining effect of the adherend on the absorption process.

3.1.1. Hygrothermal effects on matrix and adhesive characteristics

The influence of temperature and moisture on a polymeric (chiefly epoxy) matrix has been investigated extensively. Most of the data available concern effects on the matrix-dominated mechanical characteristics of FRP such as transverse and shear moduli and the strength of U.D. lamina.

Part of this great store of information is summarized in Section 2.1 of this Report as well as in refs. 2, 6, and 7; and it is also surveyed in the next Section, which deals with the effects referred to on FRP as adherends in bonded systems. The evidence trend towards a reduction in strength and stiffness with higher temperature and moisture content is common to all findings.

The effects of temperature and moisture on the mechanical performance of structural adhesives, whether as a bulk material or as a bonded phase, has been investigated much less. Some of the authors findings on this topic are summarized in Section 2.2 of this report and in refs.19, 20, 22, and 23.

The works of Althof [32,33] provide comprehensive information on the effects of temperature and relative humidity to the stress-strain relationship and dynamic response of several commercial structural adhesives as a function of exposure time.

A review by Delollis [34] provides some vital information on the long-term performance of different structural adhesives exposed to real environmental conditions (marine ambience and sun exposure). Most of the adhesives begin to degrade only after prolonged exposure. The contradicting results obtain in several cases were attributed to the differing contributions of surface treatments of the adherends to overall strength. Wegman et al. [35] proposed a method for assessing the long-term durability of structural adhesives based on short-term laboratory tests.

Recently, Almer et al. [36] have found that exposure to moisture of the adhesive prepreps before curing will affect their dynamic mechanical characteristics in service.

The trend towards a decrease in mechanical performance with hygrothermal exposure was found to characterize adhesives similar to bulk polymers. Hence, the laws which govern stress-strain-temperature-moisture vs. time and which were found to apply to bulk epoxy resins (refs.1, 2) may be adopted for predicting the long-term mechanical behavior of structural adhesives.

The effect of moisture in impairing the mechanical performance at elevated temperatures of matrix and adhesive was found to be reversible, and it could be attributed to the reduction in the glass transition temperature of the polymer.

3.2. HYDROTHERMAL EFFECTS ON THE INTERFACES

Due to the recent significant advances in structural adhesives and surface treatment, the weak link, which had previously been the adhesive-adherend interface, was shifted to the adhesive or to an imaginary boundary layer located between the adhesive and the interface.

Moisture penetrating to this region may reverse the effect by reducing stress concentration in the "plastic" adhesive on the one hand and by weakening the interfaces by a water molecule penetration mechanism, on the other.

The mechanism of interface weakening is a combination of physical, chemical, and mechanical, effects (See ref.7).

3.2.1 Physical effects

Wet interfaces have a lower surface energy and tend to be more stable than dry ones; thus high adsorption forces act at the interface against the existing interfacial physical bonding forces.

According to DeLollis [37] such forces are responsible for stress concentration which initiates, and causes the propagation of, interfacial cracking. An attempt to measure the reduction in interfacial bonds due to wetting on the basis surface energy considerations was made by Kaible et al. [38,39]. The system was a fiber-epoxy composite; but the physico-mathematical approach may be applicable to other bonded systems, too. Good agreement was found to exist between measured and predicted shear strength values of wet vs. dry systems. The main criticism of the thermodynamic-energetic approach is its inapplicability to highly brittle systems with very low interfacial bonding. A pronounced discrepancy is found between theory and experiments in the case of structural adhesives which had been subjected to high plastic deformation [40,41].

3.2.2 Chemical effects

Most metallic adherends used in adhesive bonding are sensitive to the presence of water. In the case of aluminum two processes may occur:

- a) Hydration of the oxide layer.
- b) Dissolution of the Aluminum underneath the oxide layer.

Both effects accelerate the galvanic corrosion which is initiated by the presence of copper, zinc, or magnesium, in the aluminum alloy. According to Patrick [42] the dissolution process begins with the formation of an alkaline solution due to the solubility of the amine hardener contained in the adhesive. The alkaline solution in turn releases aluminate ions (AlO_2^-) from the aluminum oxide.

Orman & Kerr [43] found that an increase in the pH of aqueous solutions has a pronounced effect on the chemical processes at the metal surfaces. It is known that a seawater ambience has a deleterious effect on bonded aluminum joints similar to that of bulk aluminum.

The contribution of a primer layer to improved interfacial strength has been widely investigated. It was found that the introduction of such a primer "interlayer" augments the resistance of interfaces to the corrosive effects of water and thus shifts the focus of weakness to the tough adhesive layer even in a severely moist ambience [44].

3.2.3 Mechanical effects

The residual strength of bonded aluminum/epoxy joints which had been loaded while being exposed to a water ambience was found to drop considerably as exposure time increased [43,45]. The failure was found to initiate at the

aluminum oxide layer. Thus reduction in residual strength is attributable to the weakening of the oxide layer due to its hydration.

Most of the reduction in residual strength was found to be reversible by drying [45,46]. Lewis and Natarajan [41] have suggested a mathematical-mechanical model for interfacial bonding consisting of an aggregation of linkage points which is progressively attacked by water molecules penetrating to it. Thus the rate of interfacial strength reduction may be related to the rate of moisture diffusion. Several works apply a fracture mechanics approach in dealing with the effects on the joint strength of moisture penetrating the interfaces. That method is represented by the contribution of Mostovoy et al. [47-49]. Recently the effects of temperature and moisture on the stresses induced at fiber-matrix interfaces was studied numerically by Adams et al. [50,51], who used a finite element (FEM) approach. Their solution takes into account the non-linear behavior of the epoxy matrix and describes the stress distribution pattern over the interfaces. That approach may be applicable to the solution of similar problems but involving hygrothermal effects at adhesive-adherend interfaces in bonded systems.

3.3 HYGROTHERMAL EFFECTS ON FRP ADHERENDS

Moisture penetration and temperature changes may affect the performance of FRP adherends in three ways:

- a) Thermoelastic (TE) and hygroelastic (HE) deformation of the laminate as governed by the TE and HE characteristics of the constituent layers.
- b) Inter and intra-laminar residual stresses induced in the FRP systems in the course of curing and as a result of subsequent stress variations due to fluctuations in ambient service conditions.
- c) Deterioration of the mechanical characteristics of FRP due to prolonged exposure (Durability).

3.3.1 Thermoelastic and hygroelastic behavior of polymeric composites

Variations in ambient conditions, viz. temperature and humidity, were found to have similar effects on deformational changes of polymers and polymeric composites. These effects, which are controlled by the polymeric matrix, are much more pronounced in the transverse, than in the longitudinal, direction. In extreme cases, such as Carbon-fiber reinforced plastics (CFRP) and Kevlar-fiber reinforced plastics (KFRP), the coefficient of thermal expansion (CTE) in the direction of the fibers is even negative but negligible. In textbooks dealing with structural design [52,53] with FRP materials both thermoelastic and hygroelastic behavior are treated in the same way because of the approximately linear, and reversible, relationship between temperature change and respective moisture content on the one hand, and the deformation response of these materials on the other. That approach is based on the analytical work of Halpin and Pagano in 1969 [54]. It is justified when the problem of hygrothermal stresses in multi-layer laminates in the curing and service stages is considered. [53,55] From a more rigorously scientific point of view, however, there is a fundamental difference between the thermoelastic and the hygroelastic phenomena and mechanisms, and they require different approaches in their respective studies.

3.3.1.1 Thermoelastic characteristics

Analytical studies aimed at predicting the coefficient of thermal expansion (CTE) from the properties of the different constituents were begun at the same time as similar efforts toward the elastic solution of the problem. Schapery [56], using energetic principles, concluded that a simple law (very similar to the "rule of mixture") can be used for the prediction of the CTE as well as for extending the results to viscoelastic behavior.

A similar micromechanics approach by Rosen and Hashin [57] resulted in a more complicated solution for the CTE of multiphase anisotropic composites having any number of anisotropic phases. That result, an "effective CTE", is given in terms of two bounds, which reduce to those of Schapery for the case of two phases.

An analytical solution for the CTE of composites was provided by Halpin and Pagano [54] and confirmed experimentally by the work of Fahmy and Ragai [58] on angle-ply CFRP composites.

In recent years several works have been devoted to the experimental investigation of the CTE of specific composite systems, which are used mainly in aircraft structural elements. Marom and Gerson [59] studied the effect of interfacial bonds on CTE of unidirectional (U.D.) CFRP and GFRP; Rogers et al. [60] investigated the effect of fibre orientation on CTE of CFRP within a wide temperature range. The effect of carbon fiber anisotropy on CTE of U.D. composites was treated by Ishikawa [61] with the aid of both experimental and analytical methods.

CTE of U.D. and of angle-ply CFRP laminates were measured by Strife and Prewé [62], the results for U.D. laminates being also examined in the light of formulas taken from micromechanics. The time and temperature dependence of CTE in different types of U.D. CFRP systems was investigated by Dootson et al. [63].

Thermally invariant characteristics of composite laminates were derived analytically by Miller [64]. In this case, as in the previously reviewed studies of thermoelastic behavior of composite laminates, the analysis is based mainly on invariant lamina properties [65] and on the classical linear laminate theory concerning the effect of the thermal loading concept [53,55,66].

In spite of the very large amount of data derived, experimentally for CTE of U.D. lamina it is difficult to establish a firm, accepted average value even for lamina of identical compositions. This is due to the high scatter found when comparing the results obtained from different sources, as shown in Table 3.1

One explanation for that scatter attributes it to the intervention of shrinkage (or swelling) due to drying (or wetting), which is responsible for the dimensional changes during the measurement of CTE. Most of the publications surveyed above took no account of the hygroelastic characteristics in this connection, nor did they mention any experimental details which might reveal the ambient conditions of humidity during the tests.

3.3.1.2 Hygroelastic characteristics

The hygroelastic behavior of composites and their hygroelastic coefficient (HEC) were studied much less extensively than the thermoelastic characteristics. The significance of the effect of moisture on the elastic and strength performance of polymeric composites has only been acknowledged in recent years. It is being attributed mainly to the effect of moisture penetrating into the matrix (adhesive) and interfaces and the resulting degradation in the mechanical characteristics of the composite and bonded system. Rather less attention was paid to the swelling and shrinkage process attending the wetting and drying of the materials through exposure to environmental changes. That phenomena, termed hygroelasticity, is often treated in a way analogous to that applied to the thermoelastic effects by virtue of its linearity and reversibility within the range of practical service conditions.

Previous research on the hygroelastic behavior of GFRP at different humidity and temperature levels is summarized in Section 2.1 of this report and discussed at some length in refs. 6, 7, and 10. A more comprehensive study is reported in ref. [24], which deals with dimensional changes in glass filled and unfilled epoxy resin at different humidity levels. The major finding of that work is the linear relationship between relative humidity, moisture absorption, and dimensional changes, which is characterized by an almost constant hygroelastic coefficient (HEC), independent of the humidity level and exposure-time history.

3.3.1.3 Hygrothermoelasticity in structural design & applications

In recent years the thermoelastic and hygroelastic concepts were introduced into the analysis and design of structural composite materials [52, 53, 55], due to the interest in thermoelastic and hygroelastic characteristics and behavior of certain graphite/epoxy composites having extremely low CTE and HEC with high stiffness and low density like Cy 70 [25]. These composites are used for structures which must possess dimensional stability under extreme temperature and moisture conditions. For example: Space structures [67], Antenna truss structures [68], and optical bench [69]. For such applications as well as in order to know the effects of the environmental history on the deformational behavior of an FRP adherend as part of a bonded structure, more information is needed on the HEC and CTE characteristics of different composites, matrices, and adhesives.

The wide scatter of the available data is attributable to the dependence of HEC on the environmental history before, and the thermal conditions during, the tests.

One of the objectives of the present research is to investigate the interdependence of thermal and hygroelastic characteristics, i.e. the effect of moisture on CTE and the effect of temperature of HEC.

3.3.2 Hygrothermal effects on stresses and failure in FRP adherends

In recent years the problem of failure initiation (first-ply failure, abbreviated FPF) and its propagation has been studied extensively [70, 71]. In the case of FRP laminates, which are composed of layers characterized by a pronounced difference between their transverse and their longitudinal CTE

(such as CFRP and KFRP), residual stresses are induced during curing due to the thermal incompatibility between laminate layers [72,73]. In severe cases, when these residual stresses exceed the laminar transverse strength, transverse cracks already appear while curing is still in progress [74,75]. In a more realistic situation, matrix swelling due to the penetration of moisture will counterbalance the residual transverse curing stresses and delay crack initiation and first-ply failure under external loading [67,77,78]. The effect of moisture penetration in service on interlaminar residual stresses in GFRP and their effect on reducing the laminar failure limit was investigated by Lee et al. [79] who measured the curvature changes of a non-symmetrical laminate during moisture absorption over a period of time. The combined effect of exposure to moisture and subsequent thermal cycles on CFRP was investigated by Lee [80] and Dvnes [80], who found that strength degradation through crack propagation was accelerated by moisture penetrating into existing microcracks. Karami, Chamis et al. have carried out an extensive analytical study on the effect of a humid ambience on the moisture profile and subsequent stress distribution through the thickness of a M.D. FRP laminate [81,82].

It may be concluded that the combined effects of thermal and moisture variations can be detrimental by inducing stresses which, in extreme cases, will cause crack initiation followed by propagation, even in unloaded FRP. On the other hand, when acting in opposite directions (i.e. drying at an elevated temperature), hygroelastic stresses counterbalance thermal stresses and may thus delay crack initiation and increase level of FRP under subsequent loading.

2.2. Hygrothermal effects on structural characteristics of FRP laminates

During the last decade a vast amount of information was accumulated concerning environmental effects on the mechanical performance of FRP structural composites. This testifies the intense effort invested in this subject and the prime importance of this field.

A brief summary of the findings up to 1977 is given in Section 2.1 and in refs. 6-9 and ref. [83]. More information is available in two Proceedings of ASTM conferences on this subject [84,85]. Most of these works were concerned with the effects of long-term hygrothermal exposure on the gross mechanical characteristics of FRP, such as stiffness and strength [86-88].

Currently more attention is devoted to the effect of moisture and temperature on interlaminar FRP characteristics under shear and compressive loading and also under curing and in environmental conditions alone. The common trend found in all these investigations is the decrease with prolonged exposure to hygrothermal conditions, in matrix-dominated characteristics such as transverse and interlaminar shear and compressive strength.

2.3. HYGTROTHERMAL EFFECTS ON ADHESIVELY BONDED SYSTEMS

The complexity of this subject stems from the complexity of the material systems involved which is characterized, in the general context, by multi-phase, anisotropic, three-dimensional unisotropic modes of behavior.

The adhesive phase by itself when bonded to the adherends is characterized by viscoelastic and viscoplastic characteristics which are highly sensitive to hygrothermal conditions. The different aspects and approaches to tackle with such systems are discussed in Section 2.3 and in refs. [14-23].

Similar to FRP, here, too, a vast body of information is available in the literature. Most of it has engineering value and concerns the effects of different conditions of prolonged service on the residual strength and fatigue characteristics of both loaded and unloaded bonded-joint models. Some of the findings are reviewed in Sections 3.1 and 3.2 of the present survey, which deal with the influences to which adhesives and interfaces are subject.

In this section the survey deals with three aspects of the hygrothermal macroeffects on the bonded system as a multilayered structure, as follows:

- a) Thermoelastic and hygroelastic behavior of the unloaded system;
- b) Durability of the unloaded bonded system; and
- c) Durability of the loaded system.

3.4.1 Thermoelastic and hygroelastic behavior of bonded systems

The analytical approach to the solution of the problem of deformation and stress of bonded systems due to HT effects is similar to that applicable to FRP laminates (Section 3.3.1). The main difference is to be seen in the fact that here the polymeric-adhesive phase can be geometrically and mechanically defined as a separate phase - in contrast to the difficult analytical representation of the polymeric matrix phase in composite materials.

In bonded systems the HE and TE problem appears whenever CTE and HEC of the adherends are incompatible, e.g. when different metals are bonded together or metals are bonded to FRP. In such cases the main objects of the analytical study are the deformation of the bonded structure and the interlaminar stresses within the adhesive layers.

The thermoelastic stresses created within the adhesive and the adherends develop in two principal stages. First, thermal stresses remain after the bonded system has cooled to room temperature following the curing process. These residual stresses undergo additional changes in the course of time and may eventually lead to delamination failure-mode [89] due to thermal fluctuations during service.

This problem is particularly severe in CFRP-aluminum bonded systems, where the difference in thermoelastic characteristics is high and delamination between the two adherends may occur, in extreme cases, even during the curing stage.

The analytical problem involved was approached on four levels:

- a) Solving the average thermal stresses in the adherends by assuming, in turn, axial stress and plane-stress, and neglecting the interlaminar and laminate stresses close to the free end [90]. This was similar to the approach of Timoshenko [91] and to the classical composite laminate theory [53,55,66].
- b) As an extension of the general study of the interlaminar behavior of laminated plates [92,76], solving the interfacial stresses while neglecting the characteristics of the interlaminar adhesive phase. In most of these solutions boundary conditions were not satisfied.

c) Solving the problem by representing the bonded joint as a three-phase model, assuming either plane stress or plane strain, and solving the differential equation for the derivation of interlaminar stress distributions [93-95].

In most of the cited works, whenever a closed-form solution was obtained, stress distribution in the critical zone close to the free ends does not satisfy boundary conditions.

d) In recent years the problem was tackled by numerical methods, such as the finite element method. Only such an approach provided solutions which satisfied boundary conditions [96-98].

The analytical study of the effect of moisture diffusion and internal profile on the stress distribution follows the trend used for ~~same~~ effects on FRP as reported by Chamis [81,82], Lee et al. [79], and others. Althof [28] found a good agreement between the analytical prediction and experimental findings concerning the moisture profile and the resulting stress distribution within a structural adhesive layer bonded to aluminum adherends.

Weitsman [99] analytically studied the effect of moisture absorption on interfacial stress-relaxation within an adhesive layer bonded to elastic adherends. Such visco-elastic behavior was found to reduce stresses but assumed to be reversible on drying.

The coupled effects of temperature and moisture fluctuations on interlaminar stresses within layered systems was studied theoretically by Pipes et al. [100], and their results showed both the magnitude and distribution of hygrothermally induced interlaminar stresses.

More recently a similar study, which took into account the time-dependency of the behavior, was reported by Sih and Shih [101].

In spite of the known significant effect of the bonded system's hygro-thermal exposure on its residual stresses, only comparatively few analytical solutions are available. This is due to the mathematical complexity of the problem, as discussed before.

Further experimental study of these effects is required in order to examine the validity of the existing solutions.

3.4.2 Durability of unloaded bonded joints

One representative source of information on this topic is that of Minfold [102,103] who carried out comprehensive investigations with unloaded joint specimens exposed to different ambient conditions (seawater immersion, freezing, and drying, at different temperatures, etc.). The variations over 4 years in bonded joint strength were measured, and the results indicated that exposure to a marine environment was the most corrosive, whereas exposure to RT water has almost no effect on joint strength. Even in the most severe cases, however, accelerated degradation only started after more than a year, so that information on short-term exposure, even under extreme conditions, could not be extrapolated for the prediction of long-term durability. Adhesives cured at elevated temperatures and under pressure are more durable than adhesive cured without pressure. The effects of different surface treatments on durability in hostile environments show contradictory results.

In most of the tests so far conducted single-lap-joint (SLJ) or double leg joint (DLJ) specimens were used, but their strength data are difficult to interpret due to the non-uniformity of the interlaminar stress distribution and the coupling of bonding moments, which together create lateral stresses (peel) at the joint edges. The combined effects of peel and shear stresses on ultimate failure complicate the failure mechanism and essentially limit these tests to qualitative comparative purposes. Recently thick adherend specimens (TA) have become widely used due to their more uniform interlaminar shear stress distribution and to the minor contribution of peel stresses to the total behavior which characterize them.

The behavior of TA joints was investigated by Althof and Brockman [32], who exposed them to different hygrothermal combinations. The resulting stress-strain curves in shear indicated the general trend of the reduction in plastic yield strength with an increase in temperature and relative humidity. Garrett et al. [104] found strength increases in bonded DLJ CFRP joint with drying at elevated temperatures. On the other hand, an increase in moisture at elevated temperatures resulted in a pronounced strength degradation.

The effects of moisture content on the strength of FRP/Metal DLJ joints were studied by Wolf [105,106]. He found that moisture may improve joint strength at a low temperature but that its influence is small at intermediate temperatures; while at elevated temperatures it reduces strength.

These findings, together with similar results obtained by Althof [33], may explain the opposing effects of moisture on bonded joints: On the one hand, it relaxes the high stresses at the joint edges, while on the other it has a weakening effect on the adhesive layer and interfaces. The mechanism that predominates will eventually determine the strength and durability of the bonded joint.

The combined effects of moisture and temperature on the strength of CFRP bonded joints was investigated by Parker [107]. His findings indicated a drop in strength with increasing moisture content of the constituent materials. The failure mode gradually changed from failure within the composite in dry conditions to cohesive failure of the adhesive in the case of specimens exposed to prolonged hygrothermal influences.

3.4.3 The durability of loaded bonded systems

The combined mechanical and hygrothermal effects on the residual strength of bonded joints was investigated by Bethune [45], who found a drastic drop in joint strength after a brief warm-water exposure of loaded specimens as compared with unloaded control specimens, which produced hardly any significant change in strength. Higher loading levels resulted in yet shorter times to failure.

Similar tests by Lohr [108] showed that under exposure to moisture the typical bond failure was cohesive when a primer was used, but adhesive without primer. In the case of specimens with primer - characterized by cohesive failure - drying resulted in the recovery of the original strength. Wegman et al. [35] showed that the curve, strength vs. exposure time, of an unloaded joint under specified hygrothermal conditions is similar to the trend derived from the test of loaded joint specimens conducted in accordance with the pertinent ASTM standards.

The durability trends of loaded joint specimens may thus be extrapolated from the corresponding data of their unloaded counterparts. A model for predicting joint durability was recently proposed by Gledhill et al. [109].

A most comprehensive study of the performance of structural bonded systems was conducted under the PABST program in the last five years. The Design Handbook for Adhesive Bonding [110] summarises a part of the findings from the points of view of technological design. The current PABST reports deal with hygrothermal effects on mechanical characteristics of the bonded system and their time-dependency [111,112].

The design handbook, however, hardly concerns itself with the hygrothermal durability of bonded joints.

3.5 CONCLUSIONS OF THE LITERATURE SURVEY

(1) There is a tremendous amount of technological information on the durability of bonded joints and their constituents, but only limited data on the fundamental time-dependent effects, both separate and combined, of moisture, temperature, and mechanical loading.

(2) The interdependence of adhesive stresses and moisture diffusion has not been investigated in any systematic manner.

(3) Temperature and moisture are predominant factors in the stress and the failure mechanisms of bonded systems in service conditions. Their combined effects may lead to significantly different trends in the failure mechanism and its location.

(4) There are contradictory views of the effects of thermo and hygroelastic characteristics on an FRP adherend. This is mainly due to the interdependence of CTE in moisture and HEC on temperature.

(5) The effect of hygrothermal conditions on the time-dependent behavior (viscoelastic, viscoplastic) of bonded system has not been adequately investigated, nor was it considered in any stress-strain analysis.

(6) The theoretical prediction of the time-dependent hygrothermal effects on the mechanical behavior of adhesively bonded systems necessitates an advanced and powerful non-linear, time-dependent and three-dimensional, numerical solution.

4. OBJECTIVES AND PROCEDURES OF PRESENT RESEARCH

The final goal of the present work may be stated to be the prediction of the deformation and the failure limit of a bonded system with time as a function of mechanical and hygrothermal conditions, which can be defined mathematically as follows:

$$F = f_1 (t, \sigma_i, H, T)$$

$$\delta = f_2 (t, \sigma_i, H, T)$$

where F - failure limit

δ - deformational characteristics

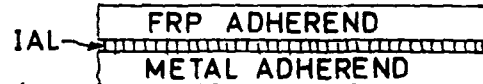
t - time

σ_i - state of stress

H - humidity conditions

T - thermal conditions

The material-structural model which forms the final objective of the theoretical and experimental investigation comprises three basic constituents, namely: The interlaminar adhesive layer (IAL), metallic and/or FRP adherends, and the different interfaces. A representative non-symmetrical version of such a model is illustrated here:



The research procedure will start with the adhesive behavior as a function of stress and time.

The second step will be concerned with hygrothermoelastic characteristics of adhesives and FRP adherends and their effect on internal stresses and deformation, only in the third stage will the overall behavior of the model be studied as a function of hygrothermo-mechanical conditions with time.

The research objectives and the procedure for their accomplishment are outlined in more detail in the following sections.

4.1 RESEARCH OBJECTIVES

4.1.1 To establish, and to verify experimentally, a "stress-strain relationship up to failure" criterion for the prediction of the mechanical behavior of the adhesive layer under combined stresses and as a function of hygrothermal conditions with time.

4.1.2 To compile basic empirical data on the time-dependent hygrothermal-mechanical characteristics of the bonded system constituents: adhesives, FRP adherends, and interface. These data will constitute the input required for the analysis of the bonded system.

4.1.3 To develop, and to verify experimentally, a numerical methodology for the prediction of the stress-strain-vs.-time behavior of the bonded system, having different hygrothermo-loading histories and subjected to different current conditions.

4.2 RESEARCH PROCEDURE

The procedure adopted and the major disciplines involved in attaining these objectives may be outlined as follows:

A MECHANICAL CHARACTERIZATION OF STRUCTURAL ADHESIVES AND ADHERENDS

- A-1 Establishment and verification of a general "effective" stress-strain-relationship concept for a combined state of stress.
- A-2 Development of a data-reduction methodology for the experimental characterization of the mechanical behavior of adhesives in time as affected by hygrothermal conditions.
- A-3 Compilation of basic experimental data on the hygrothermoelastic characteristics of adhesives and FRP adherends, required as input for the analysis of bonded systems.
- A-4 Compilation of basic experimental data of the hygrothermal effects, with time, on the mechanical behavior of adhesives and FRP adherends. These data are required as input for the analysis of bonded systems.

B STRESS ANALYSIS OF BONDED SYSTEMS AND THEIR DEFORMATION BEHAVIOR

- B-1 Analytical and experimental study of the time dependent stress distribution in an adhesively bonded model under constant load and the displacement undergone by the model.
- B-2 Analytical study and experimental investigation of temperature and moisture effects, with time, on the mechanical behavior of unloaded bonded systems (in the curing stage and subsequent service conditions).
- B-3 Investigation of the temperature and moisture effects, with time, on loaded bonded systems.
- B-4 Investigation of the history of combined hygrothermal and mechanical effects and of current such effects on loaded bonded systems.

A flow chart descriptive of the detailed research procedure towards the accomplishment of its objectives is shown in fig. 4.1.

5. MECHANICAL BEHAVIOR OF ADHESIVE MATERIALS UNDER A COMBINED STATE OF STRESS

5.1 BACKGROUND

The complexity of the stress analysis and the structural design of bonded joints stems from two main characteristics of the interlaminar adhesive layer (IAL), namely;

- The non-linearity of the stress-strain relationship, which is a reflection of the viscoelastoplastic behavior of the polymeric adhesive; and
- The three-dimensional state of stress prevailing in the critical IAL edge zone, which eventually determines the failure load and fatigue life of the bonded joint.

Analytical closed-form solutions for the IAL stress distribution are inadequate and cannot satisfy the boundary conditions in the critical edge zone, even at the linear elastic level [113-115]. Numerical solutions, on the other hand, require the input of the stress-strain relationship, which is a function of the state of stress, the strain rate, time, temperature, etc. At low strain levels a linear approximation can be made, and the finite-element (FEM) solution is relatively simple and direct [17,116]. At moderate, and certainly at higher, loading, however, the adhesive material behaves in a non-linear manner, being highly sensitive to time and to environmental effects. The stress-strain relationship in these cases is derived empirically and can easily be obtained in a simple loading mode, such as uniaxial tension or pure shear.

Hence the stress analysis of the IAL, which in the multiaxial state of stress is an involved concept, must be related to the available empirical simple stress-strain data. The "Effective Stress-Strain" concept is one approach for tackling the problem, and it was found to be successful in the IAL stress analysis in the non-linear range [18,116]. The effective stress-strain concept assumes that, in the case of a basically ductile material, plastic residual strains are induced even at a low stress level. Hence the plastic yield hypothesis can be applied, and the multi-directional state of stress can be related to a simple one through a function similar to that of Von-Mises [18,117]. A number of authors have suggested, and applied, such an approach for viscoelastoplastic polymeric materials commonly used for adhesive bonding [118-119].

The Von-Mises function and similar expressions are based on the contribution of the deviatoric stress component to the plastic yield process; but it does not account for the effect of the volumetric stress component.

In a recent investigation on bulk properties of structural adhesives, a significant difference was found between the stress-strain curves and the yield stress levels under uniaxial tension and those under compression loading [19-23,120]. It was thus concluded that a modified yield criterion and an effective stress-strain concept must be evolved for the analysis and design of structural adhesively bonded joints. The objective of the present study is thus twofold:

- a) To evolve an extended and more general effective stress-strain hypothesis, which takes into account the effect of the volumetric stress component through the linear and the non-linear ranges and up to plastic yield failure.

b) To examine the hypothesis referred to under a) above, in the light of an experimental investigation conducted on both bulk and bonded (in-situ) structural adhesive systems commonly used in bonded joints.

5.2 THEORETICAL CONSIDERATIONS

The analytical approach to the problem of the non-linear time- and temperature-dependent mechanical behavior of the interlaminar adhesive layer (IAL) must be based on the determination of an effective stress-strain relationship which can be used as an empirical input.

This relationship can be determined if a function is available which relates the tensorial components of stress and strain to their respective effective values. That function must be valid throughout the entire range of stress-strain relationship up to failure and under all combinations of compound stresses.

The common function for such an effective relationship is based on the invariant principle postulated by Von-Mises, Henky and others [121,122] for ductile isotropic materials:

$$\bar{s} = \sqrt{3}(J_{2D})^{1/2} \quad (5.1)$$

where \bar{s} - the effective stress

J_{2D}^* - the second invariant of the deviatoric stress tensor

The relationship thus established is adequate for ductile materials, in which the effect of the volumetric stress component, σ_m , is negligible.

$$\sigma_m = \frac{J_1}{3} \quad (5.2)$$

where

J_1^* - the first invariant of the general stress tensor.

For materials which are affected by σ_m eq.(5.1) should be modified, thus [22,23,123]:

$$\bar{s} = C_s (J_{2D})^{1/2} + C_v J_1 \quad (5.3)$$

where

$$C_s = \frac{\sqrt{3}(\lambda+1)}{2\lambda}$$

$$C_v = \frac{\lambda-1}{2\lambda}, \text{ and}$$

$$\lambda = \frac{\sigma_c}{\sigma_t} - \text{the ratio between compressive and tensile stress, which}$$

is a function of the effective strain level. Eq.(5.3) includes eq.(5.1) and thereby holds good for isotropic materials, where the following relationships exist:

$$J_{2D} = \frac{1}{6} [(\sigma_1 - \sigma_2)^2 + (\sigma_2 - \sigma_3)^2 + (\sigma_3 - \sigma_1)^2]$$

$$J_1 = \sigma_1 + \sigma_2 + \sigma_3$$

$$\sigma_c = \sigma_t \quad \lambda = 1 \quad C_v = 0 \quad C_s = \sqrt{3}$$

At the failure level eq.(5.3) is transformed into:

$$\bar{s}_f = C_{sf}(J_{2D})_f^{1/2} + C_{vf}(J_1)_f \quad (5.4)$$

which describes the failure envelope of the more general case of ductile materials, e.g. structural adhesives. From the comparison of pure shear and tensile loadings at the failure level, the following ratio of tensile to shear yield strength is obtained:

$$C_{sf} = \frac{F_t}{F_s} = \frac{\sqrt{3}(\sigma_f + 1)}{2\sigma_f}$$

which is also a function of σ_f .

The appropriate expression for the effective strain, $\bar{\epsilon}$, is given by eq.(5.5)

$$\bar{\epsilon} = C_s \frac{1}{1+\nu} (I_{2D})^{1/2} + C_v \frac{1}{1-2\nu} I_1 \quad (5.5)$$

where

ν - Poisson's ratio, which is a function of the effective strain level.

I_{2D}^{**} - the second invariant of the deviatoric strain tensor.

I_1^{**} - the first invariant of the general strain tensor.

Expressions (5.3) and (5.5) permit the derivation of the relationship between the effective stress and the effective strain for a general state of stress, based on simple uniaxial stress-strain curves obtained empirically. It is suggested that this procedure is adequate for those structural adhesives in which bulk and in-situ mechanical properties have been found to be correlated [15,23]. It can be used in cases in which a wide range of empirical s-s curves of different hygrothermal conditions as a function of time are available.

In this way the effects of time, of temperature, and even of humidity, on the non-linear s-s relationship, can be used as input for determining the actual mechanical behavior of each individual element within the IAL system with the aid of a numerical procedure.

$$I_{2D}^{**} = \frac{1}{6} [(\epsilon_1 - \epsilon_2)^2 + (\epsilon_2 - \epsilon_3)^2 + (\epsilon_3 - \epsilon_1)^2]$$

$$I_1^{**} = \epsilon_1 + \epsilon_2 + \epsilon_3$$

5.3 EXPERIMENTAL PROCEDURE

The main objective of the present investigation was to verify the analytical concepts postulated above. The basic tests were (i) uniaxial tensile loadings carried out with standard dog-bone specimens cut from 3 mm thick plates made of hardened adhesive in accordance with ASTM 638-641; and (ii) uniaxial compression of tubular specimens of 12 mm external diameter, 3 mm wall thickness and 24 mm length.

A state of pure shear was obtained by the torsional testing of thin-wall specimens so machined that for the gauge length, the wall-thickness was reduced. Special tabs bonded to the edges served to transfer the moment from the Instron loading machine. Instron Extensometer G57-11 enabled exact measurements to be made of small twist angles in the linear elastic range (See fig.4 in ref.15). In the non-linear range, up to failure, large deformations must be expected which may, however, not be detected by the standard Extensometer. In these measurements, the overall angle include an unknown contribution by the load transfer zone. In order to find the pure twist angle at the gauge length, this deformation was deducted by means of a correction curve (fig.5.1)* obtained by the following procedure: tubular specimens of different lengths (40-140 mm) were loaded up to failure, the torsional deformation vs. specimen length at different levels of moment, M, up to failure were plotted (See fig.5 in ref.15). The extrapolation of these curves down to length 0 is the correction curve of γ vs. l .

A compound state of stress was achieved by the simultaneous application of uniaxial and torsional loading by means of an axial spring which also served as a pressure gauge (fig.5.2).

Shear stress-strain curves of bonded adhesive in simple and compound state of stress were obtained by the napkin-ring type specimen as reported earlier [21].

5.4 EXPERIMENTAL VERIFICATION

In order to examine the relationship expressed by eqs.(5.3) and (5.5), a series of tests was conducted with different materials and under a variety of temperature conditions representing the practical range of the parameter, λ .

Behavior unaffected by the volumetric stress compound ($\lambda \approx 1$)

The investigation was based on an epoxy adhesive composed of Epon 815 and Versamide V140 in the ratio, 70/30. Uniform conditions of strain-rate, temperature, and humidity, were maintained. It was found for this material, that, $\lambda \approx 1$ throughout most of the loading range, but close to failure $\lambda \approx 1.1$. For a material of the type tested, the Von-Mises approach is accepted to hold:

$$\begin{aligned}\bar{s} &= \sqrt{3}(J_{2D})^{1/2} \\ \bar{e} &= \sqrt{3} \frac{1}{1+\lambda} (I_{2D})^{1/2}\end{aligned}\tag{5.6}$$

* Fig. 5.1 is identical with fig.6 of ref.15

The effective stress-strain relationship and Poisson's ratio were obtained empirically by the uniaxial tensile testing of the bulk adhesive (Fig.5.3), thus:

$$\begin{aligned}\bar{s} &= \sigma_t \\ \bar{e} &= \epsilon_t \\ \dot{\bar{e}} &= \dot{\epsilon}_t\end{aligned}$$

Fig. 5.1 shows a comparison between the shear stress-strain relationships obtained from the napkin-ring tests of bonded adhesive and those produced by the torsional testing of bulk tubular specimens by the described procedure. The similarity of these curves as well as previous findings [23] justify basing the effective stress-strain relationship for bonded ductile adhesives on their bulk data.

The examination of the shear test data in the light of the effective stress-strain relationship derived from the tensile test data (Fig.5.3) rests on the following relations:

$$\begin{aligned}\bar{s} &= \sqrt{3} \tau \\ \bar{s} &= \frac{\sqrt{3}}{2} \frac{1}{1+\nu} \sigma_t \\ \dot{\bar{e}} &= \frac{\sqrt{3}}{2} \frac{1}{1+\nu} \dot{\epsilon}_t\end{aligned}$$

Shear stress-strain curves obtained under different combinations of tensile-torsion loading are shown in Fig.5.4. A similar procedure, and substituting the data so obtained in eqs.(5.1) and (5.6), yields the effective stress-strain relations shown in Fig.5.3. They are in good agreement with those obtained by simple tensile tests. The small discrepancy shown at the plastic yield level is attributable to the fact that $\lambda > 1.1$ in this zone.

The experimental verification of the basic assumptions and of the analytical expressions validate the application of data obtained from tensile loading of the bulk adhesive for the derivation of empirical effective stress-strain relationships which are representative of the mechanical behavior of the bonded adhesive.

Behavior affected by the volumetric stress component ($\lambda > 1$)

Stress-strain data of a ductile structural adhesive composed of rubber-modified epoxy FM73 have shown a pronounced difference between compressive and tensile test results. The ratio between compressive and tensile stress, λ , was high at room temperature and tended to decrease to 1.0 at elevated temperatures.

Typical stress-strain relationships for bulk FM73 adhesive under tension, compression, and shear, are shown in Fig.5.5. $\bar{\sigma} = \frac{\sigma}{E_{sc}}$ derived from Fig.5.5 for $E_{sc} = E_{st}$ is plotted in Fig.5.6 as a function of $\bar{\epsilon}$. On this basis, the shear data from Fig.5.5 can be translated, through eqs.(5.3) and (5.5), into effective stress-strain relationships.

The results shown in Fig.5.6 seem to be in fair agreement with the respective effective stress-strain relationships derived from tensile test data.

The failure zone

The failure envelope of a structural adhesive material under compound stresses is expressed by eq.5.4. The results of an experimental examination of this expression are shown in Fig.5.7 for the bulk and the bonded epoxy adhesive, respectively, (at room temperature $T_f = 1.0$) and they seem to be of good agreement.

A similar representation of analytical and experimental failure envelopes for the structural adhesive FM73, is shown in Fig.5.8 as a function of the temperature level for the range of $1.0 \leq T_f \leq 1.4$. A good correlation is apparent between the test data and the expected analytical results based on the modified Von-Mises criterion, as expressed in eq.(5.4).

5.5. CONCLUSIONS

A series of tests was conducted with structural adhesives in order to examine the validity of an effective stress-strain concept for the behavior of these materials under compound stresses. The following conclusions could be drawn:

1. The mechanical behavior up to failure of ductile structural adhesives can be represented by their effective stress-strain relationship based on the Von-Mises hypothesis, suitably modified.
2. The hypothesis of (1) above takes into account the effect of volumetric stress and strain components as represented by the compressive-to-tensile stress ratio μ .
3. An analytical-empirical procedure for deriving the effective stress-strain relationship from simple uniaxial tensile tests of bulk adhesives is proposed.
4. The above procedure was verified experimentally by the test data obtained for different adhesives (21) under various combinations of shear-tension-compression loading modes.
5. Similar formulations and procedures were found to be adequate for the establishment of failure envelopes for these adhesives under the same loading conditions.

6. HYGROTHERMAL EFFECTS ON TIME-DEPENDENT CHARACTERISTICS OF
ADHESIVE MATERIALS

6.1 BACKGROUND

According to the prior assumptions, which were based on previous investigations [19-23], the bulk properties of an adhesive material may be taken to represent its characteristics as an in-situ phase within a bonded system. In Section 5 the effect of a state of stress on the stress-strain and failure characteristics of the adhesive material was discussed, the visco-elastoplastic nature of modern rubber-modified structural adhesives, such as FM73, being demonstrated.

In the present work the results of investigations on environmental effects on such time-dependent behavior will be reported.

Studies of the visco-elastic and time-dependent plastic failure characteristics of composites were conducted in the past by the present authors [1-5]. In those projects the temperature-time dependence of plastic yield and the relaxation modulus of epoxy/versamid specimens, as well as the respective matrix-dominated characteristics of glass fiber-reinforced epoxy composites were investigated.

Results, given in ref.[2], indicated the following:

- The effect of temperature on short-term yield and relaxation matrix-dominated characteristics of ductile epoxy composites and their matrix can be translated and converted to long-time behavior by shifting method.
- Relaxation behavior (in the linear visco-elastic range) is not affected by the mode of loading, whereas yield characteristics in compression are higher than their tensile counterparts.
- The relationship time-shift parameter vs. temperature, is independent of the mode of loading, and of the type and the geometry of the filament, as long as the same matrix is involved. These trends were supported recently by the work of Yoew et al. [124].

The above finding, beside its scientific, physical significance, may lead to a substantial reduction in the experimental work required for the characterization of temperature-time effects on the mechanical behavior of ductile matrix composites and similar adhesive systems.

If the above conclusions are substantiated by more comprehensive, direct long-term tests, the short-term data on an epoxy matrix under simple uniaxial tension at different temperatures will suffice or predicting the long-term behavior of different composites with the same matrix under a combined state of stress, provided RT short-term data of the respective systems are available.

More recently the effect of moisture exposure on the viscoelastic characteristics of FRP was studied [125]. Trends similar to those described above were found, which indicates that moisture effects with time can be treated in a way similar to that used for the corresponding temperature effects.

The major objectives of the present part in the research are to provide the basic hygrothermal-vs.-time characteristics of structural adhesives and to establish an efficient procedure with a view to reducing the tremendous experimental work involved.

6.2 THE EFFECT OF STRAIN RATE ON THE PLASTIC YIELD OF STRUCTURAL ADHESIVES

The effects of strain rate on the stress-strain characteristics of structural adhesives in different hygrothermal conditions were investigated in previous research work and reported in refs.[19,20,22]. The two adhesives tested are representative of the high-performance adhesives now in use in aircraft structures, namely:

FM73 - for intermediate temperatures (up to 80°C)

FM300 - for elevated temperatures (up to 130°C)

These two rubber-modified adhesives will also be the "candidates" for the present investigation.

Hence, part of the relevant previous data, which will be used at a later stage as input for interlaminar stress analysis, will be briefly reviewed here, together with the new data derived in the present research.

In the investigation mentioned above adhesive dog-bone specimens were used for tensile, and cylindrical tube specimens for compression, testing.

The fabrication and curing procedures of these specimens are given in refs.[22,23]. In wet conditions the tubular specimens were immersed in water up to almost saturation (about 2-3% moisture content) (see Fig.6.1). The modulus vs. temperature relationships which was derived for determination of glass transition temperature (T_g) for the different adhesives are shown in Fig. 6.2. The reduction in T_g due to moisture in case of FM73 specimens is evident.

Typical tensile stress-strain curves of FM73 adhesive in different hygrothermal conditions are given in Fig.6.3. Typical compressive stress-strain data of wet and dry FM73 specimens at different temperature and strain-rate levels are shown in Figs.6.4, 6.5.

In all cases the common trend is towards the reduction in modulus and yield stress with an increase in temperature and in moisture content and with a decrease in strain-rate. The effect of these variables on yield stress (σ_{yp}) is shown in Fig.4 of ref.32 for dry specimens. In all these figures the σ_{yp} relationship between yield stress and log strain-rate was found to be linear.

This linear law, which follows trends similar to those found in the past in other ductile epoxy systems [1-5], is attributable to non-newtonian flow based on a rate-process mechanism. It enables a time-temperature shifting procedure to be applied in order to provide long-term master curves for yield stress constructed from short-term data derived at different temperature levels.

Accordingly, based on Fig. 4.5 of ref.22, master curves for tensile and compressive yield stress of dry and wet FM73 specimens are given in Fig.6.6 covering almost 12 decades of strain-rate.

Moreover, the shifting parameter $\log a_T$ was found to be almost linear with temperature and independent of moisture conditions or mode of loading, as shown in Fig. 6.7. Similar trends were found for FM300K adhesives, as shown in Figs. 6.6, and 6.7.

It can be concluded that the yield-time characteristics of structural adhesives used in the present investigation follow general laws which also dictate the behavior of other ductile epoxy materials.

6.3. HYGROTHERMAL EFFECTS ON VISCO-ELASTIC CHARACTERISTICS OF STRUCTURAL ADHESIVES

6.3.1 Previous data

The visco-elastic mode of behavior most relevant to the redistribution of interlaminar stress vs. time is the relaxation modulus.

Summarized results of previous investigations are given in refs. 2, 5. The data are related to the stress relaxation of epoxy-versamid systems, whose temperature-time mode of behavior was found to be representative of other ductile polymers as well.

Three conclusions can be drawn from these results:

1. The stress-relaxation function (in the linear visco-elastic range) is nearly the same under tension, compression, and flexure, i.e. it is invariant with the mode of loading.
2. The time scale can be considerably extended on a log scale by the time-temperature shift procedure.
3. Matrix-dominated relaxation characteristics of FRP laminates which contain a ductile matrix show trends similar to the pure matrix behavior, and its time shift vs. temperature relationship is almost unaffected by composite composition (above the glassy range).

One of the objective of the present investigation is to examine the viscoelastic behavior of the two representative structural adhesives : FM73 and FM300K in light of the above findings.

6.3.2 Experimental procedure

Two types of adhesives were used, viz.: FM73 and FM300K. The specimens were prepared by lay-up of adhesive films in a closed mould composed of two thick aluminum plates.

The curing process was as follows:

- Application of 10 atm by a press.
- Heating to 120°C in 30 minutes (FM73)
- to 170°C " " " (FM300K)
- Holding at 120°C (170°C) and 10 atm for 1 hour.
- Slow cooling to room temperature.
- Release of the pressure.

The following specimens were prepared:

For tensile tests: Dog-bone shape in accordance with ASTM D638, machined from a laminate consisting of about 20 layers to achieve 3mm thickness.

For compressive tests: Cylinder of about 12mm diameter, 24mm height, machined from a thick laminate consisting of about 80 adhesive layers.

The specimens were loaded uniaxially by Instron tester to different strain levels at a constant strain rate of 5mm/min. Strain levels (ranged from $\epsilon_0 = 0.5\%$ to 2.5%). While constant strain was maintained, load vs. time was recorded up to 30 minutes. These relaxation tests were conducted at different temperatures, ranging from 20°C to 80°C in the case of FM73 and from 20°C to 150°C in that of FM300K.

Diagrams showing the relaxation modulus (stresses per unit constant strain) vs. time are given in Figs. 6.8, 6.9 for FM73 in tension and compression.

The plot of relaxation vs. time at the different temperatures is given on a log scale in Fig.6.10 in which tension data for FM73 are compared with the respective compression data. This demonstrates almost identical behavior under both tension and compression, showing it to be similar to that previously found in the case of ductile epoxy material (Ref.2).

The trends of the curves in Fig.6.8 permit a master curve for the relaxation modulus to be obtained by the shifting method. The curve - relating to FM73 - is expected to be common for tension and compression, covering a range of about 12 decades as shown in Fig.6.11. The linear relationship of log shift data vs. temperature shown in Fig.6.12 is similar to the findings for other ductile epoxies shown before.

Stress-relaxation data for FM300K adhesives in tension under different temperature levels is shown in Fig.6.13. The corresponding master curve and shift vs. temperature relationship are given in Figs.6.11 and 6.12. The trends are similar to those found for FM73 adhesive.

The relaxation modulus data given above in terms of master curves for tension and compression serve two causes: (a) They confirm one of the basic assumptions, viz. that the representative structural adhesives used in the present investigation obey time-temperature laws common to ductile polymers. (b) They provide relaxation data for long-term behavior at different temperatures, to be used as input in the following analytical study of interlaminar stresses and strain distribution, as functions of time, within the adhesive layer of loaded bonded systems.

7. THE TIME-DEPENDENT MECHANICAL BEHAVIOR OF AN INTERLAMINAR ADHESIVE LAYER WITHIN A LOADED BONDED SYSTEM

7.1 BACKGROUND

The interlaminar adhesive layer (IAL) serving as a bonding phase between structural elements may be treated as an equivalent material layer in the multi-material laminate. The particularity of the IAL, however, stems from its low stiffness and strength, its non-linear viscoplastic stress-strain-time behavior, and its sensitivity to hygrothermal effects.

The solution of IAL stress and strain distribution, which is crucial for the failure prediction of the bonded system, is highly involved due to these characteristics. Singularities stemming from geometrical edge effect, material heterogeneity, and the three-dimensional state of stress, eliminate the close-form analytical solution and lead to numerical solutions, e.g. the finite element method (FEM) [126,127]. Such methods can deal with complex geometrical and material parameters but leave the problem of material non-linearity and time-dependency still to be tackled. Most of the numerical solutions are confined to the elastic linear range [17] where they could, in certain cases, be extended to deal with a simplified elasto-plastic model [128] or with bilinear behavior [129]. Recently the problem was analyzed in the non-linear range by being referred to a bonded double model [18]. That solution was based on an empirical effective stress-strain relationship according to the Von-Mises assumption. Results permit the evaluation of IAL behavior up to the plastic range and even beyond it.

The object of the present study was the extension of that solution to the treatment of the time-dependency of the stress and strain distribution within the IAL at different viscoplastic stages.

7.2 THE BONDED MODEL

A symmetrical doubler was selected as the model to represent the complex material system typical of a bonded structure. The model consists of a central uniaxially loaded adherend layer and two external adherends bonded to the central layer by two interlaminar adhesive layers (IAL) (Fig.7.1).

The adherend materials were either aluminum 2024-T3 or unidirectional carbon-fiber-reinforced plastic (CFRP). The IALs were made of epoxy resin consisting of 70% epon 815 monomer and 30% Versamid V-140 hardener. (See section 5). For the numerical solution the adhesive layer was successively divided into 2 and 4 sub-layers so as to represent the effect of thickness on stress distribution, as shown in Fig.7.2.

7.3 THE ANALYTICAL APPROACH

The IAL stress-strain-time relationship is non-linear and cannot be adequately represented by the linear viscoelastic theory even at a moderate stress level. To tackle this problem, an empirical numerical approach was developed involving an iterative FEM related to the effective stress-strain relationship, which in turn was taken to be representative of the IAL behavior at different levels of loading and in different time intervals [18]. The

solution is based on the assumption that the material behavior of the IAL can be treated, after a modification of material parameters of the different elements, as a function of stress, strain, and time, variables. The representation of the stress and strain states by means of their respective effective values is justified, when a functional relationship exists between the effective stress (\bar{s}) and the effective strain (\bar{e}), on the one hand, and the respective stress and strain second invariants. Such a functional relation must hold good throughout the whole range of the stress-strain relationship and for any combined state of stress.

For the present study the functional relationship according to Von-Mises, Hencky and others were assumed to apply, as follows [130]

$$\bar{s} = \frac{\sqrt{2}}{2} [(\sigma_1 - \sigma_2)^2 + (\sigma_2 - \sigma_3)^2 + (\sigma_3 - \sigma_1)^2]^{1/2} \quad (7.1)$$

$$\bar{e} = \frac{\sqrt{2}}{2(1+\nu)} [(\epsilon_1 - \epsilon_2)^2 + (\epsilon_2 - \epsilon_3)^2 + (\epsilon_3 - \epsilon_1)^2]^{1/2} \quad (7.2)$$

$\bar{\nu}$ - effective Poisson's ratio, which is dependent on the strain and stress levels.

7.4 THE EMPIRICAL NUMERICAL SOLUTION

The validity of the effective stress-strain relationship of the adhesive material investigated was verified experimentally by combined torsion-tension loading tests [21] as shown in Fig.5.3.

Based on other investigations, [23] it can be assumed that, as long as the failure mode of the bonded system is cohesive and initiates within the IAL, the mechanical in-situ behavior of a bonded adhesive is represented by the corresponding bulk properties of the adhesive (See Fig.5.1). Thus, the uniaxial-tension bulk stress-strain relationship of the epoxy adhesive can provide the effective loading function for the numerical FEM solution. In this way the nonlinear relationship between effective stress (\bar{s}) and effective strain (\bar{e}) is expressed as a function of strain rate, temperature, and humidity, viz: $\bar{s} = F(\bar{e}, \dot{\bar{e}}, T, RH)$, which follows the real material behavior as determined empirically (Fig.7.3).

7.5 STRAIN RATE EFFECT

When strain-rate effect is considered, such a relationship may be expressed by the Ramberg-Osgood function [131] as expanded by McLellan [132] to represent nonlinear curves obtained empirically from loading tests at different strain-rate levels:

$$\bar{e} = \frac{\bar{s}}{c\dot{\bar{e}}^d} + a\dot{\bar{e}}^b \bar{s}^n \quad (7.3)$$

where a, b, c, d, and n are material constants derived experimentally.

The above relationship provides the basis for deriving the strain-rate effect on stress and strain distribution within the IAL. The solution takes into account the different strain-rate conditions at each IAL element under a certain external loading rate applied to the bonded model. The modified stress-strain curves under the actual strain-rate at the different IAL elements are shown in Fig.7.3. IAL stresses τ_{xzo} and σ_{zo} in the critical zone, determined when non-linearity and strain-rate effect are considered, are significantly lower than the corresponding data derived by the simplified linear elastic solution (Figs.7.4,7.5).

Varying the adhesive thickness produces two different effects: Along most of the IAL boundary zone, stresses are lower with thicker IAL as was expected, whereas in the critical zone close to the IAL edge, this trend is reversed, higher normal stresses, σ_{zo} , prevailing in the thicker IAL case (Figs.7.6,7.7).

7.6 STRESS RELAXATION

Stress relaxation data of the adhesive bulk material under uniaxial tension are shown in Fig.7.8 in terms of stress (σ) as a function of time (t) for different constant strain levels (ϵ_0). It can be seen that for a relatively short period after the initial loading stage ($t=0$), the instantaneous inertia effects - which depend on the strain and strain-rate levels - are negligible.

An attempt to assess the states of stress and strain within the IAL for a time interval Δt was made following the endochronic approach [133,134]. The solution is based on the empirical effective stress-strain relationships for different time intervals Δt_i (Fig.7.9) derived from the experimental stress-relaxation curves of Fig.7.8. The FEM solution provides an approximate estimate of the states of stresses and strains at each element after a given time interval, Δt .

The effect of time on the stress relaxation, as demonstrated by the shear, τ_{xzo} , and normal σ_{zo} stress distribution within the IAL, is shown in Figs.7.10 and 7.11. Here the trend of IAL stress reduction with time is evident.

7.7. CONCLUSIONS

The following conclusions can be drawn based on the empirical-numerical FEM solution for the stress and the strain distributions within the IAL of a bonded doubler model:

1. IAL stresses which are determined from the strain-rate dependent non-linear stress-strain behavior of the adhesive material are significantly lower than the stresses predicted on the basis of linear behavior.

2. The increase of the strain-rate was found to effect a redistribution of the IAL stress distribution by reducing the more highly strained elements as compared with those of a lower strain level.

3. The general tendency of loaded bonded systems after initial loading is towards a reduction of stresses at the critical elements, and an increase in corresponding strains with time.

4. These trends point to a possibility of the strain level limit being exceeded and the viscoplastic zone propagating with time within the critical zones of the polymeric IAL.

8. THERMOELASTIC AND HYGROELASTIC CHARACTERISTICS OF ADHESIVES AND FRP ADHERENDS, CONSTITUENTS OF THE BONDED SYSTEM

8.1 BACKGROUND

During the fabrication process and in service exposure the bonded system is subjected to fluctuations temperature and moisture. These hygro-thermal environmental changes induce elastic stresses and strains in the different constituents of the bonded system, viz., the adhesive layer and the FRP adherends.

The resulting residual stresses may affect the mechanical behavior or possibly lead to the failure of the system even before, or without, the application of any external mechanical loading.

Recent information on these effects and available data on the coefficient of thermal expansion (CTE) and hygroelastic coefficients (HEC) of different FRP materials are surveyed in section 3.3 (refs.24-26, 52-64). Some findings on the hygroelastic behavior and the HEC of structural adhesives are also found in ref.[135]. It was found that the available information is characterized by high scatter and inconsistency. This is attributable mainly to the fact that most investigations did not consider the dependence of the CTE on moisture content and that of the HEC (which was rarely derived) on the temperature level.

In the present part of the research project it is intended to investigate these dependences by measuring CTE of dry and of moist specimens, and similarly the HEC at different temperature levels.

8.2 TEST PROCEDURE

8.2.1 Specimens

The tests for deriving thermoelastic and hygroelastic characteristics were conducted on two adhesive materials, FM73 and FM300K, and four CFRP 5208/T300 configurations, namely -

| | |
|-----------------------------------|----------|
| Longitudinal U.D. specimens | (0°) |
| Transverse U.D. specimens | (90°) |
| Cross-ply Bidirectional specimens | (0°/90°) |
| Angle-ply Bidirectional specimens | (±45°) |

The adhesive specimens were cut from laminates, the preparation of which is described in Section 6.3.2

The CFRP specimens were cut from laminates prepared by lay-up of prepreg layers and autoclave curing following the producer's instructions (Narmco). The laminates were prepared at the Material Process Engineering Department of Israel Aircraft Industry.

Specimens of unidirectional CFRP configurations (0° and 90°) consisted of 24 layers; their dimensions were 140x10x3mm.

Specimens of angle-ply configurations (0/90° and ±45°) consisted of 8 layers, and their dimensions were 140x10x1mm. The approximate dimensions of adhesive specimens were 140x10x3mm.

8.2.2 Environmental history

Three different test cycles were conducted, constituting environmental histories as follows:

(figs.8.1, 8.2)

Stage a: Drying of specimens at 110°C for 3 days and keeping them in vacuum

Stage b: Heating and cooling of dry specimens between 23°C and 90°C (for deriving the CTE of dry specimens).

Stage c: Exposing the dry specimens to high humidity at 23°C.

Stage d: Immersion of the specimens in warm water at 36°C for several weeks (for deriving the HEC at intermediate temperature).

Stage e: Heating the water from 36°C to 70°C,

Stage f: Immersion in hot (70°C) water at constant temperature for several weeks (for deriving the HEC at elevated temperature)

Stage g: Cooling and heating the water bath (between 70°C and 36°C) (for deriving the CTE of saturated specimens).

The first cycle (I) consisted of all the above stages (fig.8.1) whereas Cycles II and III consisted of stages a,b,d, and a,b,f,g, Cycles II and III respectively, (fig.8.2) differ from cycle I by the fact that the specimens are exposed to warm and hot water directly from dry state, without any intermediate heating and wetting stages.

8.2.3 Test procedure

The different specimens formed two identical sets. One set was designated for the measurement of deformational changes, whereas the other was for determining weight changes.

Deformational changes were measured by means of a special device (fig.8.3) which consisted of an aluminum bench to which a dial gauge had been attached (accuracy of about 10^{-4} inch). The aluminum device was calibrated by means of metallic and quartz control specimens of known CTE. After drying, specimens were placed on the aluminum bench and zero reading was taken. Following each change in environmental conditions, readings were taken every few hours, and later once or twice per day. Weights were recorded simultaneously with deformational changes, an analytic balance with an accuracy of 10^{-5} gr, being employed. Specimens for both deformation and weight change measurements were stored in an "Areus"-type oven, which permitted the temperature to be accurately controlled and readings to be made through its glass window.

8.3 TEST RESULTS

Detailed representative data on hygroelastic and thermoelastic strains and on absorption values as functions of exposure time during cycles I, II, and III are given in Appendix 1, 2, and 3 respectively. Relative weight

changes ($w = \frac{\Delta W}{W_0}$), moisture content, and hygrothermoelastic strain changes (ϵ),

as functions of exposure time in cycle I are shown in fig.8.4, for longitudinal and transverse FRP specimens. The trends are as follows: Simultaneous increases of deformation and of absorption with time, and increase in the rate of change with increasing temperatures. Whereas the absorptions of longitudinal and of transverse specimens are almost the same, the deformation of the longitudinal specimen is almost negligible compared with its transverse counterpart.

Similar trends, but with significantly higher deformations and absorption rates, were found for both adhesives (fig.8.5).

The effect of temperature on the absorption process and the resulting swelling of all tested systems is demonstrated by comparisons with the behaviors in cycle II (exposure to warm water) and in cycle III (exposure to hot water) - figs.8.6 to 8.9).

In the transverse specimens (thickness 3mm) absorption during immersion in warm water for 4 weeks reaches about half the absorption level attained in hot water during a similar period. The swelling in hot water, too, is more than double that in the corresponding warm water exposure (fig.8.6 vs. 8.8). A much smaller difference between absorptions at different temperatures was found in the case of 0/90° and ±45° specimens (thickness 1mm) (fig.8.7 vs fig.8.9). This distinction between the two types of specimens is attributable to a thickness effect. In thin specimens the absorption approached the saturation limit in a relatively short period even in warm water. In thick specimens saturation will be reached only after much longer periods in warm water, but the process can be shortened by heating the water. In hot water, similar levels of absorption were found in thick transverse specimens (fig.8.8) and thin cross-ply specimens (fig.8.9). A comparison of characteristics indicates much lower deformation, by an order of magnitude, of the angle-ply and cross-ply specimens compared with their transverse counterparts, in all cases.

A peculiar tendency, to a slight decrease in swelling after prolonged hot water exposure, was observed in angle-ply and cross-ply specimens (fig.8.9). This is attributable to an interlaminar matrix stress relaxation process, as will be explained later. Adhesive materials show similar trends as functions of time and temperature with significantly higher levels of absorption and swelling (figs.8.6,8.8) than in their composite counterparts. FM73 specimens appeared to have lost their stiffness after a week's exposure to hot water. This was reflected by the inconsistency of deformational changes after the period mentioned, whereas the absorption process continued normally. Hence, data for FM73 above this level were not analyzed (figs.8.5,8.8).

8.4 DISCUSSING TEST RESULTS

8.4.1 Unidirectional CFRP Specimens

The relationships between thermal strains and temperature in transverse specimens exposed to dry and wet conditions during the different environmental cycles are shown in fig.8.10. A linear relationship was found to exist in all cases, at any rate within the temperature range investigated in the present series of tests, 23° - 90°. A slightly higher CTE was found in wet specimens.

The relationship between swelling strains and moisture content at different temperatures of water exposure are shown in fig.8.11 for the cycles involved.

Similar linear trends characterize all cases above absorption levels of $w=0.1-0.2\%$. Clear linearity was found in cases of hot water exposure in cycle III. The HEC was found to increase significantly with temperature.

Deformations of longitudinal specimens as a result of temperature changes as well as in the course of absorption were relatively very small and were moreover characterized by high scatter. Based on data available from different sources (see ref.53, and table 4.1), it is reasonable to assume that the CTE and the HEC for longitudinal specimens are almost zero for most practical purposes ($B_1 = \alpha_1 \approx 0$). That value will therefore be used for the theoretical prediction of laminate HT characteristics in table 8.1.

8.4.2 Bidirectional CFRP specimens

Thermoelastic deformations of cross-ply specimens were found to be significantly smaller than those of their transverse counterparts (fig.8.12). The relationships between deformation and temperature under dry and wet conditions were found to be closely similar.

The behavior of angle-ply specimens ($\pm 45^\circ$) in heating-cooling cycles was similar to that of the cross-ply specimens, but with higher scatter, which did not permit its CTE to be accurately derived.

The relationship between swelling and moisture content in cross-ply specimens was found to be linear and to show very similar trends at different temperature levels (fig.8.13). HEC values were much lower than those of their U.D. transverse counterparts and are still further reduced at higher temperatures. In both cases, swelling is seen to level off above 1.2% of moisture content which seems to be close to the saturation limit. This effect was particularly pronounced in the case of hot water exposure, a finding that may also be explained by the viscoelastic effect, which acts to relax the hygroelastic stresses in the matrix. This process, which is enhanced in hot humid conditions, may compensate for the swelling deformations, especially after prolonged hot water exposure, when the absorption-swelling mechanism tends to level off.

In the case of angle-ply ($\pm 45^\circ$) specimens, a similar linearity in the swelling absorption relationship was found during warm water (36°) exposure (Cycle III) (see fig.8.9), obscures the hygroelastic relationship at this stage. However, after prolonged hot-water exposure, a similar trend of leveling-off and even slight reduction in swelling was observed, similar to the case of cross-ply specimens.

Results of the experimentally derived CTE (α) and HEC (β) in all cases are given in table 8.1.

The α and β values for angle-ply and cross-ply specimens were calculated from the available data on U.D. specimens and based on classical HT laminate theory (refs.53,55,66). Fair agreement between experimental and computed values is evident from table 8.1

8.4.3 Structural adhesives

A linear relationship between strain and temperature was found to exist in both adhesives under wet and dry conditions (fig.8.14), whereas CTE values for FM73 were found to be higher than for FM300K (table 8.1). Wet specimens were characterized by higher CTE values.

The relationship between swelling and moisture content is much more complicated (fig.8.15).

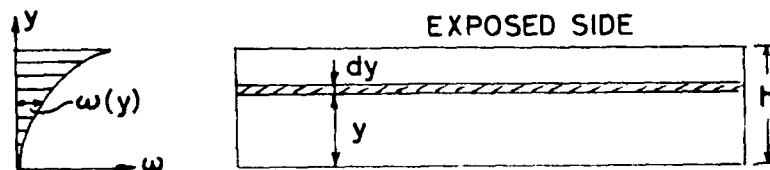
In all cases three stages may be distinguished: a slow rate of swelling up to about 0.2% of moisture, followed by a linear relationship up to about $\omega = 1.5\%$. In the case of exposure to hot water a tendency to a decrease in the swelling rate vs. moisture absorption was found as the moisture content approached saturation.

The HEC values were derived from the linear portion of the curves. These portions cover the practical range for service exposure (0.2% ω to 2.0%). β was found to be higher in FM300K adhesive than in FM73. Exposure to higher temperatures was found to increase HEC values (table 8.1)

8.5 INVARIANCE OF THE HYGROELASTIC COEFFICIENT (HEC) WITH MOISTURE HISTORY AND PROFILE

In previous studies (ref.24) and other publications on the hygro-elastic behavior of polymers and polymeric composites, the swelling and shrinkage deformations were found to be linearly related to the amount of moisture absorbed or desorbed during most of the absorption or drying processes. The HEC, β , which was defined as the HE deformation per unit moisture absorbed was found to be constant at constant temperatures, independent of humidity, environmental history, and specimen thickness. This is somewhat unexpected considering the variations in moisture distribution throughout the specimens during the absorption process, which is strongly dependent on external humidity, exposure time and specimen geometry.

The following simple analysis aims to verify these experimental findings, analytically based on the classical lamination approach. Let us assume a general moisture profile $\omega(y) = f(y)$ as illustrated below:



Other assumptions are:

- Planes remain planes following HT deformations;
- HEC, β , is constant for thin sublayers (dy);
- The state of stressing is assumed to be uniaxial;
- Macro-homogeneous material is involved, having constant stiffness and β throughout the thickness;
- Stress-absorption coupling is negligible.

Hence:

$$\epsilon_x(y) = \omega(y)\beta - \frac{\sigma_x(y)}{E} \quad \text{for any sublayer}$$

By integration and applying equilibrium conditions:

$$\frac{1}{E} \int_0^h \sigma_x(y) dy = \int_0^h \omega(y)\beta dy - \int_0^h \epsilon_x(y) dy = 0$$

Hence:

$$\frac{1}{h} \int_0^h \omega(y)\beta dy = \frac{1}{h} \int_0^h \epsilon_x(y) dy$$

where:

$$\frac{1}{h} \int_0^h \omega(y) dy = \bar{\omega} \quad - \quad \text{average moisture content}$$

and

$$\frac{1}{h} \int_0^h \epsilon_x(y) dy = \bar{\epsilon} \quad - \quad \text{average hygroelastic axial strain}$$

Hence $\epsilon = \beta \bar{\omega}$ for the laminate as a whole.

It can thus be concluded that HE strains are linear functions of the average amount of absorbed water, and β is independent of all factors liable to affect moisture distribution throughout the thickness.

8.6 CONCLUSIONS

The following conclusions can be drawn from the experimental results and analytical considerations regarding the hygro-thermoelastic behavior of the constituents of bonded systems;

1. Thermoelastic strains are linear functions of temperature in the case of macro-homogeneous U.D. composites adhesives within the temperature range, 23°-90°C.
2. CTE values are only slightly affected by moisture content, and they attain their highest values in unfilled polymeric adhesives, while in longitudinal U.D. composites they approach close to zero.
3. Bidirectional composites are characterized by significantly lower CTE values than their transverse U.D. counterparts, as predicted by analysis.

4. Hygroelastic strains above a certain level are linearly related to the average amount of absorbed water and independent of the level of external humidity, the specimen's environmental history or its thickness, all of which may affect internal moisture distribution.

5. HEC, β , is relatively high in unfilled polymeric adhesives and almost zero in U.D. longitudinal specimens. It is significantly lower in bidirectional CFRP specimens than in their U.D. transverse counterparts, as predicted by HE analysis. This conclusion is basically common to both HEC and CTE parameters, indicating the strong interdependence of thermoelastic and hygroelastic behavior.

6. In bidirectional CFRP composites, swelling deformations close to saturation seem to level off with increasing absorption. This phenomenon which was not found in U.D. specimens, is more pronounced in hot water exposure. It is attributable to an interlaminar stress-relaxation effect, which becomes more active than swelling process in this range of moisture absorption.

9. SUMMARY AND CONCLUSIONS

The present report covers the results of the first year's research on the durability of bonded systems. Three major topics were dealt with:

Nonlinear behavior of the adhesive systems under a combined state of stress, the time dependency of their mechanical behavior, and the effect of hygrothermal conditions on the adhesive and the adherend phases.

The first section of the present report shows the connection between previous investigations on this topic as recorded in the literature, briefly surveys them, and draws conclusions which provide the basic assumptions for the present study.

The second section describes an attempt to generalize the effective stress-strain concept for nonlinear structural adhesives, which will enable the time-dependency and hygrothermal effects to be included. This was examined in the light of experimental evidence.

The third section contains a numerical example for solving the time-dependent stress relaxation behavior of an adhesively bonded metal, and presents an empirical methodology for deriving the viscoelastic input characteristics as functions of time and temperature.

The fourth section is concerned with the thermoelastic and hygroelastic characteristics of the constituents of bonded systems, namely structural adhesives and FRP adherends. The interdependence between the coefficient of thermal expansion and (CTE) hygroelastic coefficients (HEC) on the one hand and temperature and moisture content on the other, was investigated.

The following general conclusions may be drawn:

1. The structural adhesives used in the present research (FM73, FM300K) follow the general laws that dictate the behavior of ductile polymers as a function of stress, time, and temperature.
2. A simplified approximation for the experimental characterization of such structural adhesives can be based on testing representative bulk specimens under an uniaxial state of stress for short times at different temperature levels. This can, with good approximation, be extrapolated to the behavior of the same adhesive in its bonded state under multi-axial stressing for much longer periods.
3. The time-dependent mechanical behavior of the bonded system under mechanical loads can be predicted by a numerical nonlinear iterative FEM procedure, provided the stress-strain-time characteristics of the adhesive as indicated above are available. Differences in hygrothermoelastic characteristics of the FRP adherends layers induce additional stresses within them and interlaminar stress in the adhesives.

4. The temperature and moisture content have same effect on hygrothermal characteristics: The CTE of wet specimens is higher than its dry counterpart, the HEC at elevated temperatures seems to be higher than under moderate conditions.
5. The hygrothermal time-dependent behavior of multiple FRP laminates seems to be different from that of adhesives and U.D. plies. The overall deformational behavior vs. moisture content as a function of exposure time seems to be affected by the relaxation of the hygrothermal (HT) stresses induced in this case. This effect is enhanced at elevated temperatures by the action of moisture with time.

10. FUTURE RESEARCH

The second year of the present research will concentrate on the HT behavior of a bonded system composed of FRP or metal layers bonded by structural adhesives.

The following topics will be investigated;

- a. The stresses in, and deformational behavior of, the bonded system following cooling down during the curing stage.
- b. The hygrothermoelastic behavior of the system when subsequently exposed to thermal fluctuations of moisture absorption.
- c. The effect of HT exposure on the mechanical behavior of the bonded system under load.

The emphasis throughout the above experimental and analytical study will be on the behavior of the interlaminar adhesive layer under hygrothermal-mechanical interactions.

LITERATURE CITED

1. O. Ishai, "The effect of temperature on the delayed yield and failure of 'plasticized' epoxy resin", Polymer Engineering and Science, 9, No.2, 131-140 (1969).
2. A.E. Moehlenpah, O. Ishai, and A.T. De Benedetto, "The effect of time and temperature on the mechanical behavior of a 'plasticized' epoxy resin under different loading modes", J. of Applied Polymer Science, 13, 1231-1245 (1969).
3. O. Ishai, A.E. Moehlenpah, and A. Preis, "Yield and failure of glass-epoxy composites" ASCE J. of Engineering Mechanics Division, 96, No. EM5, 739-752 (1970).
4. O. Ishai, "Failure of unidirectional composites in tension", ASCE J. of the Engineering Mechanics Division, 97, No. EM2, 205-222 (1971).
5. A.E. Moehlenpah, O. Ishai, and A.T. Di Benedetto, "The effect of time and temperature on the mechanical behavior of epoxy composites", Polymer Eng. and Sci., 11, No. 2, 128-138 (1971).
6. O. Ishai, and A. Mazor, "The effect of environmental-loading history on longitudinal strength of glass-fiber reinforced plastics". Rheologica Acta, V.13, No.3, 381-394 (1974).
7. O. Ishai, "Environmental effects on deformation, strength and degradation of unidirectional GRP laminates", J. of Polymer Engineering and Science (in two parts), 15, No.7, 486-499 (1975).
8. O. Ishai, and A. Mazor, "The effect of environmental-loading history on the transverse strength of GRP laminate", J. of Composite Materials, 9, 370-379 (1975).
9. O. Ishai, and U. Arnon, "The effect of hygrothermal history on residual strength of glass-fiber reinforced plastic laminates", ASTM Journal of Testing and Evaluation, 5, 320-326 (1977).
10. S. Gazit, and O. Ishai, "Hygroelastic behavior of GRP exposed to different relative humidity levels", Proc. of Conference on "Environmental degradation of engineering materials", Virginia Polytechnic Inst., Blacksburg, VA, U.S.A., 383-392 (1977).
11. M. Meron, Y. Bar Cohen, and O. Ishai, "Nondestructive evaluation of strength degradation in glass-reinforced plastics due to environmental effects", ASTM J. of Testing and Evaluation, V5, 394-396 (1977).
12. O. Ishai, and U. Arnon, "Instantaneous Effect of Internal Moisture Conditions on Strength of GFRP", Advanced Composite Material - Environmental Effects, ASTM, STP 658, 267-276 (1978).
13. O. Ishai, D. Peretz, and N. Galili, "Mechanical behavior of multimaterial composite system - Interlaminar behavior", Final Technical Report for the year 1974, sponsored by the European Research Office, U.S. Army, Contract No. DAJA-74-G-2531, 87 (1975).

14. O. Ishai, D. Peretz, and S. Gali, "Mechanical behavior of multimaterial composite system - interlaminar behavior", Final Technical Report for the second research year, sponsored by the European Research Office, U.S. Army, Contract No. DAJA-37-75-C-1890, 94 pp (1976).
15. O. Ishai, D. Peretz, and S. Gali, "Mechanical behavior of multimaterial composite system - Interlaminar behavior", Final Technical Report for the third research year, sponsored by the European Research Office, U.S. Army, Contr. No. DAERO-76-G-062, 66 pp (1977).
16. O. Ishai, D. Peretz, and S. Gali, "Direct determination of interlaminar stresses in polymeric adhesive layer", Journal of the Society for Experimental Stress Analysis, 265-270 (1977).
17. O. Ishai, and S. Gali, "Two-dimensional interlaminar stress distribution within the adhesive layer of a symmetrical double model", J. of Adhesion, 8, 301 (1977).
18. S. Gali, and O. Ishai, "Interlaminar stress distribution within an adhesive layer in the non-linear range", J. of Adhesion, 9, 253-266 (1978).
19. O. Ishai, and G. Dolev, "Mechanical characteristics of structural adhesives", Technical report for the first research year sponsored by Israel Defence Ministry, Contract No. 953/1164, MML-65, 106 (1979). (in Hebrew)
20. O. Ishai, and G. Dolev, "Mechanical characteristics of structural adhesives", Technical report for the second year, MML-68, 93 (1980) (in Hebrew).
21. D. Peretz, and O. Ishai, "Mechanical characterization of an adhesive layer in-situ under combined load", J. of Adhesion 10, 317-320 (1980).
22. O. Ishai, and G. Dolev, "Mechanical characterization of bonded and bulk adhesive specimens as affected by temperature and moisture", Proc. of the 26th SAMPE Symposium, April (1981).
23. G. Dolev, and O. Ishai, "Mechanical characterization of adhesive layer in-situ and as a bulk material", to be published in the J. of Adhesion (1981).
24. S. Gazit, "Dimensional changes in glass filled epoxy resin as a result of absorption of atmospheric moisture", J. of Applied Polymer Science 22, pp 3547-3556 (1976).
25. F.M. Crossman, and D.L. Flaggs, "Dimensional stability of composite laminates during environmental exposure", SAMPE Journal 15, No. 4, pp 15-20 (1979).
26. C.H. Shen and G.S. Springer, "Moisture absorption and desorption of composite materials", J. Composite Materials 10, pp 2-20 (1975).
27. A.C. Loos, and G.S. Springer et al., "Moisture absorption of polyester-E glass composites", J. of Composite Materials 14, pp 142-153 (1980)

28. W. Althof, "The diffusion of water vapour in humid air into the bond-line of adhesively bonded metal-joint" Proceed. of the 11th SAMPE Technical Conference, (Nov. 1979).
29. E.R. Long, "Moisture diffusion parameter characteristics for epoxy composite and neat resins", NASA Technical Paper 1474 (1979).
30. P.E. Sandorff, and Y.A. Tajima, "The experimental determination of moisture distribution in carbon/epoxy laminates", Composites J. 10, pp 37-38 (1979).
31. P.E. Sandorff, and Y.A. Tajima, "A practical method for determining moisture distribution, solubility and diffusivity in composite laminates", SAMPE Quarterly 10, No. 2, pp 21-28, (1979).
32. W. Althof, and W. Brockman, "New test methods for the prediction of environmental resistance of adhesive bonded joints", SAMPE, 21 (1976).
33. W. Althof et al., "Environmental effects on the elastic-plastic properties of adhesives in bonded metal joints", Royal Aircraft Establishment, Library Translation 1999, (Jan 1979).
34. N.J. De Lollis, "Durability of structural adhesive bonds: A Review", Adhesive Age, p 41, (Sept. 1977).
35. R.F. Wegman et al., "A new technique for assessing the durability of structural adhesives", SAMPE Journal 14, No. 1, p 20 (1976).
36. G.J. Almer, and A.V. Pocius, "Physical properties of aerospace structural adhesives displaying resistance to open time in high humidity", 12th National SAMPE Technical Conference, pp 924-934 (1979).
37. N.J. Delollis, "Adhesives for metals", Industrial Press Inc. pp 10-29, N.Y. (1970).
38. Kaelble et al., "Interfacial bonding and environmental stability of polymer matrix composites", J. of Adhesion 6, p 23 (1974).
39. Kaelble et al., "Interfacial mechanism of moisture degradation in graphite-epoxy composites", J. of Adhesion 7, p 25 (1974).
40. J.L. Gordon, "Variables and interpretation of some destructive cohesion and adhesion tests", Treatise on Adhesion and Adhesives", 1, pp 319-322 (1973).
41. A.F. Lewis, and R.T. Natarajan, "System approach to permanence and endurance of adhesive joints", Annual SAMPE Conference, p 520 (1974).
42. R.L. Patrick, "The use of scanning electron microscope, from "Treatise on Adhesion and Adhesives" 3, pp 163-228 (1973).
43. S. Orman, and C. Kerr, "The effect of water on aluminum epoxide bonds" from "Aspect of Adhesion" 6, pp 64-79, Editor J.D. Almer, University of London Press (1969).

44. D.M. Brewis et al., "The durability of some epoxide adhesive bonded joints on exposure to moist warm air", International J. of Adhesion and Adhesives 1, No.1, pp 35-39 (1980).
45. A.W. Bethune, "Durability of bonded aluminum structures", SAMPE Journal 4, July-Sept. (1975).
46. J.E. Lohr, "Factors affecting the survivability of stressed bonds in adverse environments", 18th SAMPE Symposium, p 386 (1973).
47. S. Mostovoy and E.J. Ripling, "Influence of water on stress corrosion cracking of epoxy bonds", J. of Applied Polymer Science, 13, pp 1083-1111 (1969).
48. S. Mostovoy et al., "Fracture toughness of adhesive joints", J. of Adhesion 3, p 125 (1971).
49. S. Mostovoy et al., "Stress corrosion cracking of adhesive joints", J. of Adhesion 3, p 145 (1971).
50. D.F. Adams, "Temperature and moisture induced stresses at the fiber/matrix interface in various composite materials", 24th SAMPE Symposium 24, pp 1458-1469 (1979).
51. A.K. Miller, and D.F. Adams, "Inelastic element analysis of a heterogeneous medium exhibiting temperature and moisture dependent material properties", Fibre Science and Technology 13, pp 135-153 (1980).
52. S.W. Tsai, and H.T. Hahn, "Composite materials workbook", Technical Report AFML-TR-77-33 (1977).
53. S.W. Tsai, and H.T. Hahn, "Introduction to composite materials", Technomic Publishing Co., pp 329-378 (1980).
54. J.C. Halpin, and N.J. Pagano, "Consequences of environmentally induced dilation in solids", Technical Report AFML TR-68-395 (1969).
55. J.E. Ashton, J.C. Halpin, and P.H. Petit, "Primer on composite materials: analysis, Technomic, Public. 10, pp 88-91 (1969).
56. R.A. Schapery, "Thermal expansion coefficients of composite materials based on energy principles", J. Composite Materials 2, pp 380-404 (1968).
57. B.W. Rosch, and Z. Hashin, "Effective thermal coefficients and specific heats of composite materials", In J. Engng.Sci. 8, pp 157-173 (1970).
58. A.A. Fahmy, and N. Ragai, "Thermal expansion of graphite-epoxy composites", J. of Applied Physics 41, pp 5112-5115 (1970).
59. G. Marom, and B. Gershon, "Interfacial bonding and thermal expansion of fibre-reinforced composites", J. Adhesion 7, pp 195-201 (1975).
60. K.F. Rogers et al., "The thermal expansion of carbon fibre-reinforced plastics", J. of Materials Science 12, pp 718-734 (1977).

61. Takashi Ishikawa, "Thermal expansion coefficients of unidirectional composites", J. of Composite Materials, 12, pp 153-166 (1978).
62. J.R. Strife, and K.M. Prew, "The thermal expansion behavior of unidirectional and bidirectional Kevlar/Epoxy composites", J. of Composite Materials, 13, pp 264-277 (1979).
63. M. Dootson et al., "Time and temperature-dependent effects in the thermal expansion characteristics of carbon fibre-reinforced plastics", Composite, 11, pp 73-78 (1980).
64. A.K. Miller, "Thermal expansion coefficients for laminates obtained from invariant lamina properties", Fibre Science and Technology Journal 13, pp 397-409 (1980).
65. S.W. Tsai, and N.J. Pagano, "Invariant properties of composite materials" in "composite materials workshop" (Ed. S.W. Tsai, J.C. Halpin and N.J. Pagano), Technomic Publishing Co., Inc., pp 233-253 (1968).
66. R.M. Jones, "Mechanics of composite materials", McGraw-Hill Book Company, New York (1975).
67. J. Hertz, "Moisture effects on spacecraft structures", Proceedings of 24th National SAMPE Symposium, 24, pp 965-978 (1979).
68. R.L. Kirlin, and G.E. Pyncheon, "Dimensional stability investigation graphite/epoxy truss structure", Proceeding os 24th National SAMPE Symposium 24, pp 1356-1371 (1979).
69. B.K. Gruenwald, and M. Schneerman, "Development work on optical bench structure with high thermal stability", Proceeding of 24th National SAMPE Symposium 24, pp 1332-1342 (1979)..
70. H.T. Hahn, and S.W. Tsai, "On the behavior of composite laminates after initial failure", J. of Composite Material 8, pp 288-303 (1974).
71. B.D. Agarwal, and L.J. Broutman, "Analysis and performance of fiber composites", John Wiley & Sons, pp 183-191 (1978).
72. H.T. Hahn, and N.J. Pagano, "Curing stresses in composite laminate", J. of Composite Materials 9, pp 91-106 (1975).
73. I.M. Daniel, and T. Liber, "Lamination residual strains and stresses in hybrid laminates", ASTM STP 617, pp 330-343 (1977).
74. D.R. Doner, and R.C. Novac, "Structural behavior of laminated graphite filament composites", 24th Annual Tech. Conf. SPI paper 2-D (1969).
75. A. Molcho, and O. Ishai, "Thermal cracking of CFRP laminates", Proceed. of the 10th National SAMPE Technical Conference, pp 255-262 (1978).
76. H.T. Hahn, "Residual stresses in polymer matrix composite laminates", J. of Composite Materials 10, pp 266-278 (1976).

77. N.J. Pagano, and H.T. Hahn, "Evaluation of composite curing stresses", Composite Materials, Testing and Design, ASTM STP 617, pp 317-329 (1977).
78. R.Y. Kim, and H.T. Hahn, "Effect of curing stresses on the first ply-failure in composite laminates" J. of Composite Materials 11, pp 2-16 (1979).
79. B.L. Lee, R.W. Lewis and R.E. Sacher, "Environmental effects on the mechanical properties of glass fiber-epoxy resin composites", Technical Report of the Army Material & Mechanics Research Center, AMMRC TR 78-18, April (1978).
80. D.H. Kaeble, and P.J. Dynes, "Moisture diffusion analysis for composite microdamage" 24th National SAMPE Symposium, 24, pp 351-363 (1979).
81. C.C. Chamis, R.F. Lark and J.H. Sinclair, "An integrated theory for predicting the hydrothermomechanical response of advanced composite structural components", NASA TM-73812, Sept. (1977).
82. C.C. Chamis, R.F. Lark and J.H. Sinclair, "Effects of moisture profiles and laminate configuration on the hygro stress in advanced composites", Proceed of 10th SAMPE Technical Conference, pp 684-700 (1978).
83. O. Ishai, U. Arnon and A. Molcho, "Environmental effects on mechanical performance of structural GRP laminate", Final Technical Report, Israel Council for Research and Development (1976).
84. J.L. Christian, W.E. Witzell and B.A. Stein, "Environmental effects on advanced composite materials", American Society for Testing and Materials, Proceed. of 78 Annual Meeting, STP 602 (1975).
85. J.R. Vinson, "Advanced composite materials - environmental effects", American Society for Testing and Material, Proceed. of Conference, Sponsored by Committee D-30, STP 658 (1977).
86. H.W. Bergmann, and C.W. Dill, "Effect of absorbed moisture on strength and stiffness properties of graphite-epoxy composites", Proceed. of 8th National SAMPE Conference, 8, pp 244-256 (1976).
87. J.V. Gauchel, and H.C. Nash, "The effect of long-term water immersion on the fracture toughness, strength and modulus of graphite-epoxy composites", Proceed, of the 21st National SAMPE Symposium, pp 948-957 (1976).
88. C.H. Shen, and G.S. Springer, "Effects of moisture and temperature on the tensile strength of composite materials", J. Composite Materials 11, pp 2-16 (1977).
89. G.L. Roderick, R.A. Everett, and J.A. Crews, "Cyclic debonding of uni-directional composite bonded to aluminum sheet for constant amplitude loading, NASA-TND-8126 (1976).
90. A.H. Nayfeh, and S.R. Baker, "Thermoelastic distortion of composite panels Fiber Science and Technology, 10, pp 139-149 (1977).

91. S. Timoshenko, "Analysis of bi-metal thermostats", J. of Strain Analysis 11, pp 233-255 (1923).
92. P.B. Grimado, "Interlaminar thermoelastic stresses in layered beams", J. of Thermal Stresses 1, pp 75-86 (1978).
93. L.J. Hart-Smith, "Adhesive bonded double-lap joints", NASA-CR-112235 (1973).
94. P.K. Sinha, and M.N. Reddy, "Thermal analysis of composite bonded joints", Fiber Science and Technology 9, pp 153-159 (1976).
95. D. Peretz, "Interlaminar behavior of bonded bimaterial systems", Composites, pp 153-156 (1977).
96. A.S.D. Wang, and F.W. Crossman, "Some new results on edge effects in symmetric composite laminates", J. of Composite Materials 11, pp 92-106 (1977).
97. A.S.D. Wang, and F.W. Crossman, "Edge effects on thermally induced stresses in composite laminates", J. of Composite Materials 11, pp 300-312 (1977).
98. T.A. Weishaar, and R. Gracia, "Analysis of graphite/polyamide rail shear specimens subjected to mechanical and thermal loading", NASA-CR-3106, March (1979).
99. Y. Weitzman, "Interfacial stresses in viscoelastic adhesive-layers due to moisture sorption", Int. J. Solids Structures 15, pp 701-713 (1979).
100. R.B. Pipes, J.P. Vinson and T.W. Chou, "On the hygrothermal response of laminated composite system", J. Composite Materials 10, pp 129-148 (1976).
101. G.C. Sih, and M.T. Shih, "Hygrothermal stress in a plate subjected to antisymmetric time-dependent moisture and temperature boundary conditions, J. of Thermal Stresses 3, pp 321-340 (1980).
102. J.D. Minfold, "Durability of adhesive bonded aluminum joints from treatise on adhesion and adhesives", Editor, R.L. Patrick, Marcel Dekker Inc. N.Y., pp 79-120 (1973).
103. J.D. Minfold, "Effect of surface preparation on adhesive bonding of aluminum" Adhesive Age, p 24 (July 1974).
104. R.A. Garrett, R.E. Bohlmann, and E.A. Derby, "Analysis and test of graphite/epoxy sandwich panel to internal pressure resulting from absorbed moisture", Presented at ASTM Conf. on "Environmental effects on advanced composite materials", STP 658 pp 234-253 (1977).
105. R.V. Wolf, "Effects of moisture upon mean strength of composite to metal adhesively bonded joint elements", Proceed of SAMPE Symp. 22, p 183 (1977).
106. R.V. Wolf, "Moisture/temperature effects upon mean strength of composite to metal adhesively bonded joint elements", Proceed. of 10th SAMPE Conf. pp 108-123 (1978).

107. B.M. Parker, "The effect of hot-humid conditions on adhesive bonded CFRP-CFRP joints", Symposium: "Jointing in fibre reinforced plastics", Proceedings, IPC, Science and Technology Press, pp 95-103 (1978).
108. E. Lohr, "Factors affecting the survivability of stresses bonded in adverse environments, 18th National SAMPE Symposium, p 418 (April 1973).
109. R.A. Gledhill, A.J. Kinloch, and S.J. Shaw, "A model for predicting joint durability", J. Adhesion 11, pp 3-15 (1980).
110. Primary adhesively bonded structure technology (PABST), Design Handbook for Adhesive Bonding Douglas Aircraft Company, AFFDL-TR-79-3129 Final Report, November (1979).
111. PABST "Industry review, primary adhesively bonded structure technology, Douglas Aircraft Company, Book 2 of 3, pp 207-232, Sept. (1977).
112. PABST, "Industry review primary adhesively bonded structure technology", Douglas Aircraft Company, Book 3 of 3, pp 165-181, Sept. (1977).
113. M. Goland, and E. Reissner, "The stresses in cemented joints", J. of Applied Mechanics 11, pp A17-A27 (1944).
114. O. Volkersen, Construction Metallianne, 4, pp 3-13 (1965).
115. J.W. Renton, and J.R. Vinson, "Analysis of adhesively bonded joints between panels of composite materials", J. Appl. Mechanics, 44, pp 101-106 (1977).
116. A.K. Miller, and D.F. Adams, "Advanced composite materials environmental effects", ASTM STP 658 J.R.Vinson Editor, pp 121-142 (1978).
117. R.D. Adams, and J.J. Coppedale, "The stress-strain behavior of axially-loaded butt joint", J. Adhesion 10, pp 49-62 (1979).
118. R.D. Adams, and N.A. Peppiatt, and J.J. Coppedale, "Prediction of strength of joints between composite materials", Symposium of Jointing in FRP IPC Science and Technology Press, pp 64-78 (1978).
119. N.W. Tschoegl, "Failure surfaces in principal stress space", J. Polymer Science, V C(32) p 239 (1971).
120. K. Ikegami, M. Gajiyama, S. Kaniko, and E.J. Shiratori, "Experimental studies of the strength of an adhesive joint in a state of combined stress", J. Adhesion 10, pp 25-38 (1978).
121. H. Liebowitz, Fracture II, Academic Press, pp 315-384 (1968).
122. T. Alfrey, "Nonhomogeneous stress in viscoelastic media", Quarterly Applied Mathematic 2, pp 113-119 (1944).
123. C.K. Lim, M.A. Acitelli, and W.C. Hamn, "Failure criterion of a typical polyamide cured epoxy adhesive", J. Adhesion 6, pp 281-288 (1974).

124. Y.T. Yeow, D.H. Morris, and H.F. Brinson, "Time-temperature behavior of a unidirectional graphite/epoxy composite", Composite Material Testing and Design STP 674, pp 263-281 (1978) (5th Conference).
125. K.G. Kibler, "Time-dependent environmental behavior of epoxy-matrix composites. Proceedings of the 5th Annual "Mechanics of Composites Review", AFWAL-TR-80-4020, pp 78-82 (1980).
126. R.D. Adams, and N.A. Peppiatt, "Stress analysis of adhesive bonded tubular lap joints", J. Adhesion 9, pp 1-18 (1977).
127. W.J. Renton, and J.R. Vinson, "The efficient design of adhesive bonded joints", J. Adhesion 7, pp 175-193 (1975).
128. L.J. Hart-Smith, "Analysis and design of advanced composite bonded joints", Final Report NASA-CR-2218 (1973).
129. T.S. Ramamurthy, and A.K. Rao, "Influence of adhesive non-linearities on the performance and optimal length of adhesive bonded joints", Mechanics Research Communication 5, pp 9-14 (1978).
130. J.O. Smith, and D.M. Sidebottom, "Inelastic time-temperature behavior of load carrying members", Wiley, pp 84-89 (1965).
131. W. Ramberg, and W.R. Osgood, "Description of stress-strain curves by three parameters", Technical Notes NACA, Washington, July (1943).
132. D.L. McLellan, "Constitutive equations for mechanical properties of structural materials", AIAA J. 5, pp 446-450 (1967).
133. K.C. Valanis, and U. Hon-Chin, "Endochronic representation of cyclic creep and relaxation of metals", J. of Applied Mechanics 42, pp 67-73 (1975).
134. Z.P. Bazant, "Endochronic and classical theories of plasticity in finite element analysis", International Conference on Finite Element in Non-Linear Solid and Structural Mechanics, 1, pp B01.1 (1977).
135. J.P. Sargent, and K.H.G. Ashbee, "High resolution optical interference investigation of swelling due to water uptake by model adhesive joints", J. Adhesion 11, pp 175-189 (1980).

GLOSSARY

| | |
|-----------------------|--|
| a_T | - time-temperature shift factor |
| b | - constant |
| c_i | - constants |
| $c (w)$ | - moisture content, relative moisture absorption |
| d | - constant |
| E | - elastic modulus |
| ϵ | - effective strain |
| $\dot{\epsilon}$ | - effective strain rate |
| F | - failure limit |
| f | - failure index |
| H | - humidity (Hygro) |
| h | - laminate and specimen thickness |
| I | - strain invariants |
| J | - stress invariants |
| n | - power constant |
| s | - effective strain |
| T | - temperature (ΔT - temperature difference) |
| T_g | - glass transition temperature |
| t | - time, (Δt - time interval) |
| w | - weight (Δw - weight change) |
| x, y, z | - cartesian coordinates |
| α | - coefficient of thermal expansion (CTE) |
| β | - hygroelastic coefficient (HEC) |
| γ | - shear strain |
| $\dot{\gamma}$ | - shear strain rate |
| ϵ_n | - normal strain |
| $\dot{\epsilon}_n$ | - normal strain rate |
| ϵ_d | - deformation |
| σ_c / σ_t | - ratio between compressive and tensile stresses |
| ν | - poisson ratio |
| γ_s | - shear strain |
| σ_n | - normal stress |
| $c (w)$ | - moisture content, relative moisture absorption |

ABBREVIATIONS

| | |
|------|---|
| FRP | - fiber-reinforced plastics |
| CFRP | - carbon-fiber-reinforced plastics |
| GFRP | - glass-fiber-reinforced plastics |
| KFRP | - kevlar-fiber-reinforced plastics |
| BFRP | - boron-fiber-reinforced plastics |
| U.D. | - unidirectional |
| B.D. | - bidirectional |
| M.D. | - multidirectional |
| MMS | - multimaterial multilayer systems |
| DLJ | - double lap joint |
| SLJ | - single lap joint |
| TA | - thick adherend |
| SD | - symmetrical doubler model |
| NSD | - non-symmetrical double model |
| IAL | - interlaminar adhesive layer |
| HT | - hygrothermal |
| TE | - thermoelastic |
| HE | - hygroelastic |
| HTM | - hygrothermomechanical |
| RT | - room temperature |
| CTE | - coefficient of thermal expansion (α) |
| HEC | - hygroelastic coefficient (β) |
| VE | - viscoelastic |
| EP | - elastoplastic |
| VEP | - viscoelastoplastic |
| FPP | - first ply failure |
| FEM | - finite element method |

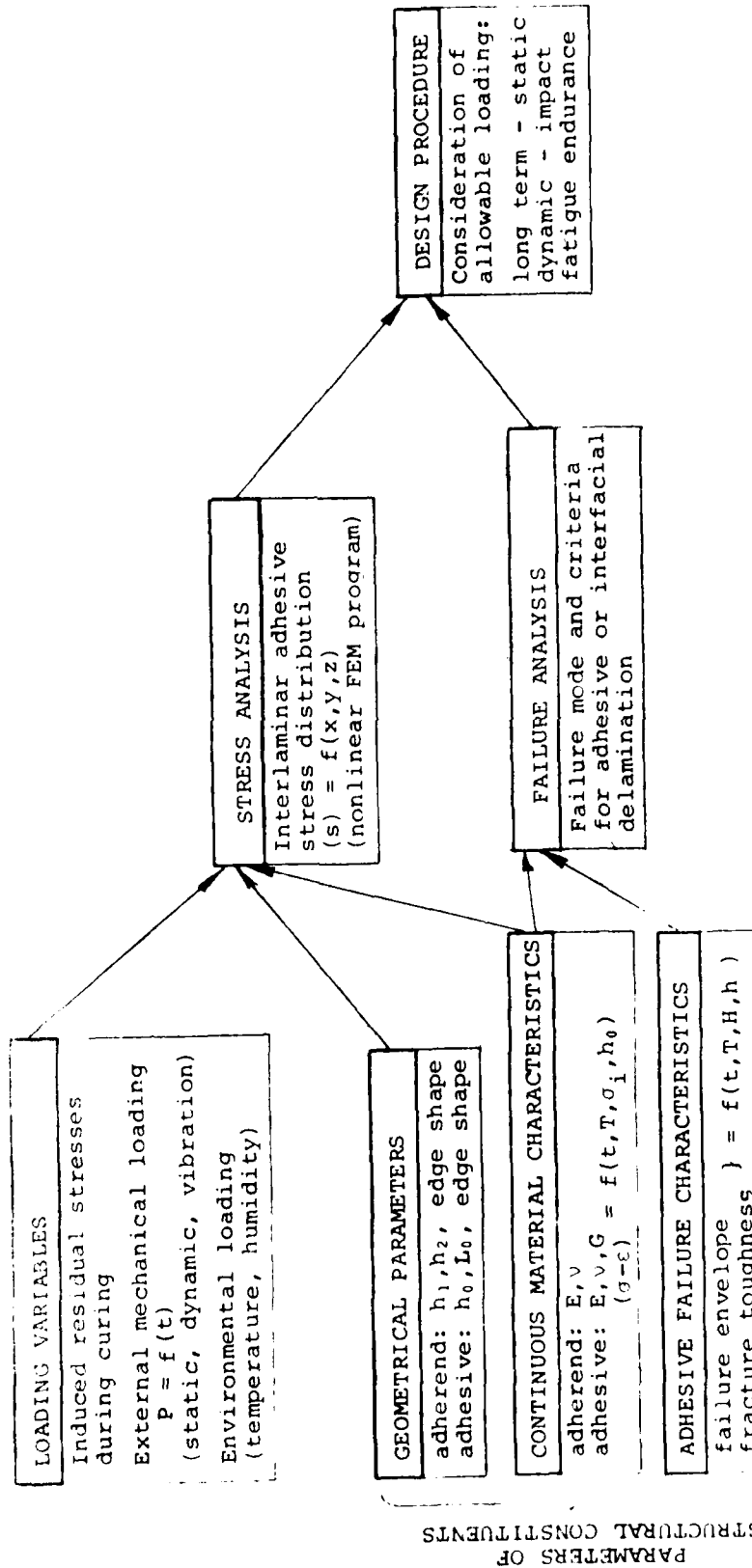
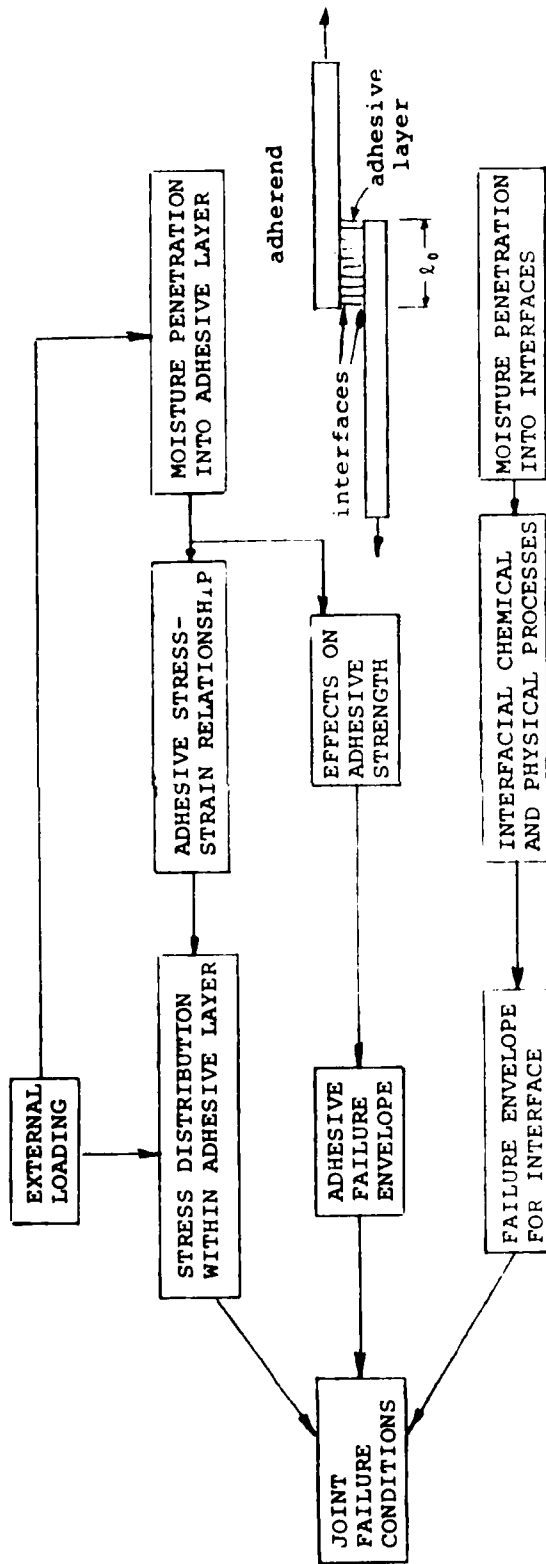


Fig. 1.1 STRESS AND FAILURE ANALYSIS PROCEDURE FOR THE STRUCTURAL DESIGN OF BONDED SYSTEM



Flow Chart for Research Program on:

Fig. 1.2 THE EFFECT OF MOISTURE ON FAILURE OF BONDED JOINTS

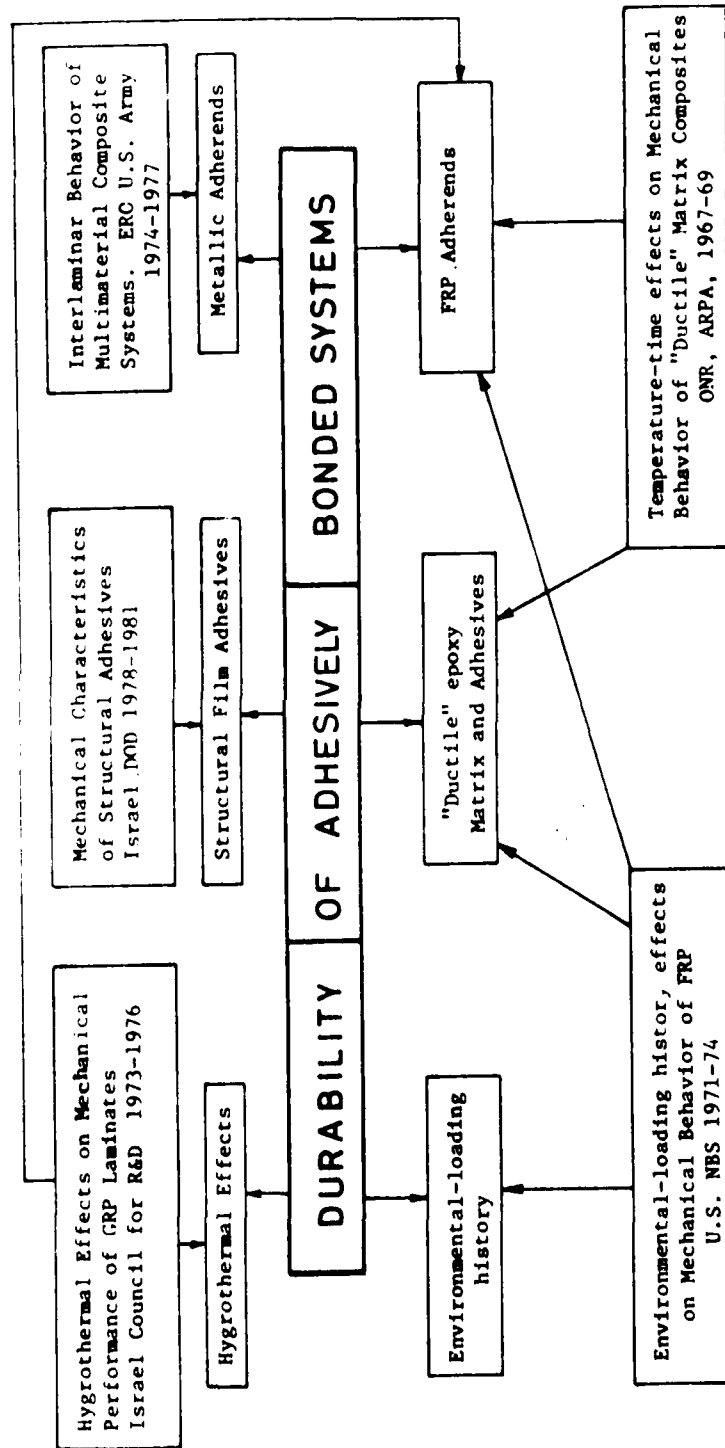


Fig. 1.3 RELEVANCE OF PREVIOUS INVESTIGATIONS TO PRESENT RESEARCH

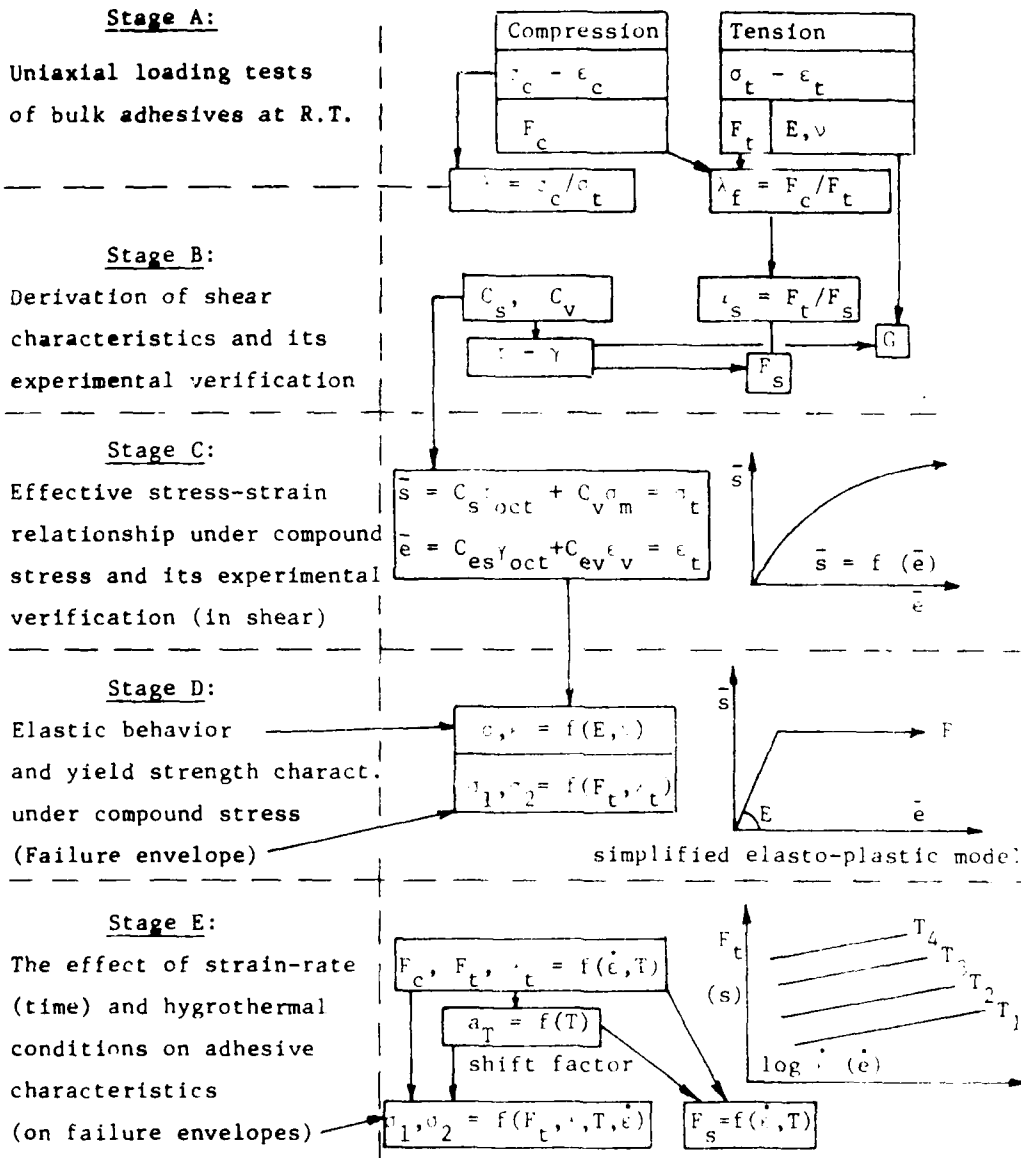


Fig. 2.1 PROPOSED PROCEDURE FOR MECHANICAL CHARACTERIZATION OF STRUCTURAL ADHESIVES

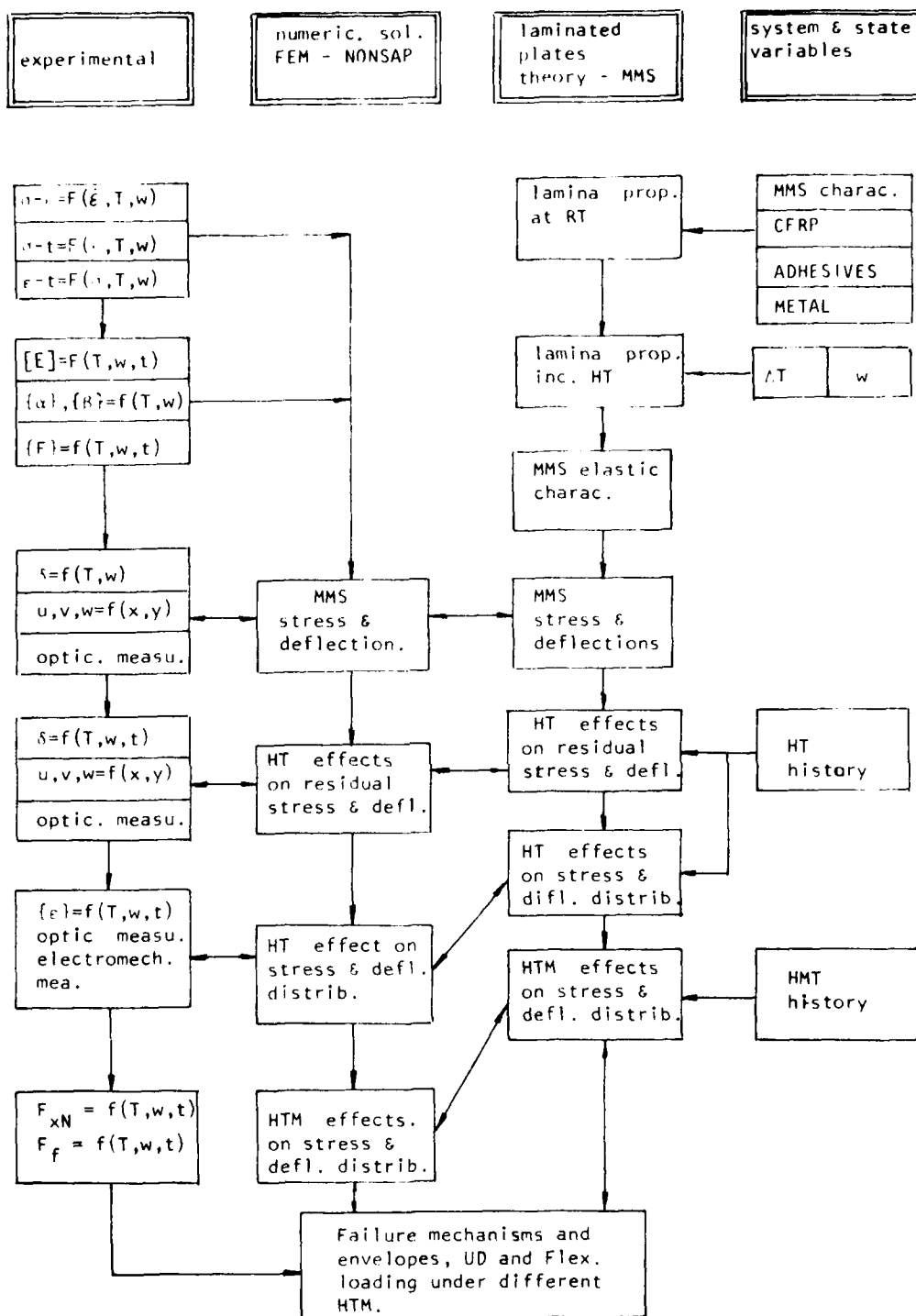


Fig. 4.1 Flow chart of present research objectives and procedure.

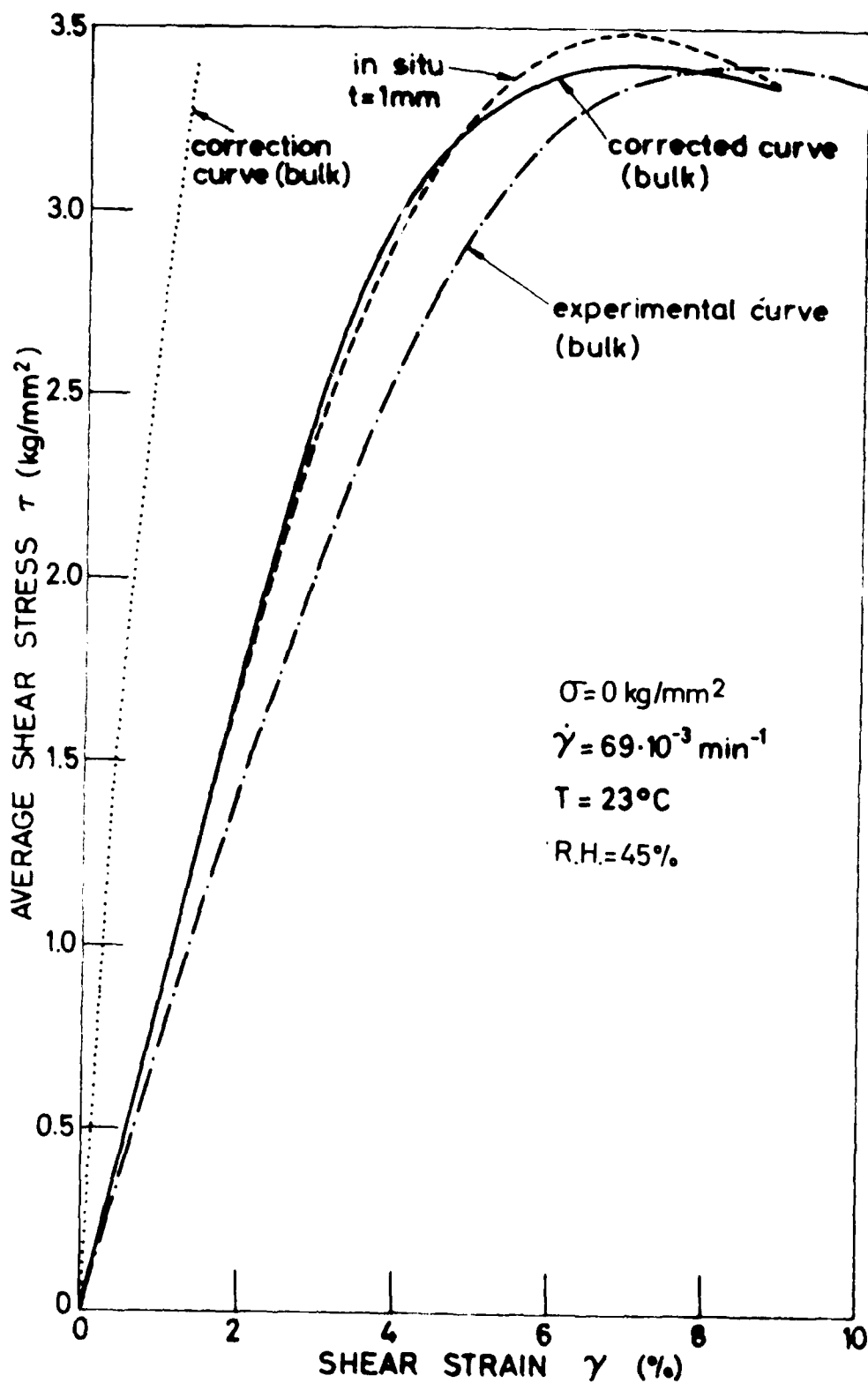


Fig. 5.1 Shear stress-strain relationship based on torsional test of tubular specimen compared with ring specimen of the adhesive insitu.

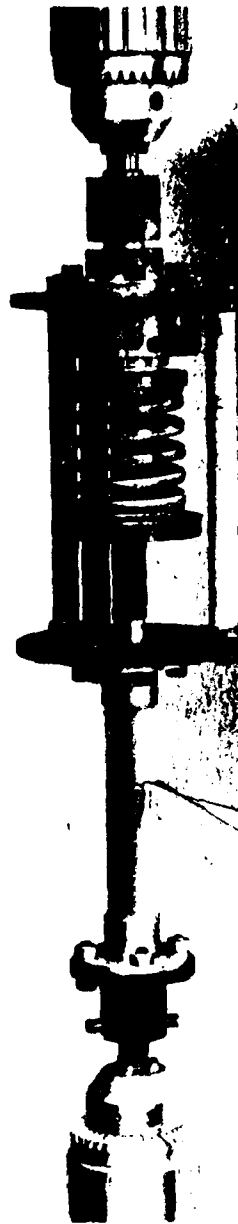


Fig. 5.2 Illustration of device for combined uniaxial and shear loading of tubular specimens.

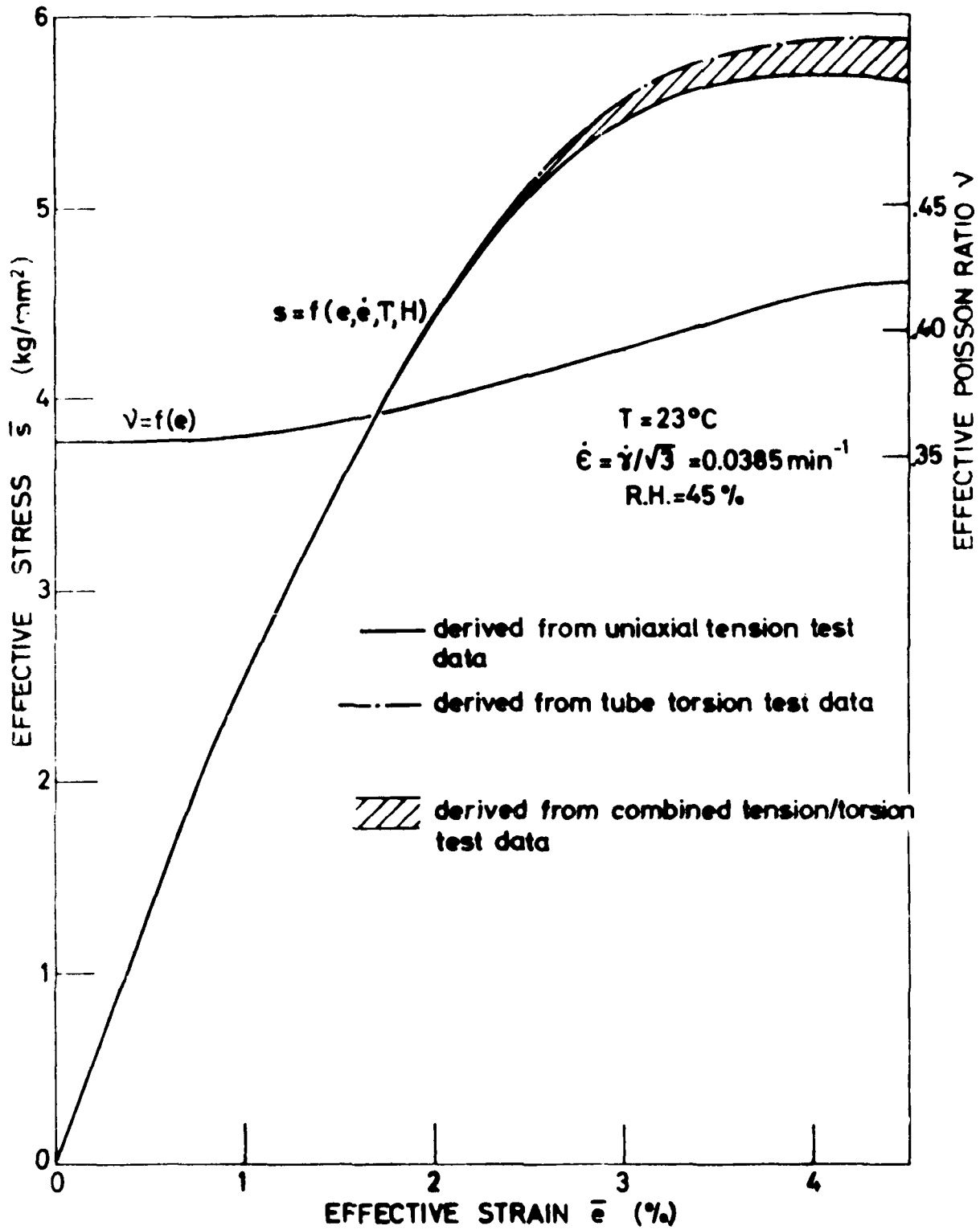


Fig. 5.3 Effective stress-strain relationship for epoxy resin derived from different loading mode combinations.

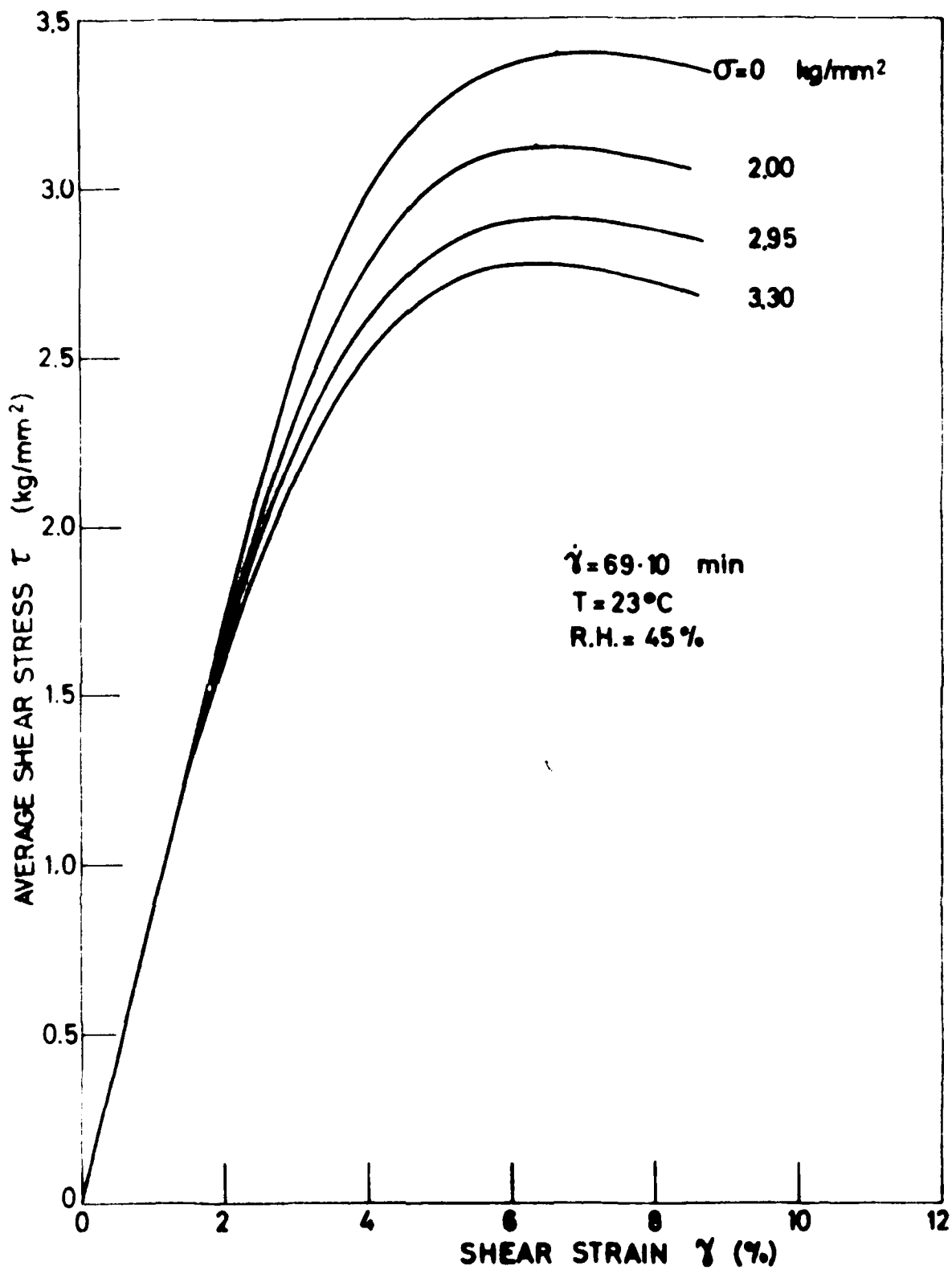


Fig. 5.4 Shear stress-strain relationship at different levels of normal stresses, as achieved by special device.

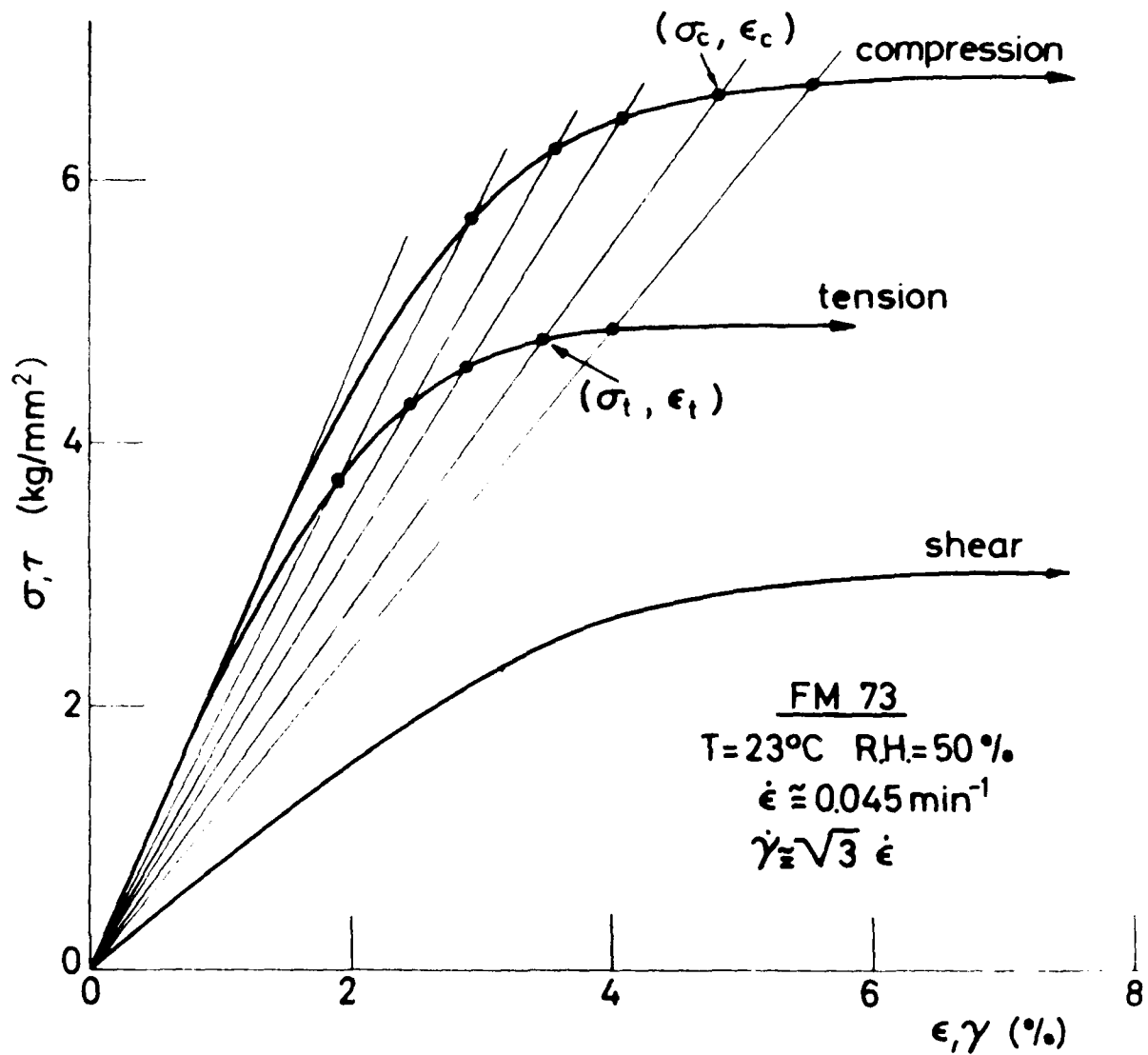


FIG. 5.5 Basic stress-strain curves under uniaxial loading in tension and compression of bulk FM73 adhesive vs. shear stress-strain curve.

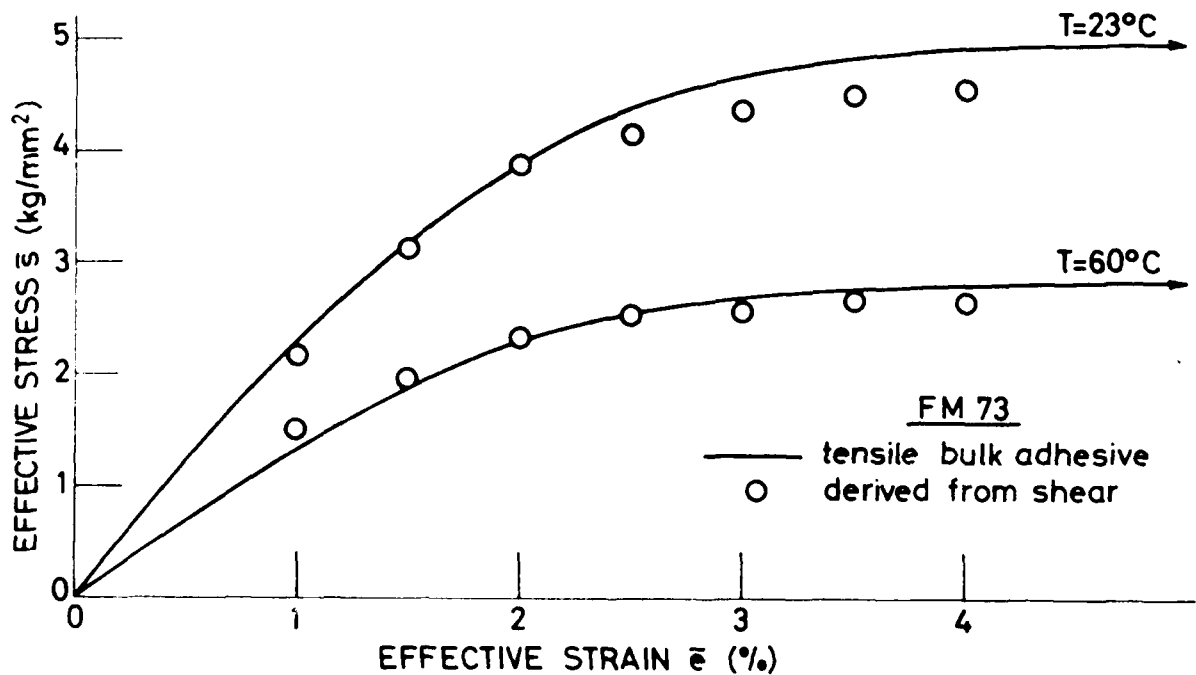
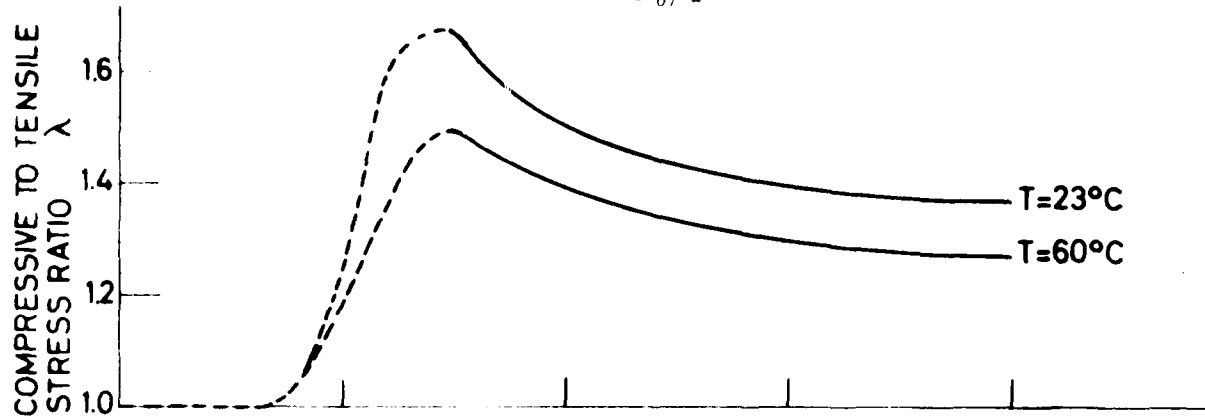


Fig. 5.6 Effective stress-strain relationship for FM73 adhesive based on uniaxial tensile test, as examined by shear test.

Fig. 5.7 Failure envelope for bulk and bonded epoxy adhesive derived from different loading mode combinations.

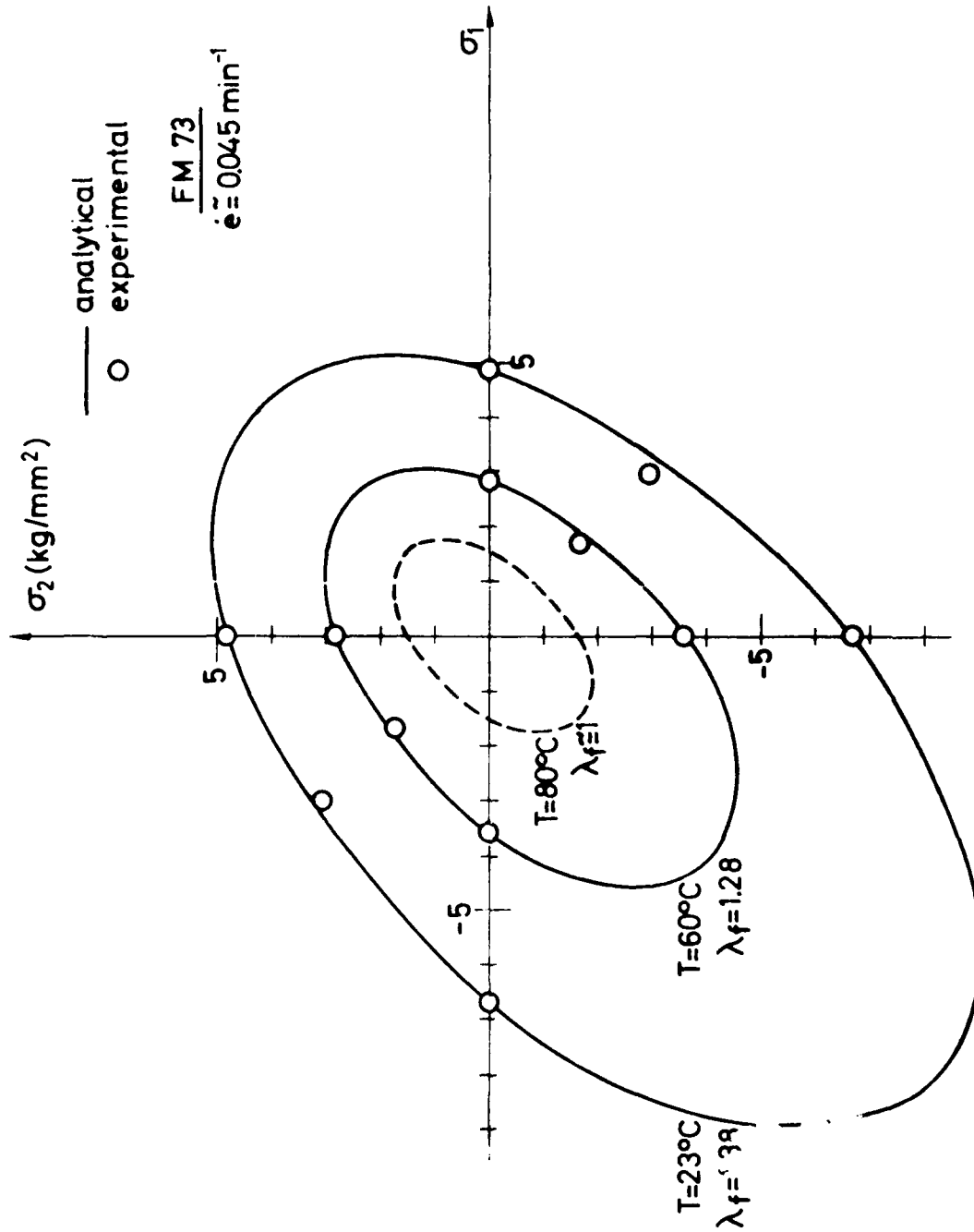


Fig. 5.8 Failure envelopes for structural adhesive FM73 at different temperature levels.

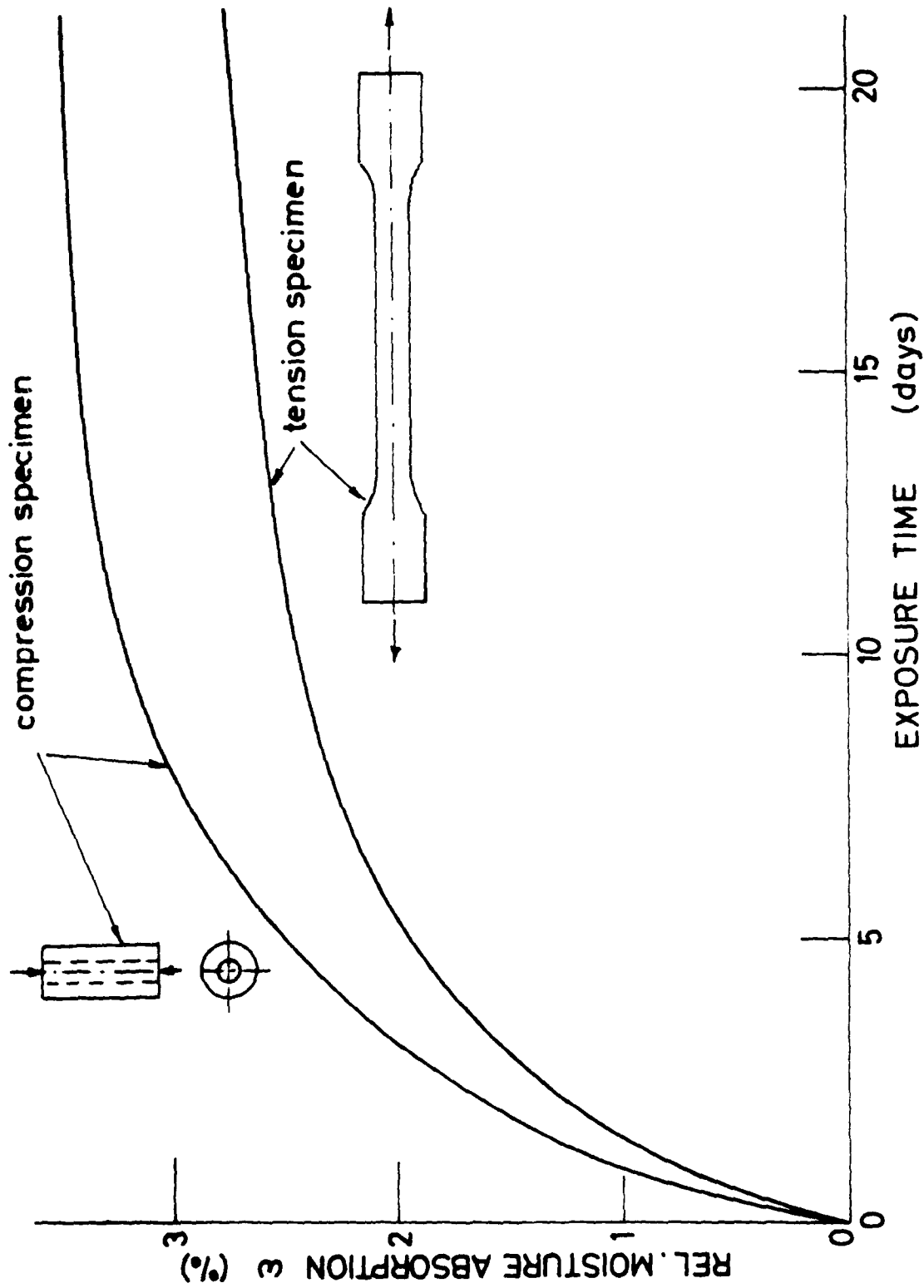


Fig. 6.1 Weight changes with time of bulk PMMA specimens immersed in R1 water, (23°C)

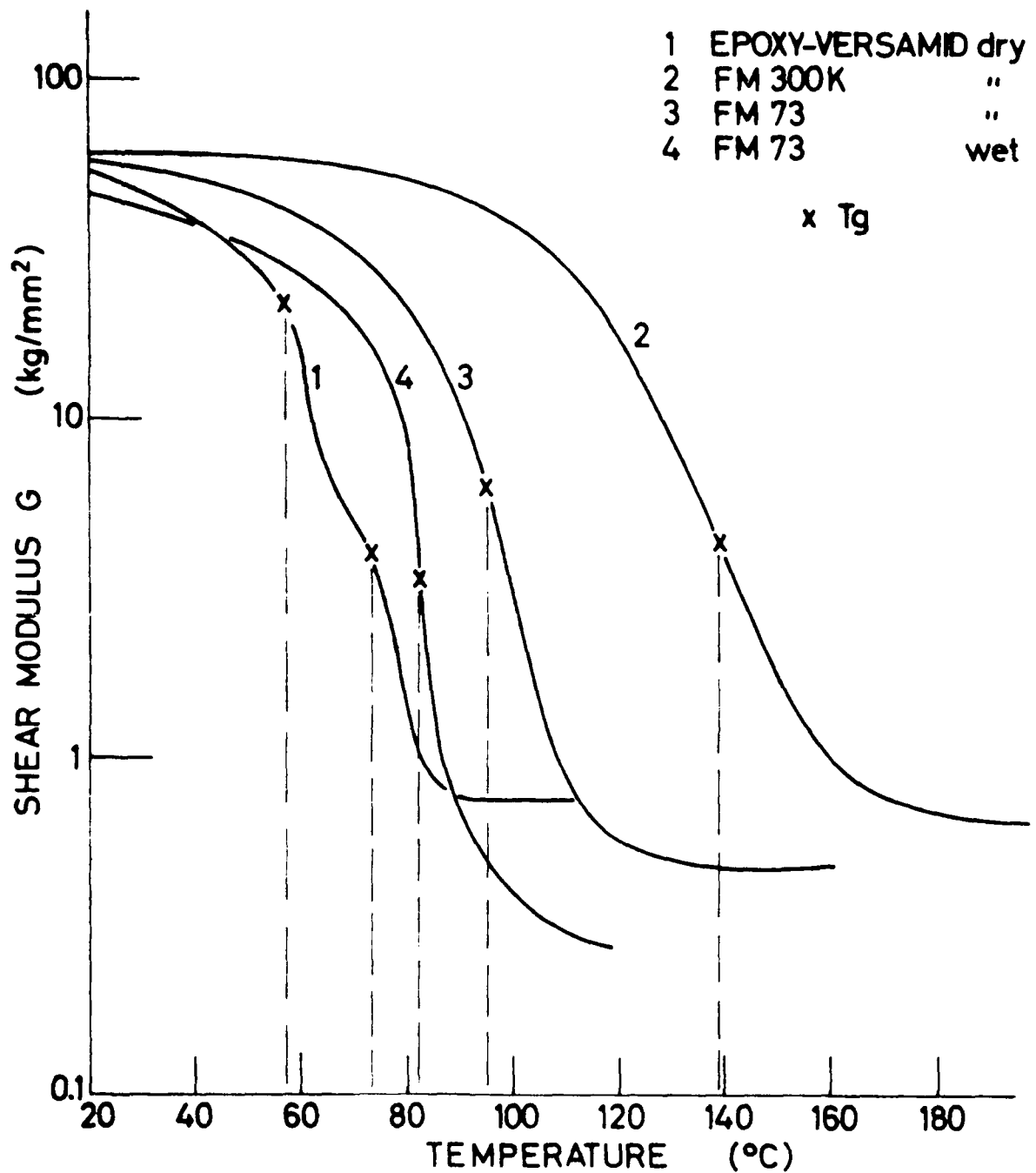
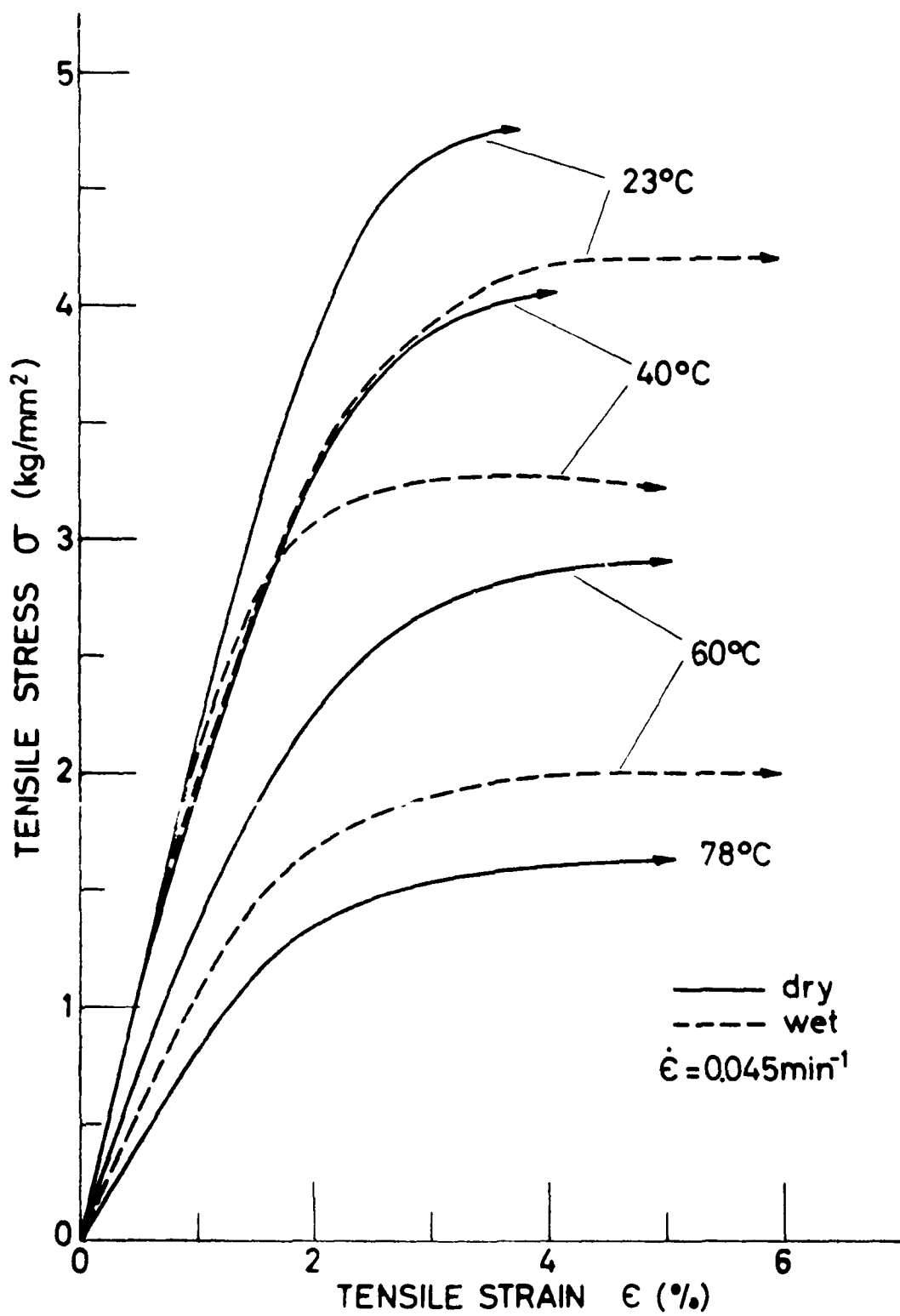


Fig. 6.2 Temperature dependence of shear modulus - for the determination of glass-transition temperature (Tg) of different adhesives.



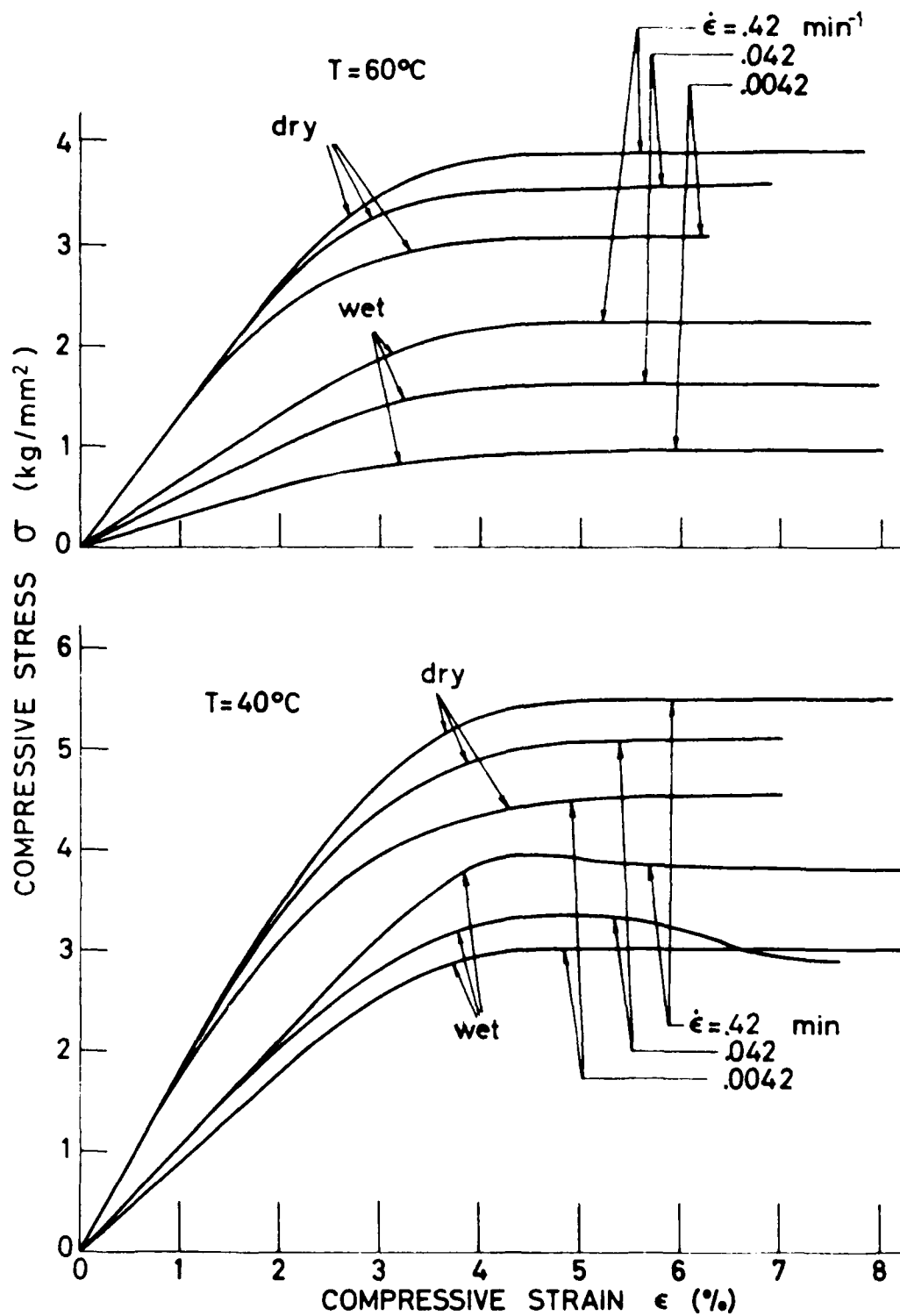


Fig. 6.4 Compressive stress-strain curves of wet and dry PM73 specimens under different strain rate and temperature conditions. ($T = 40^\circ\text{C}, 60^\circ\text{C}$).

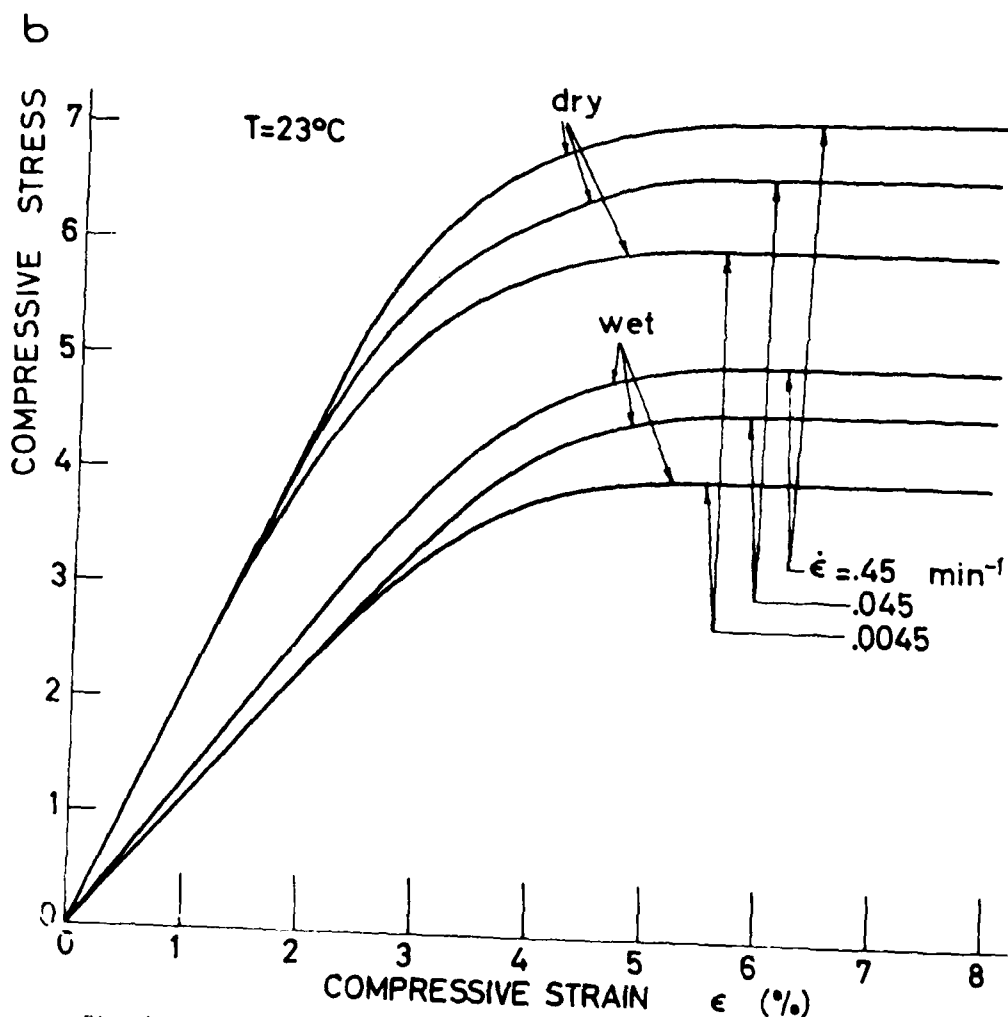
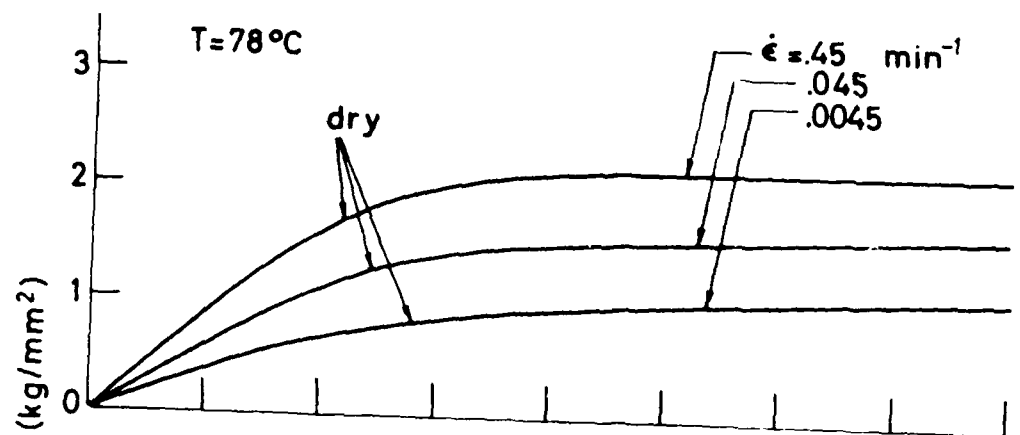


Fig. 6.5 Compressive stress-strain curves of wet and dry FM73 specimens under different strain rate and temperature conditions. ($T = 23^\circ\text{C}$, 78°C).

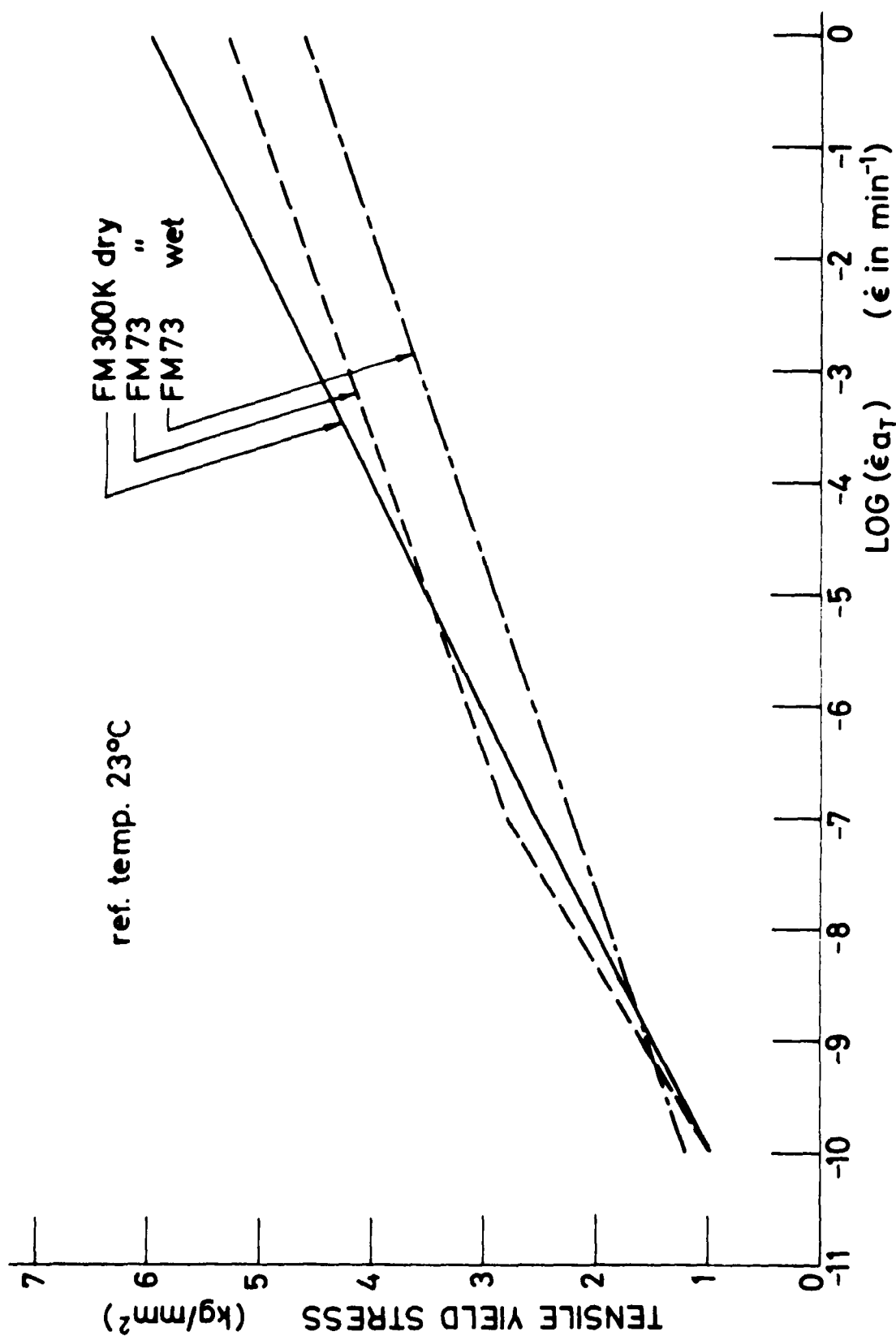


Fig. 6.6 Master curve for tensile yield stress of FM 300 K adhesive specimens.

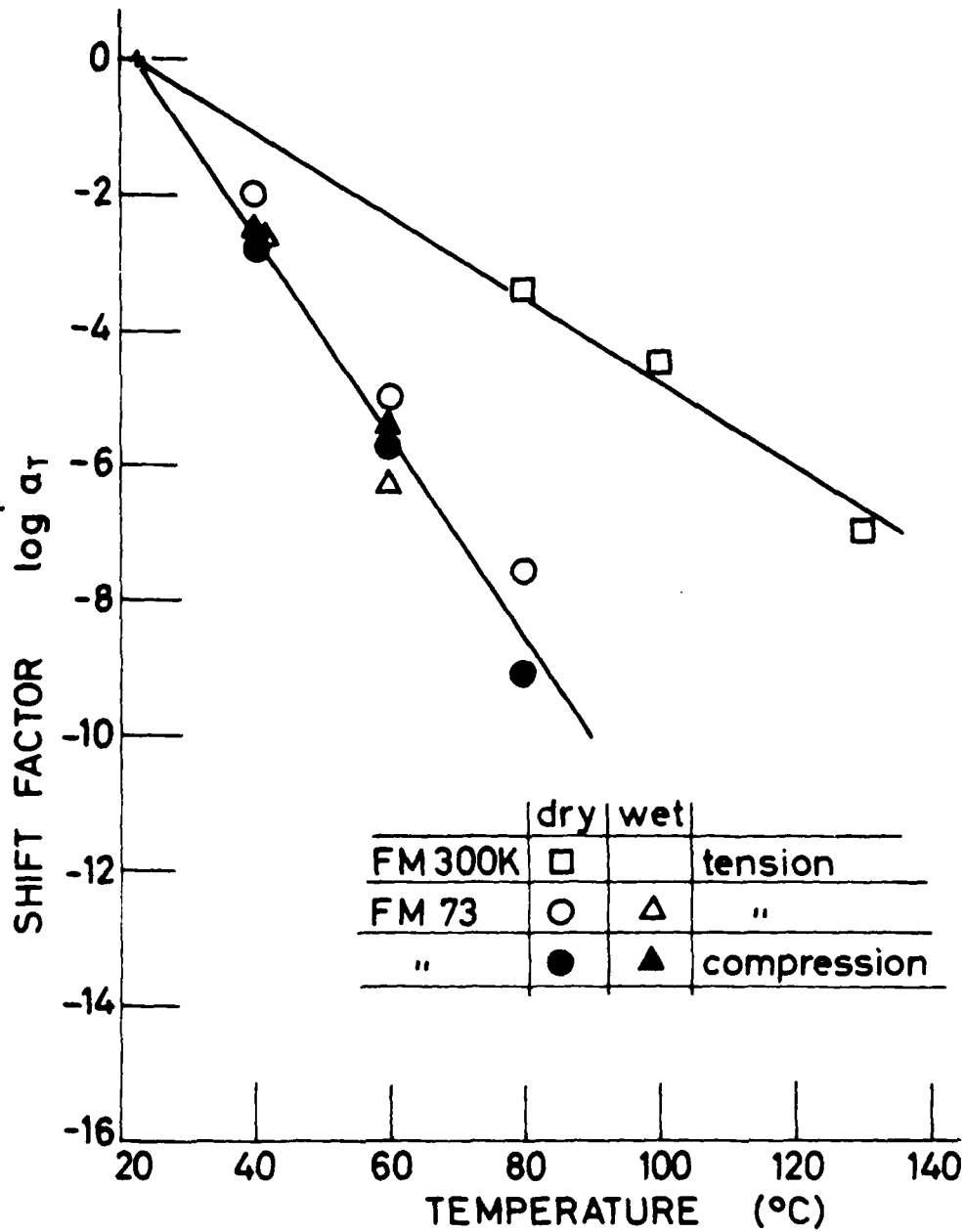


Fig. 6.7 Shift factor vs. temperature for tensile yield stress master curve of FM73 and FM 300 K adhesive specimens.

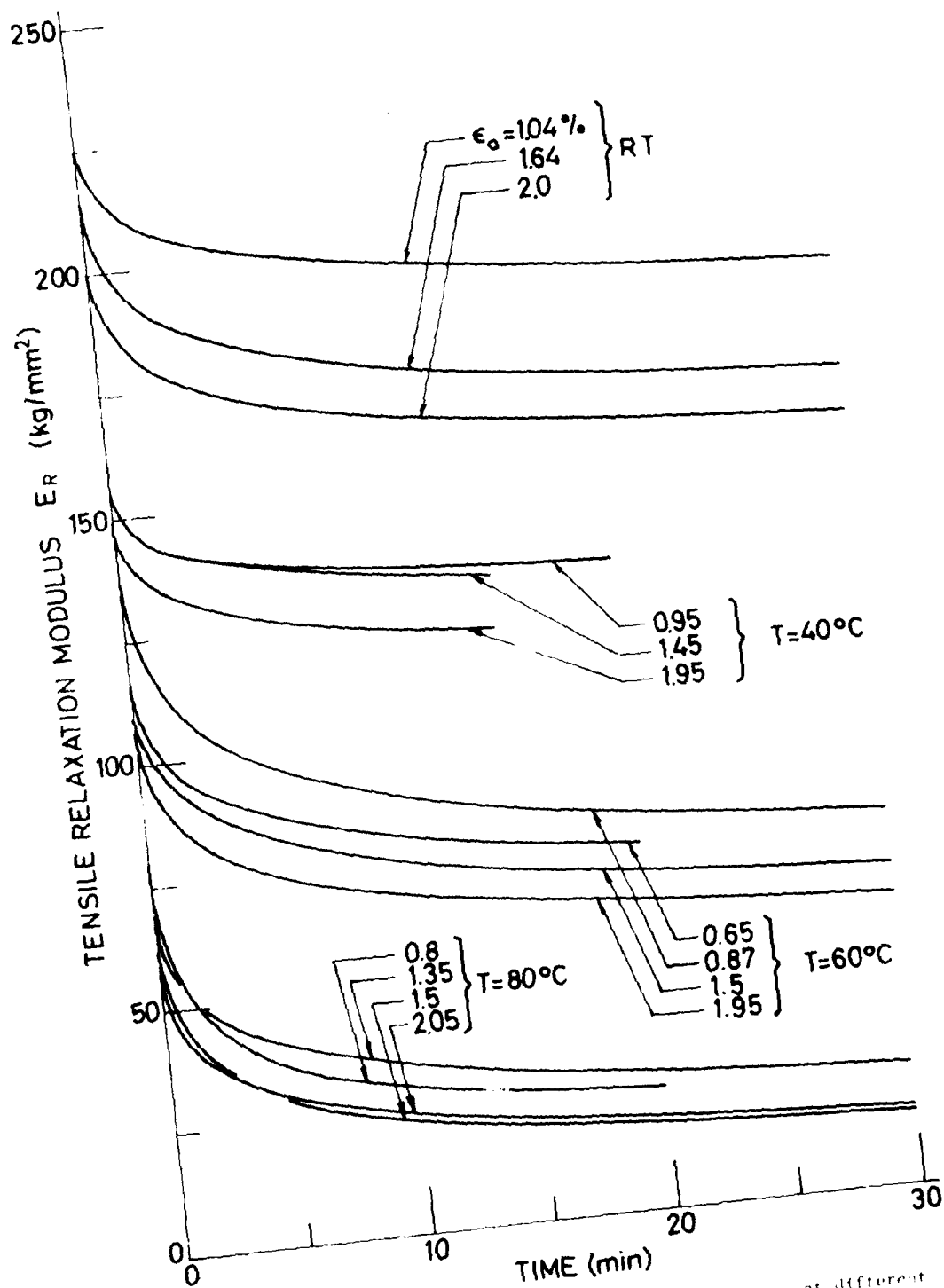


Fig. 6.8 Tensile stress relaxation curves of TM3 specimens at different strain and temperature levels.

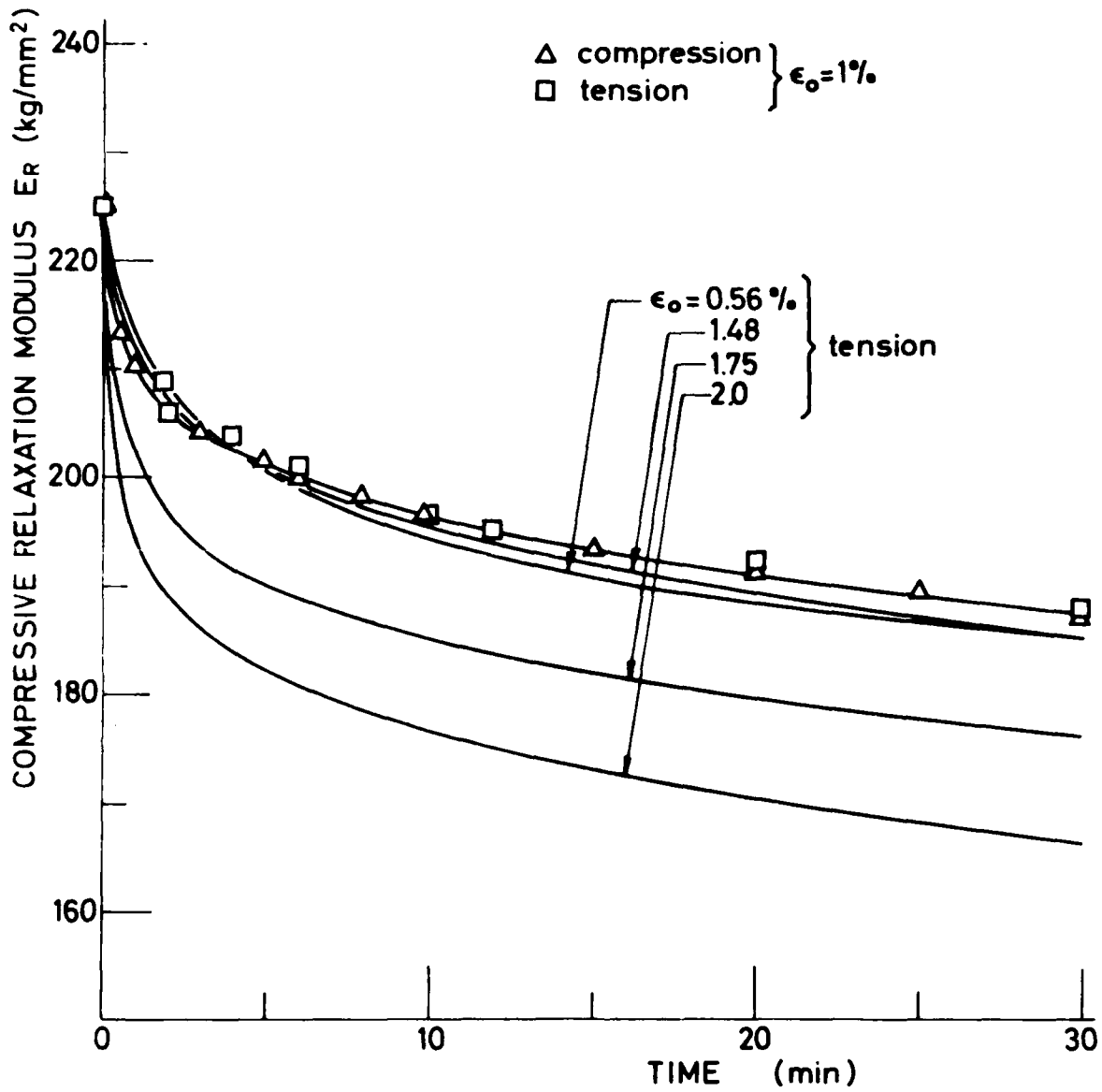


Fig. 6.9 Compressive stress relaxation curves of FM73 specimens at different strains at RT, as compared to tensile stress relaxation.

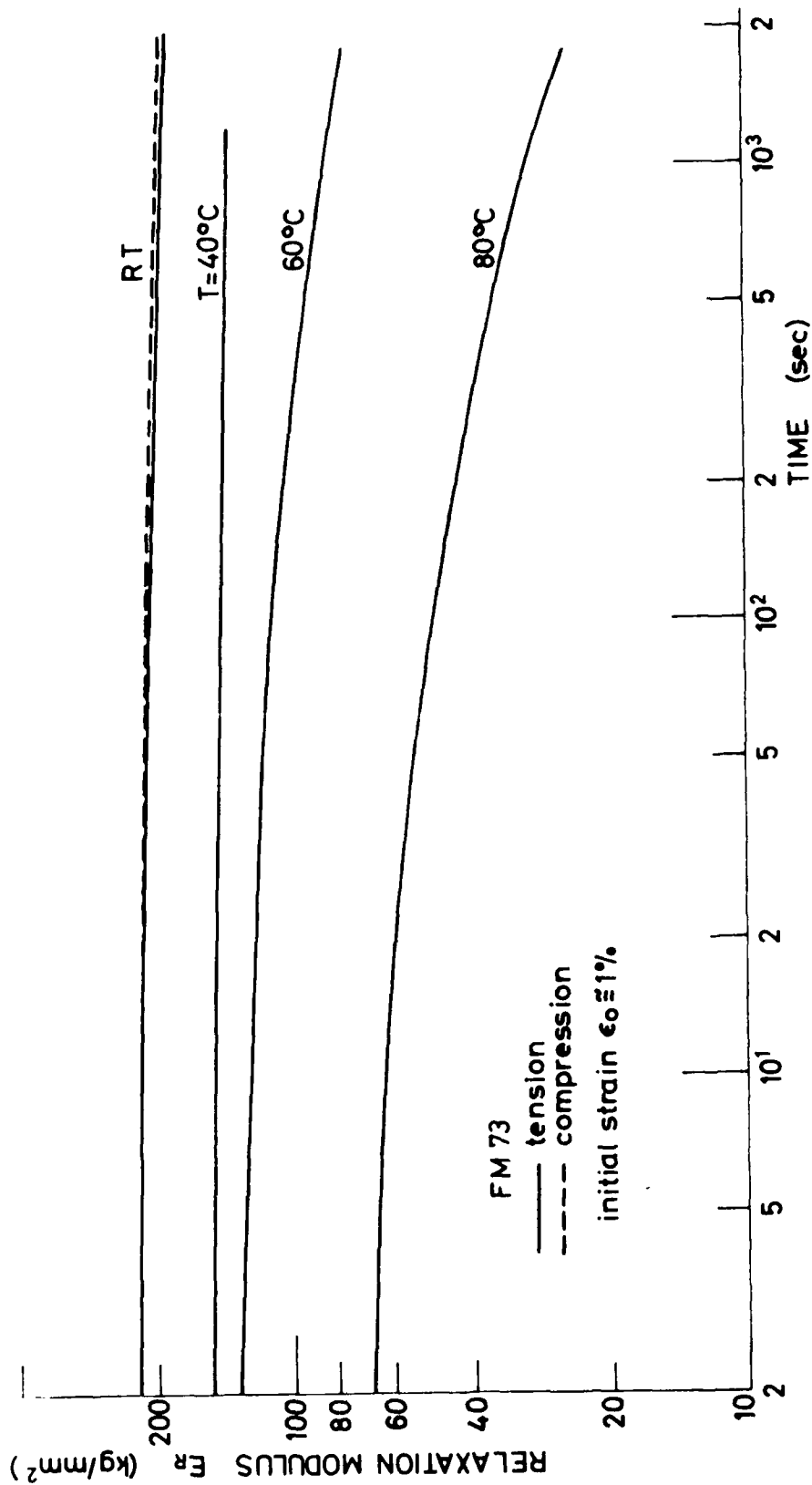


Fig. 6.10 Stress-relaxation curves vs. time of FM 73 specimens at different temperature levels on log-log scale.

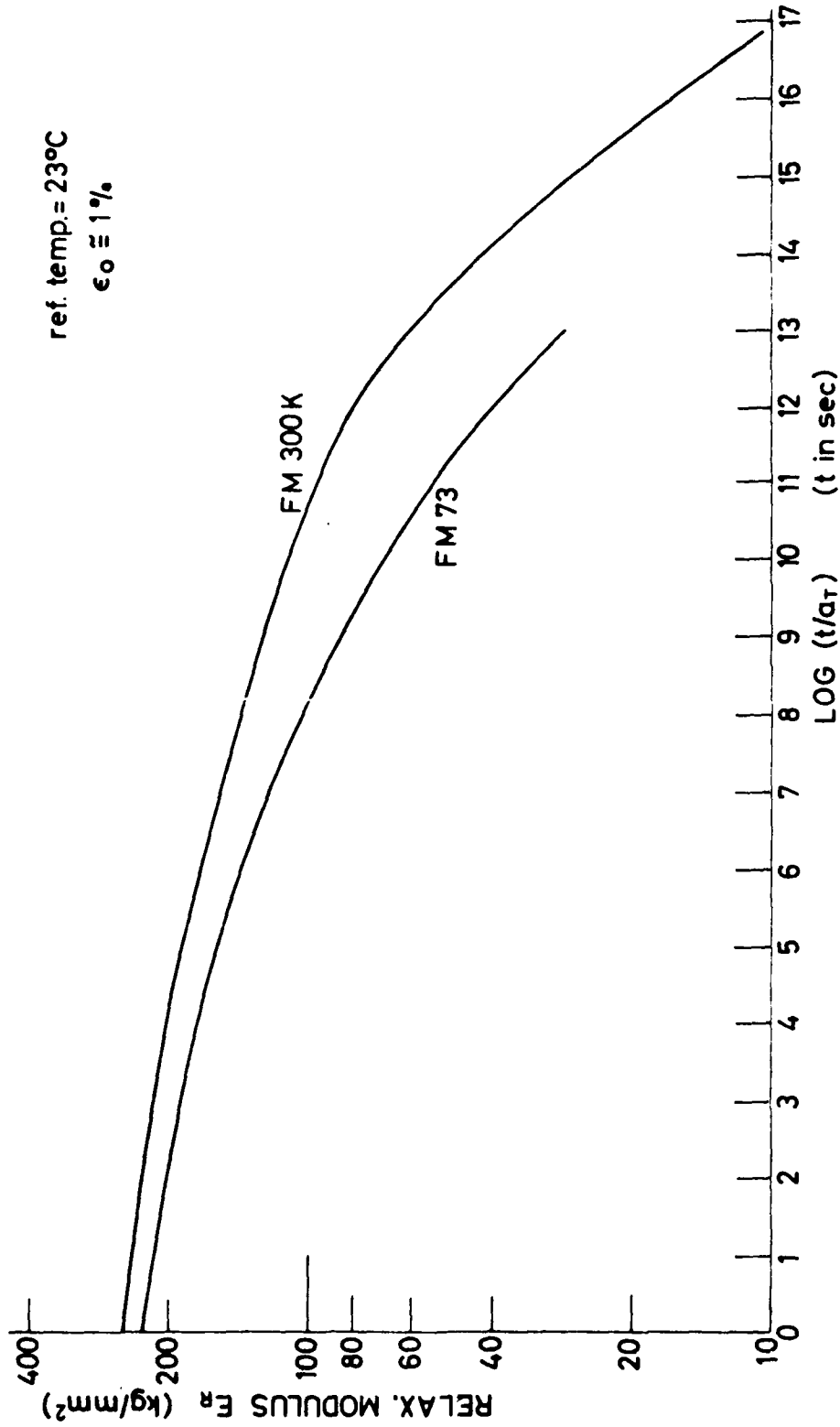


Fig. 6.11 Stress relaxation master curve of FM 73 and FM 300 K adhesive specimens. ($T_{ref} = 23^\circ\text{C}$).

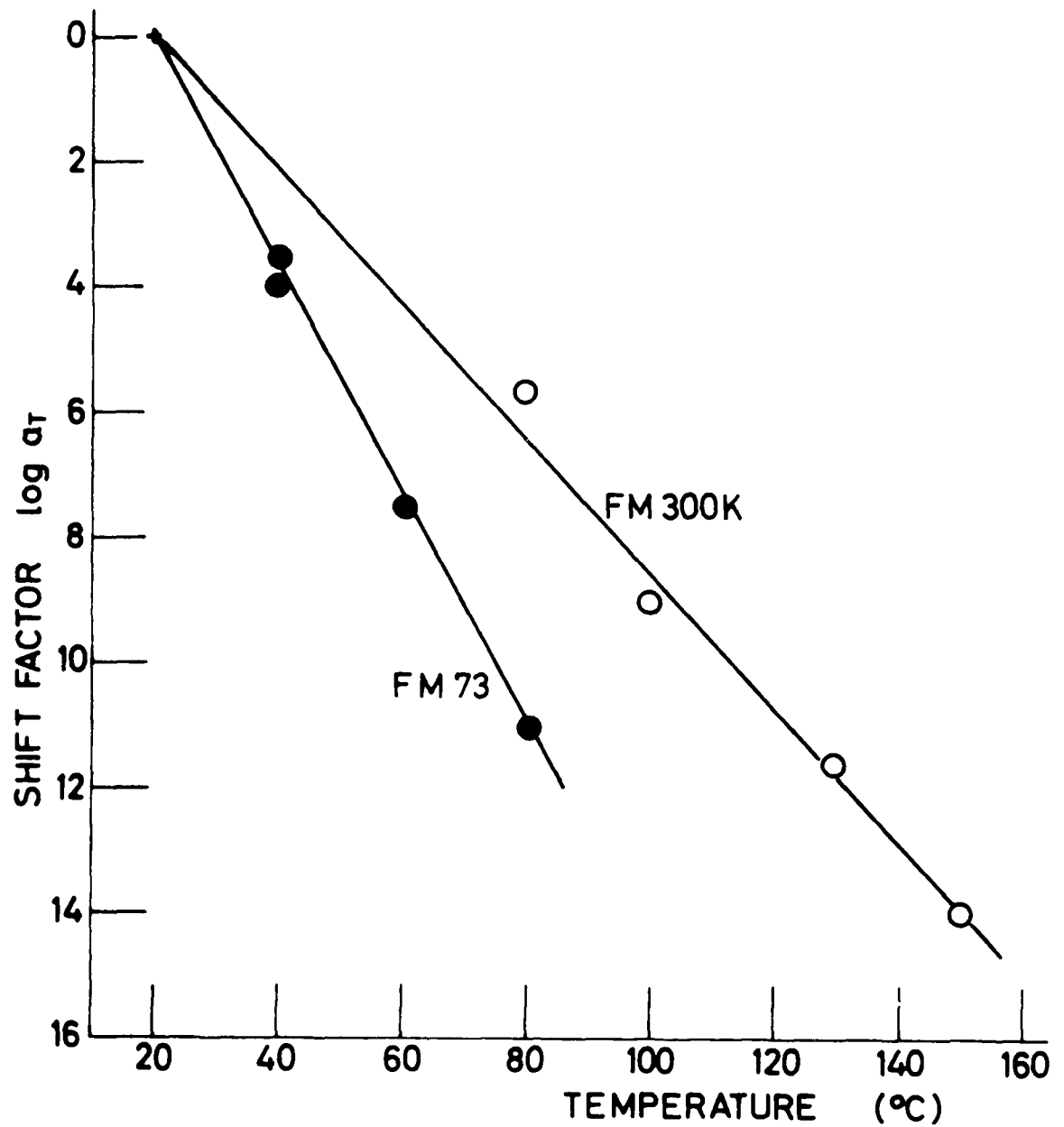


Fig. 6.12 Shift factor vs. temperature for stress relaxation master curve of FM73 and FM 300 K adhesive specimens.

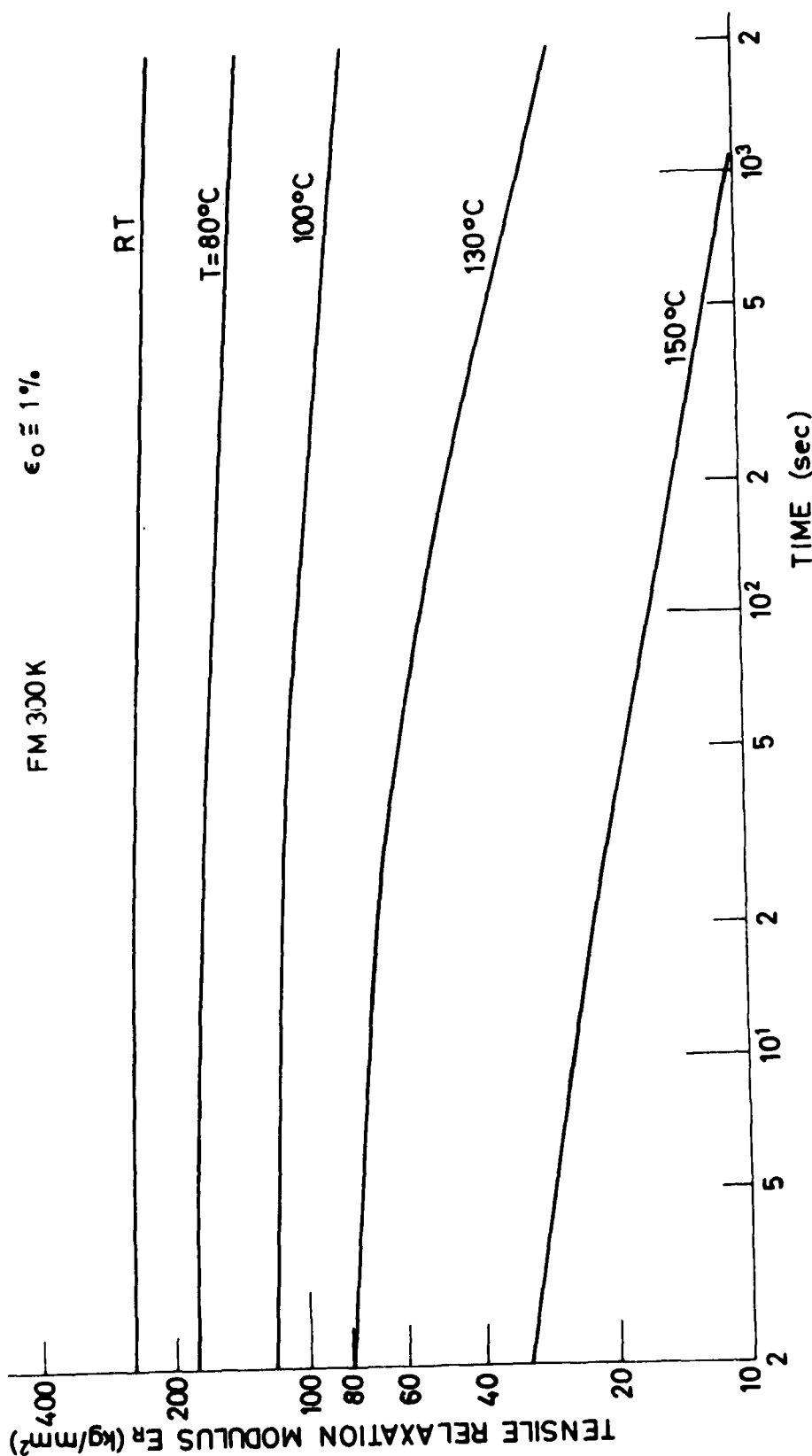


Fig. 6.13 Tensile stress relaxation curves for FM 300 K adhesive specimen at different temperature levels.

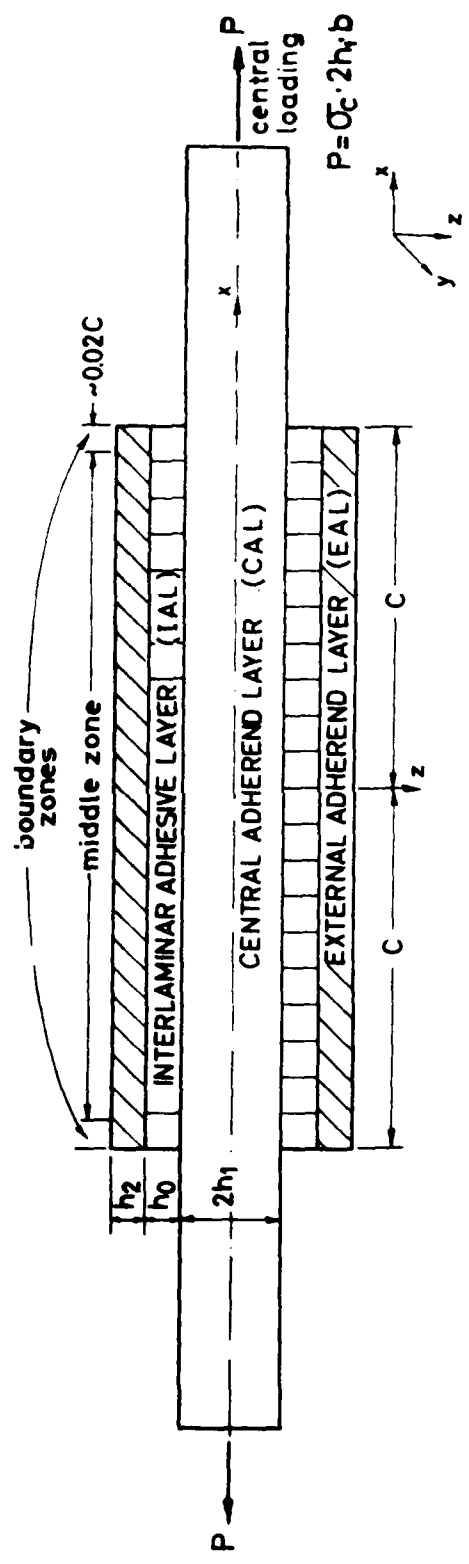


Fig. 7.1 Symmetrical doubler model.

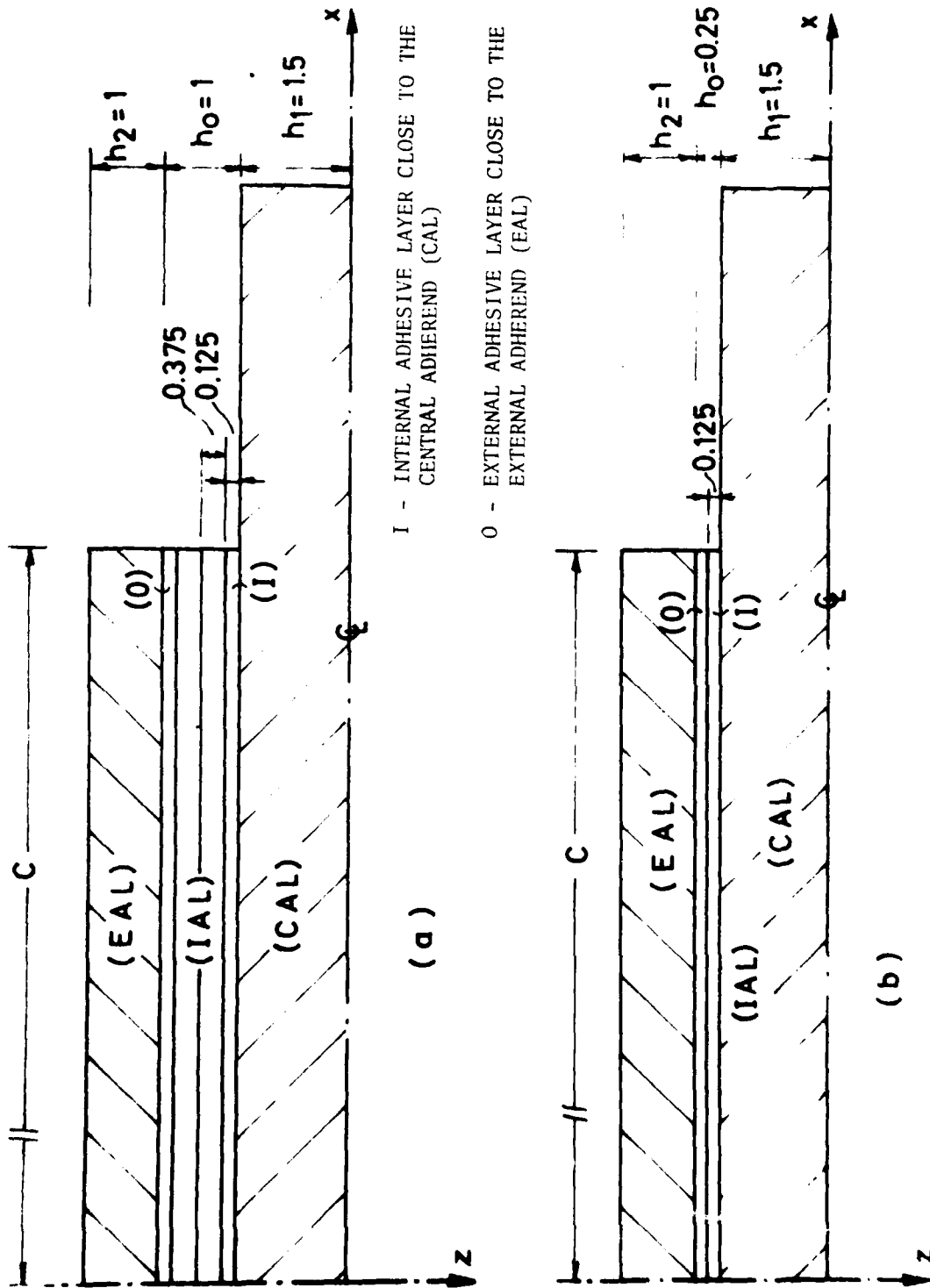


Fig. 1.2 Illustration of IAL scheme for different IAL Thicknesses.

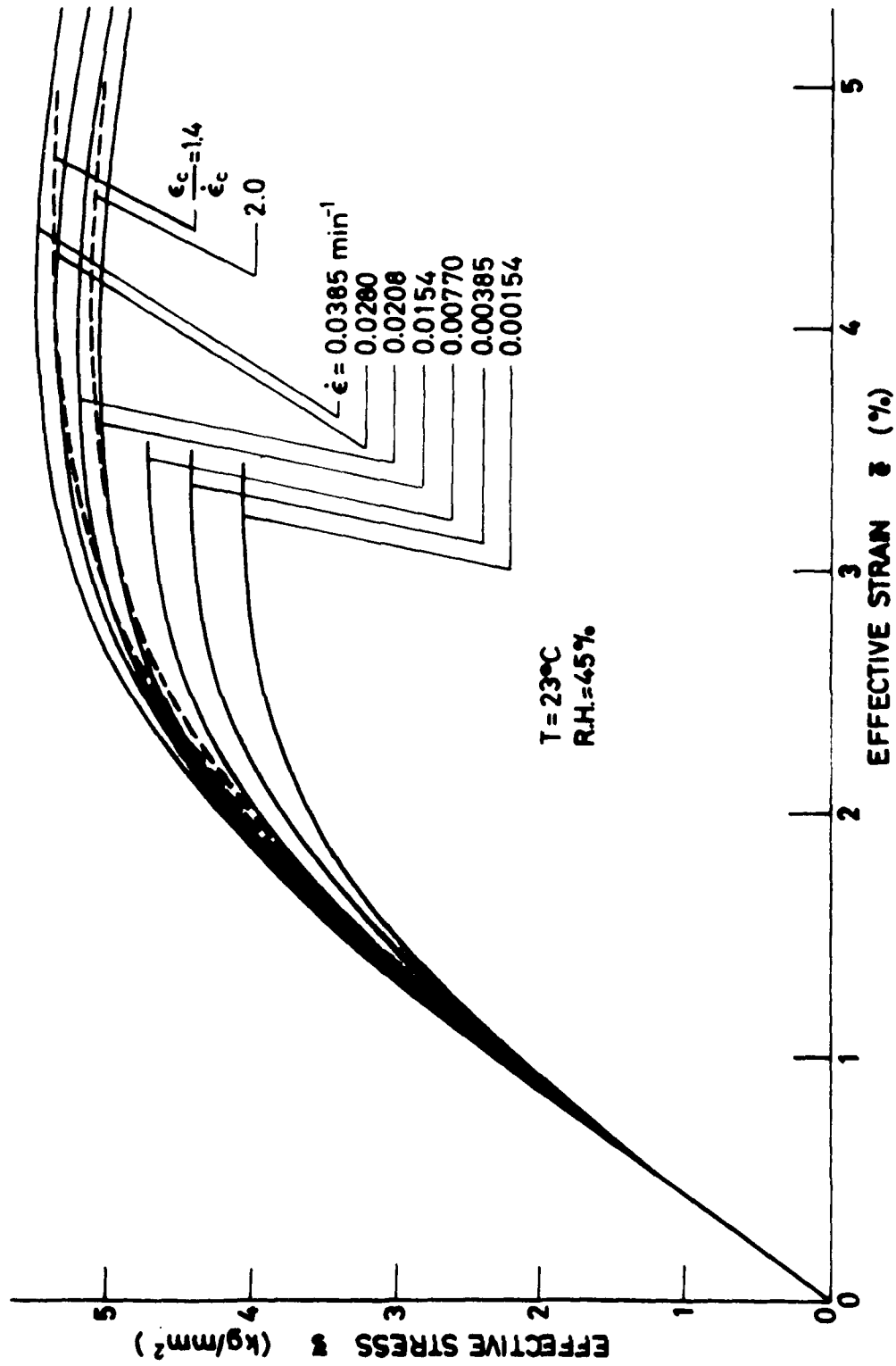


Fig. 7.3 Effective stress-strain curves of epoxy resin at different strain rates and relevant work curves in different external loading conditions $\frac{\dot{\epsilon}_c}{\dot{\epsilon}}$

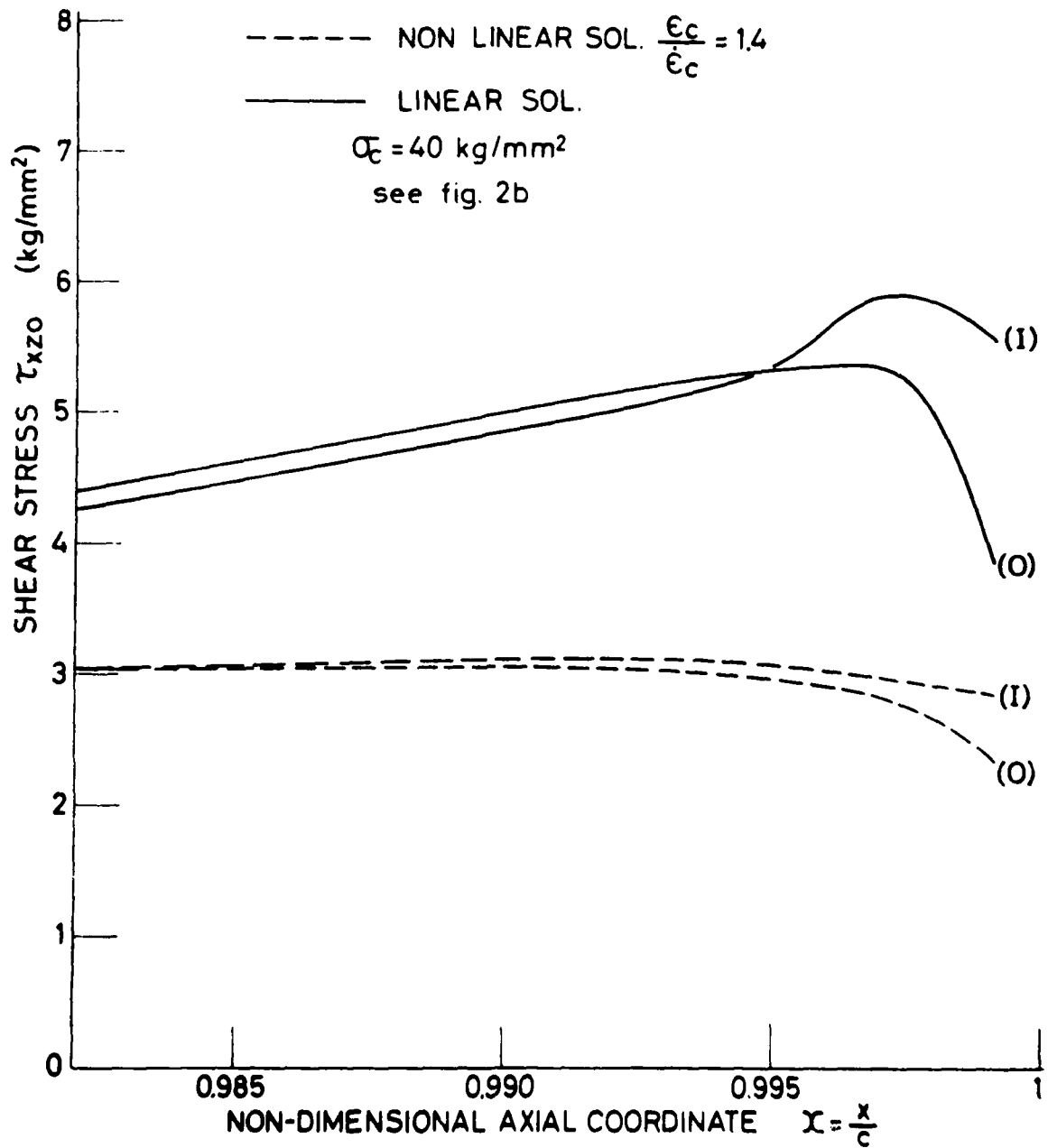


Fig. 7.4 Shear stress (τ_{xzo}) distribution within the IAL boundary zone - non-linear solution with strain rate effect (i.e. linear solution).

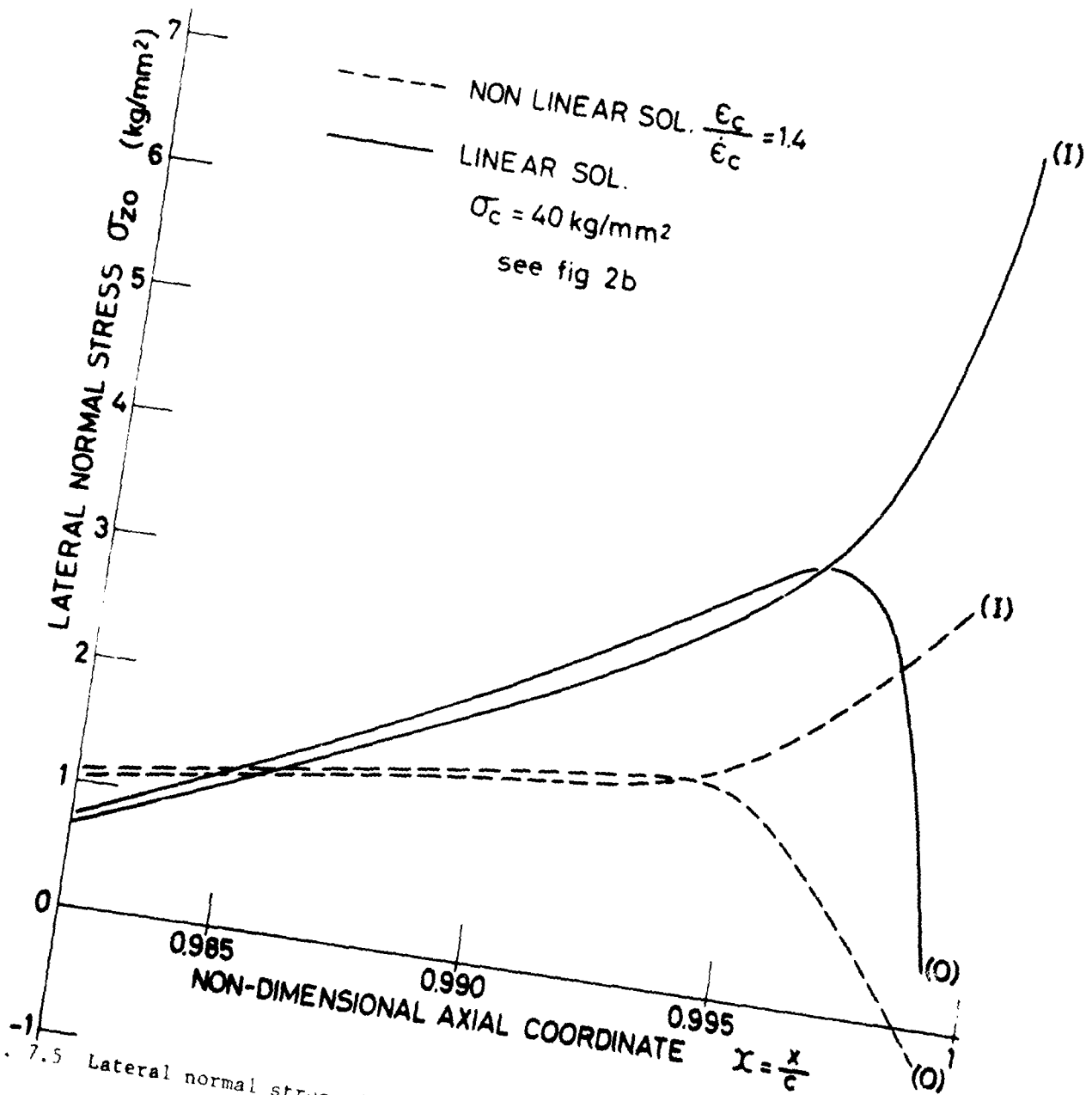


Fig. 7.5 Lateral normal stress (σ_{z0}) distribution within the IAL boundary zone - non-linear solution with strain-rate effect (i.e. linear solution).

AD-A111 209

TECHNION RESEARCH AND DEVELOPMENT FOUNDATION LTD HAI--ETC F/S 11/1
DURABILITY OF STRUCTURAL ADHESIVELY BONDED SYSTEM.(U)
JAN 81 O ISHAI, S GALI, S YANIV

DAJA37-80-C-0303

UNCLASSIFIED

NL

2 of 2
AL 4/1/89



END

DATE

FILED

9-82

DTIC

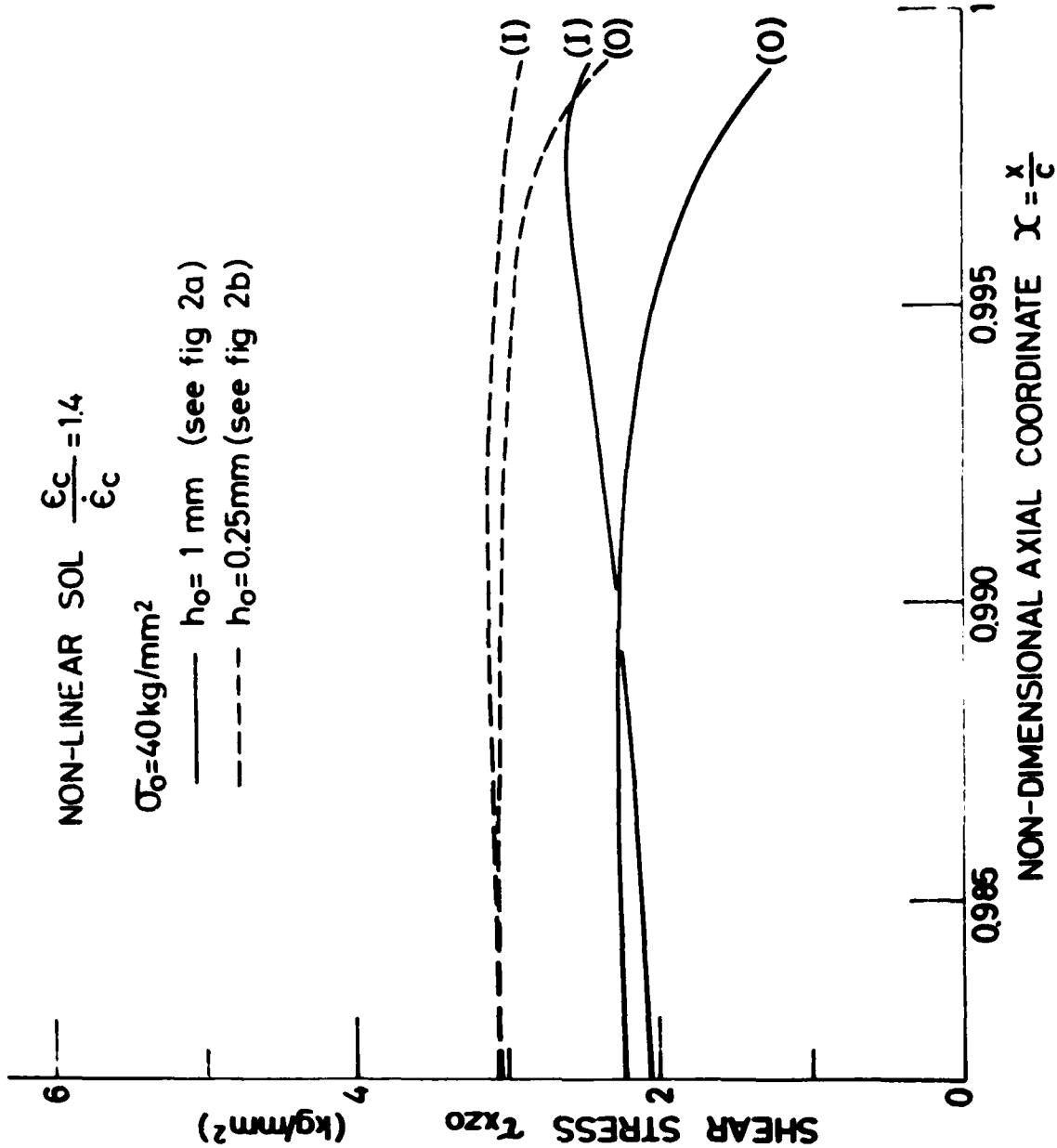


Fig. 7.6 The effect of IAL thickness on the shear stress (τ_{xz0}) distribution (non-linear solution with strain-rate effect).

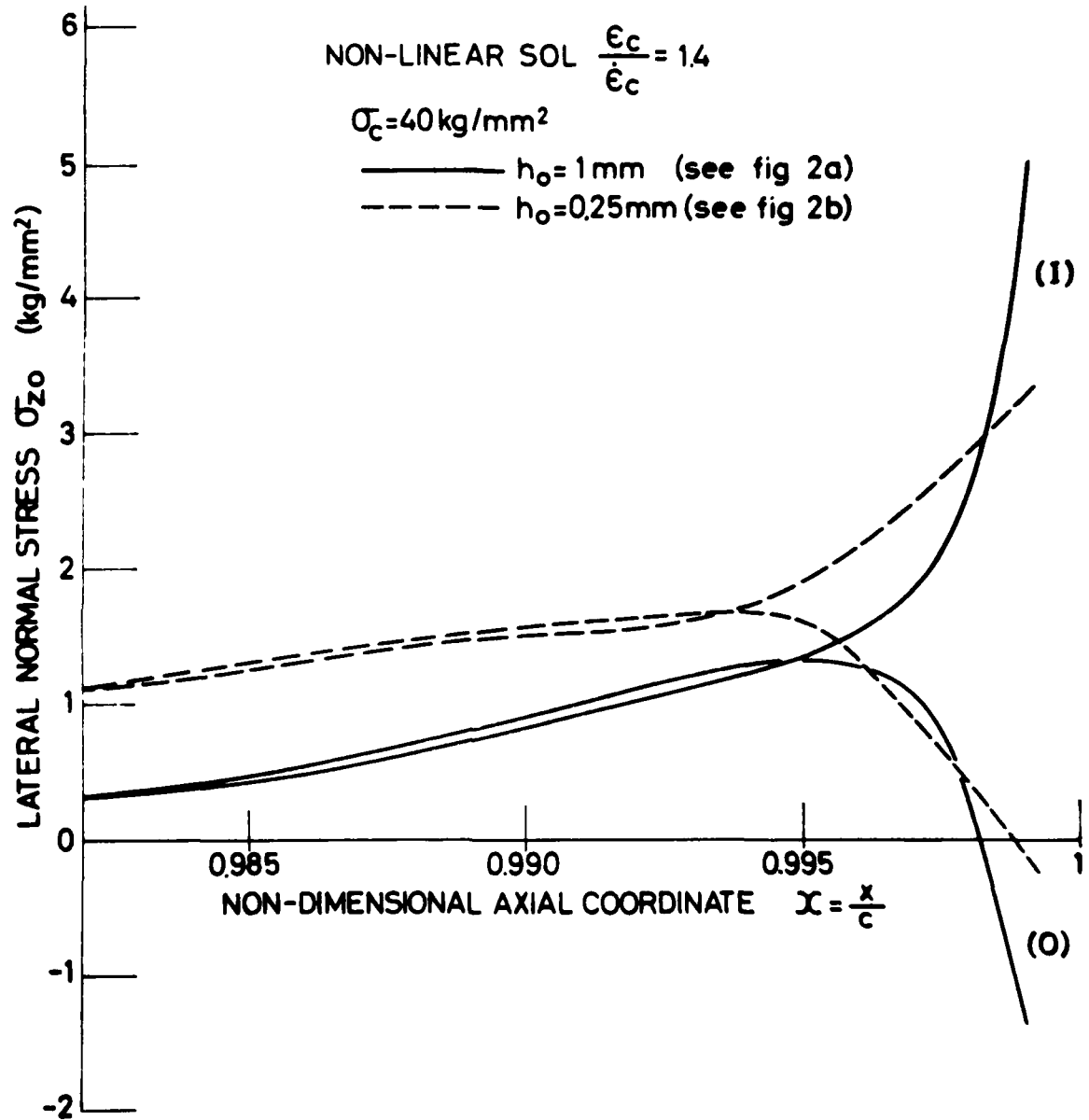


Fig. 7.7 The effect of IAL thickness on the lateral normal stress (σ_{z0}) distribution (non-linear solution with strain-rate effect).

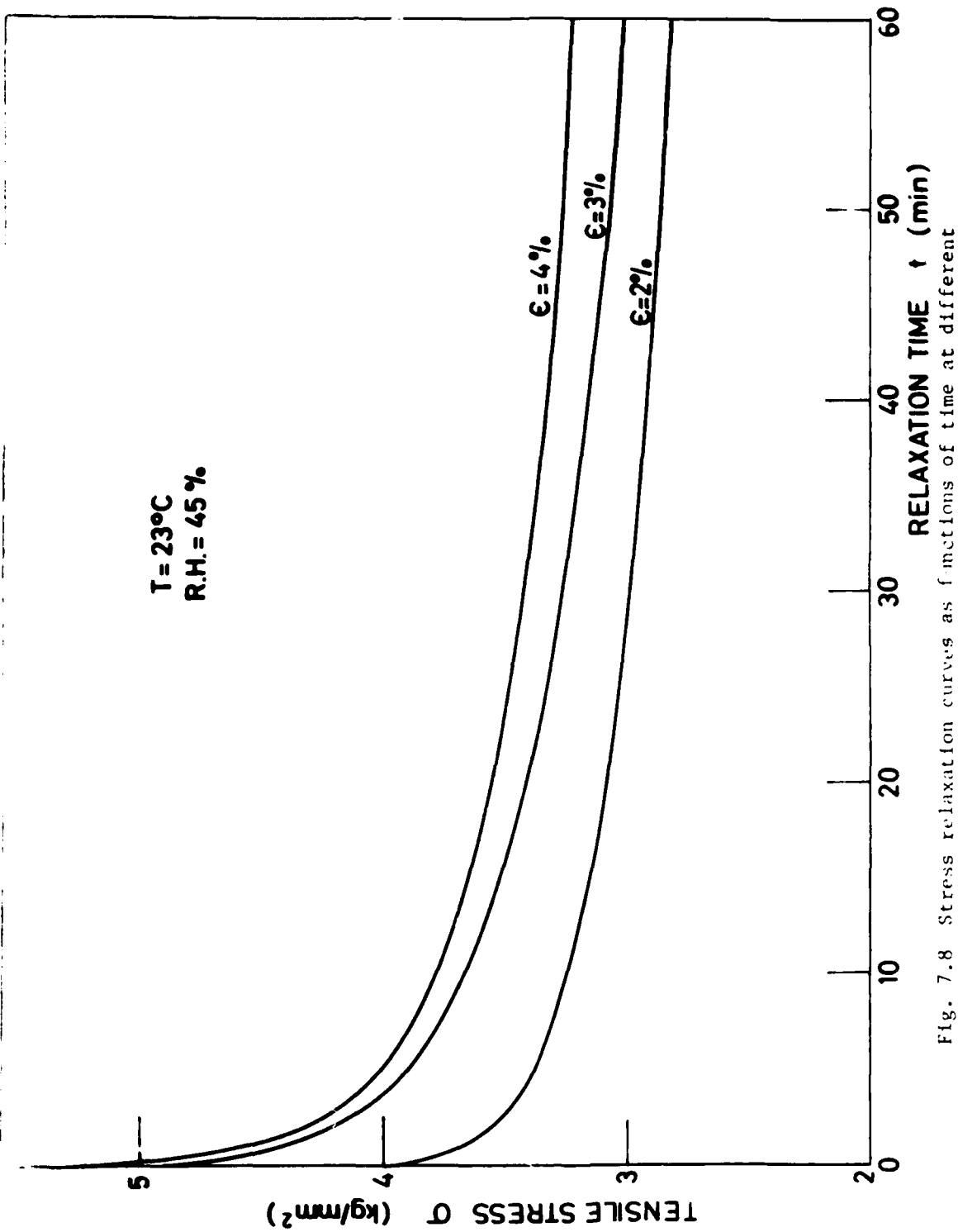


Fig. 7.8 Stress relaxation curves as functions of time at different strain (ϵ_0) levels.

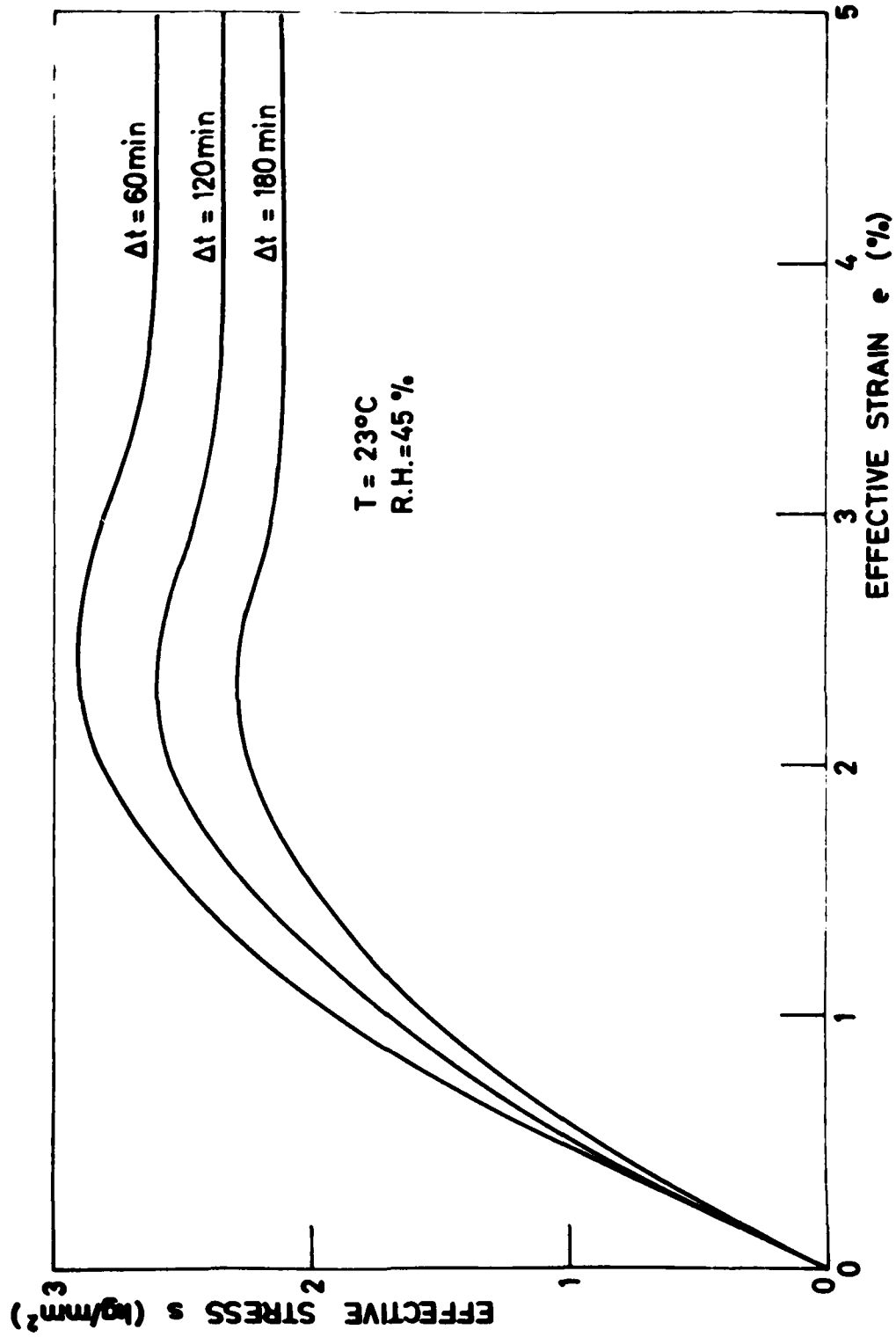


Fig. 7.9 Effective stress-strain relationships for different time intervals (Δt).

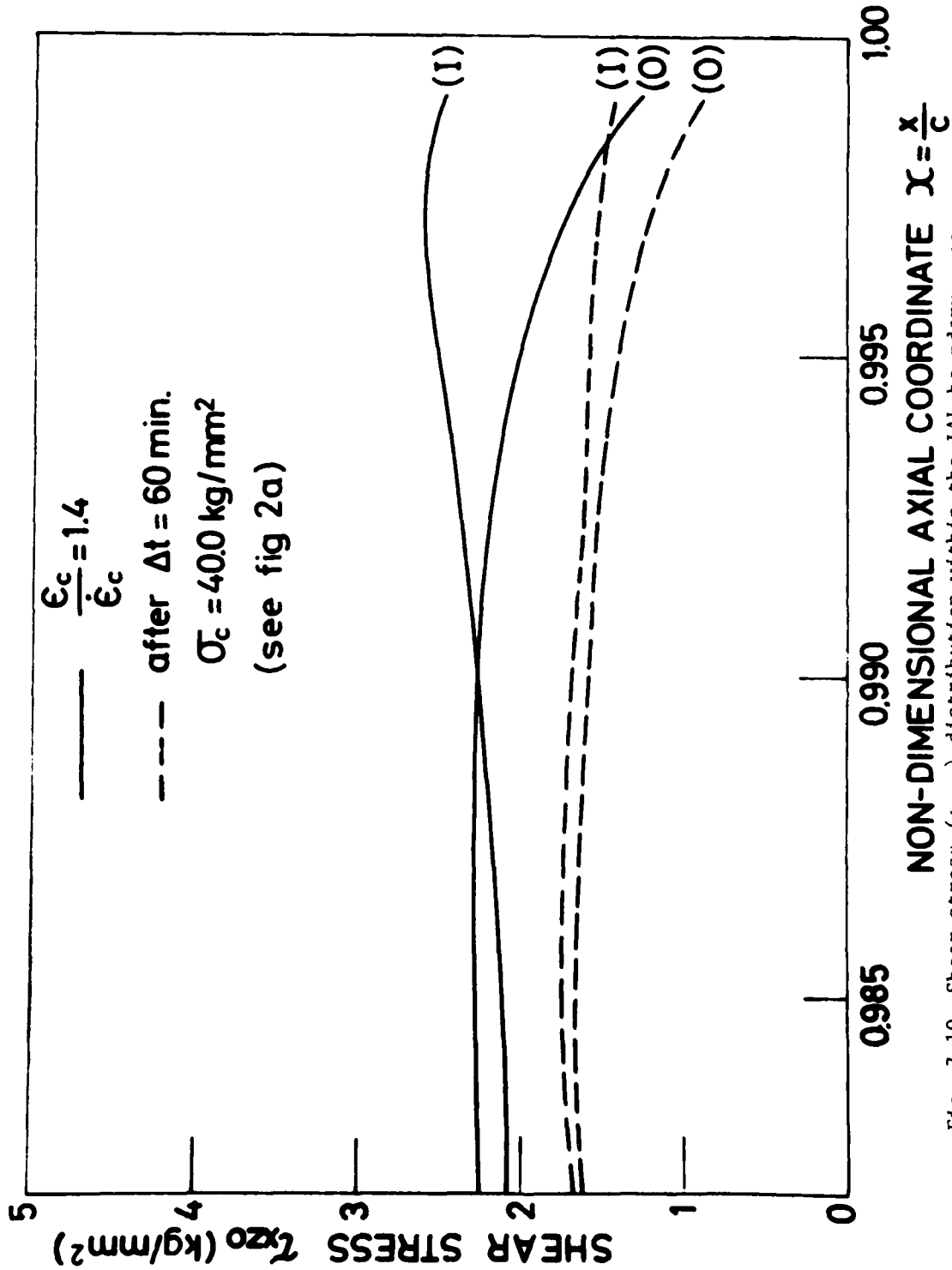


Fig. 7.10 Shear stress (τ_{xz0}) distribution within the IAL boundary zone
 at a time interval of $\Delta t = 60$ minutes (i.e. non-linear with
 strain rate effect solution).

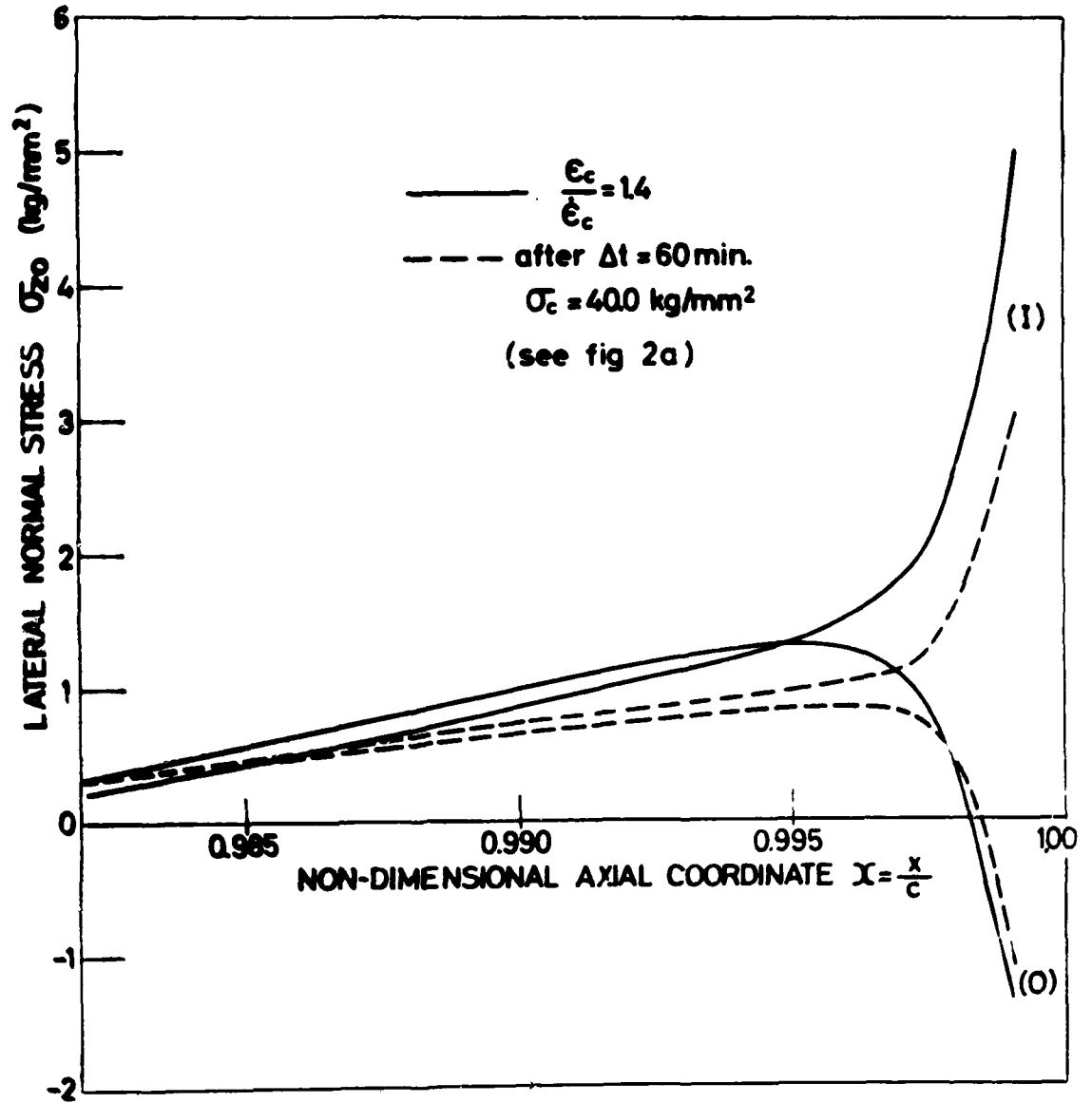


Fig. 7.11 Lateral normal stress (σ_{zo}) distribution within the IAL boundary zone at a time interval of $\Delta t = 60$ minutes (i.e. non-linear with strain rate effect solution).

cycle I

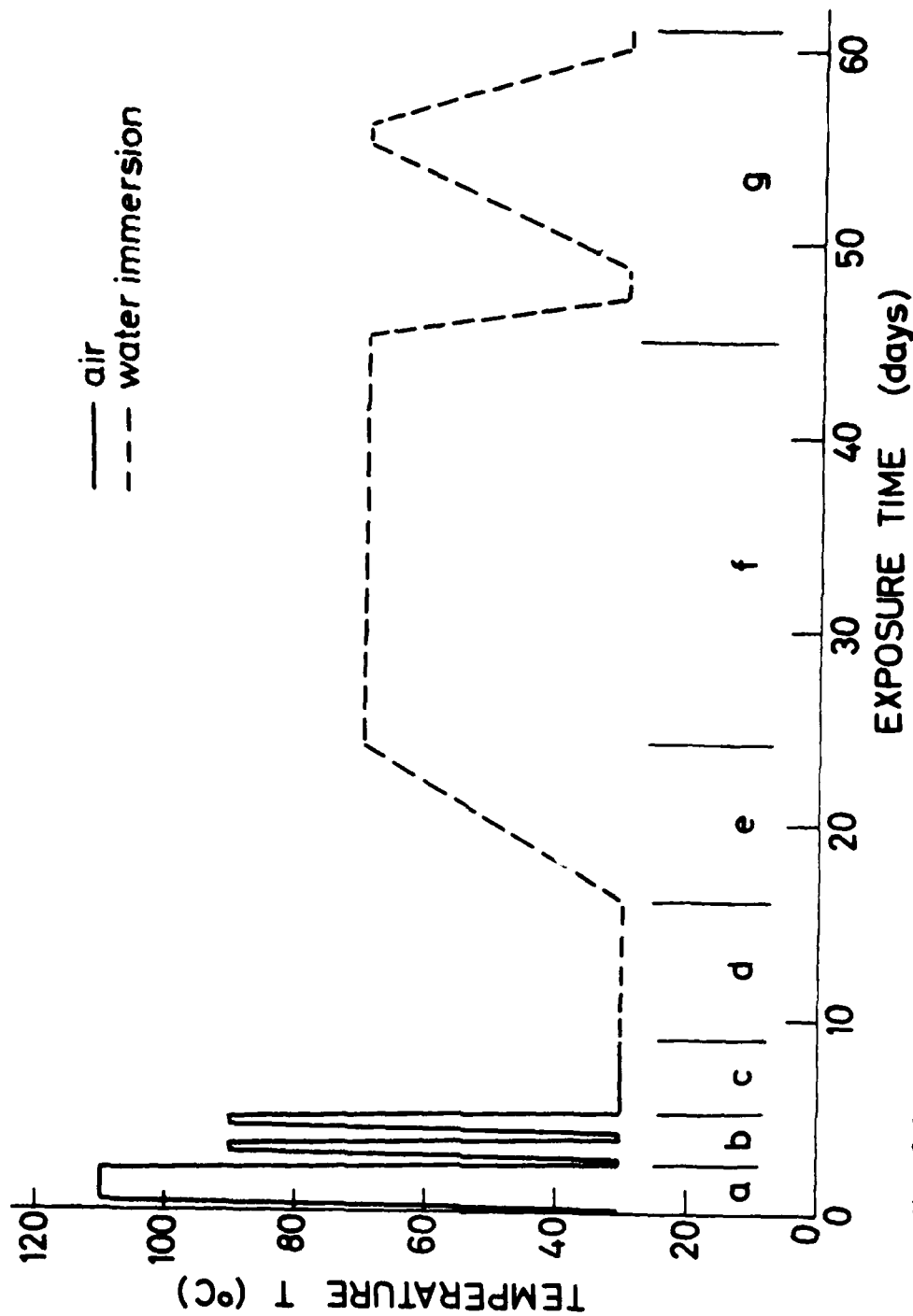


Fig. 8.1 Sequence of environmental history cycle No. I, for investigation of hygrothermal behavior of GFRP and adhesive specimens, representing the material constituents of a bonded system.

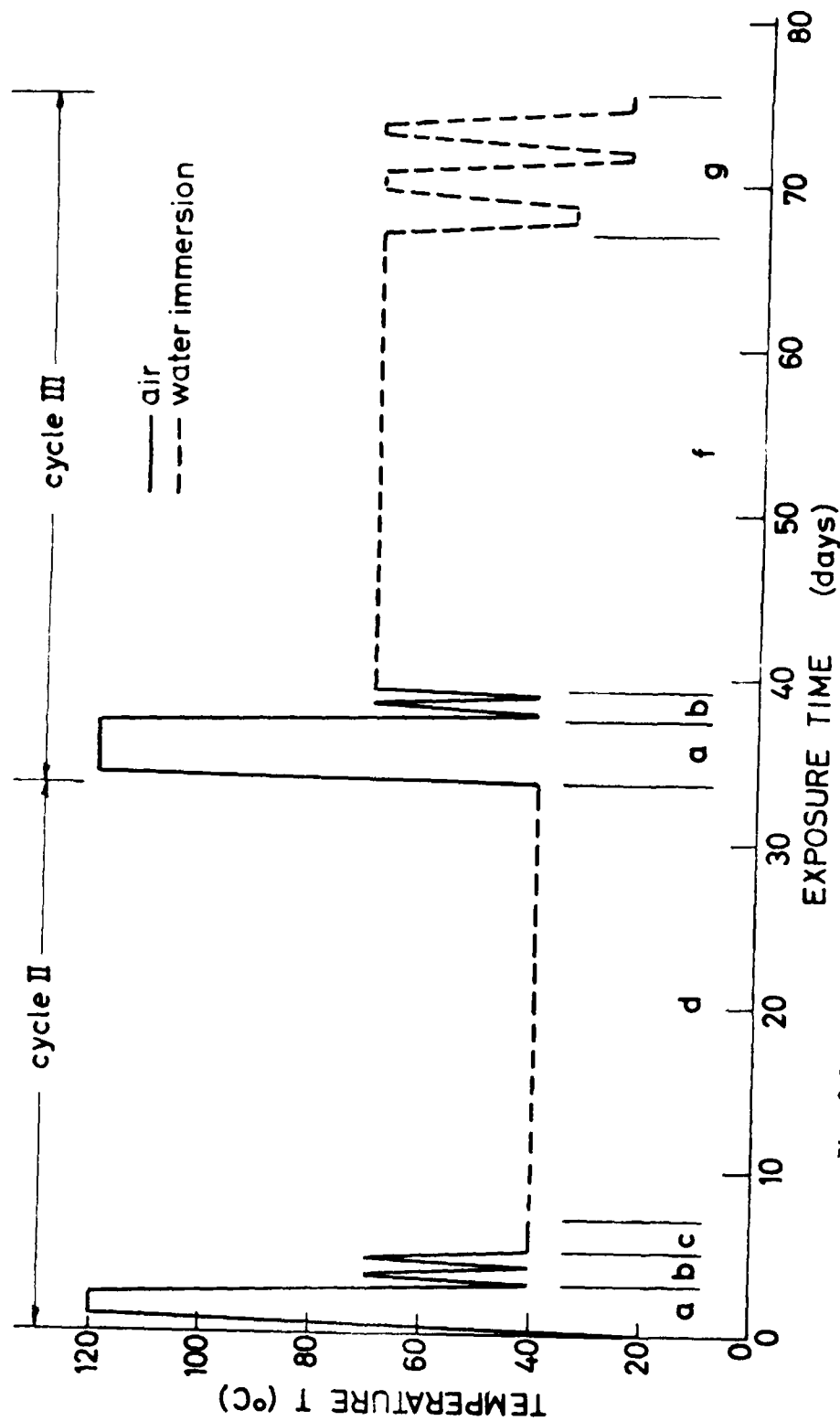


Fig. 8.2 Sequence of environmental history cycle Nos. II and III, for investigation of hygrothermal behavior of GFRP and adhesive specimens, representing the material constituents of a bonded system.

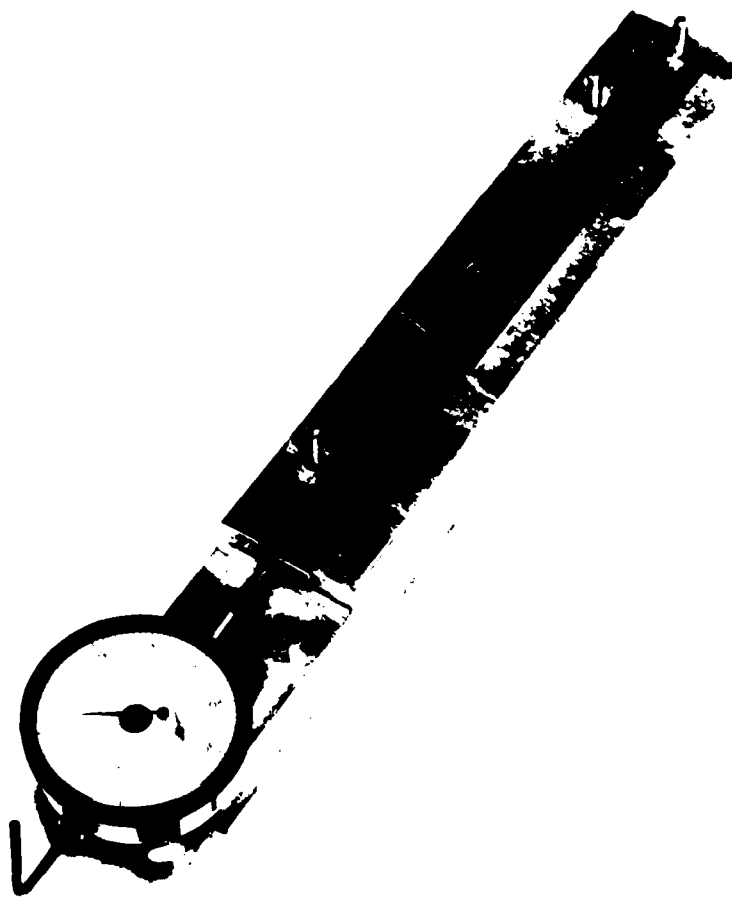


Fig. 8.3 Device for measuring the thermoelastic and the hygroelastic deformations of adhesive and FRP specimens under exposure to different hygrothermal (HT) conditions.

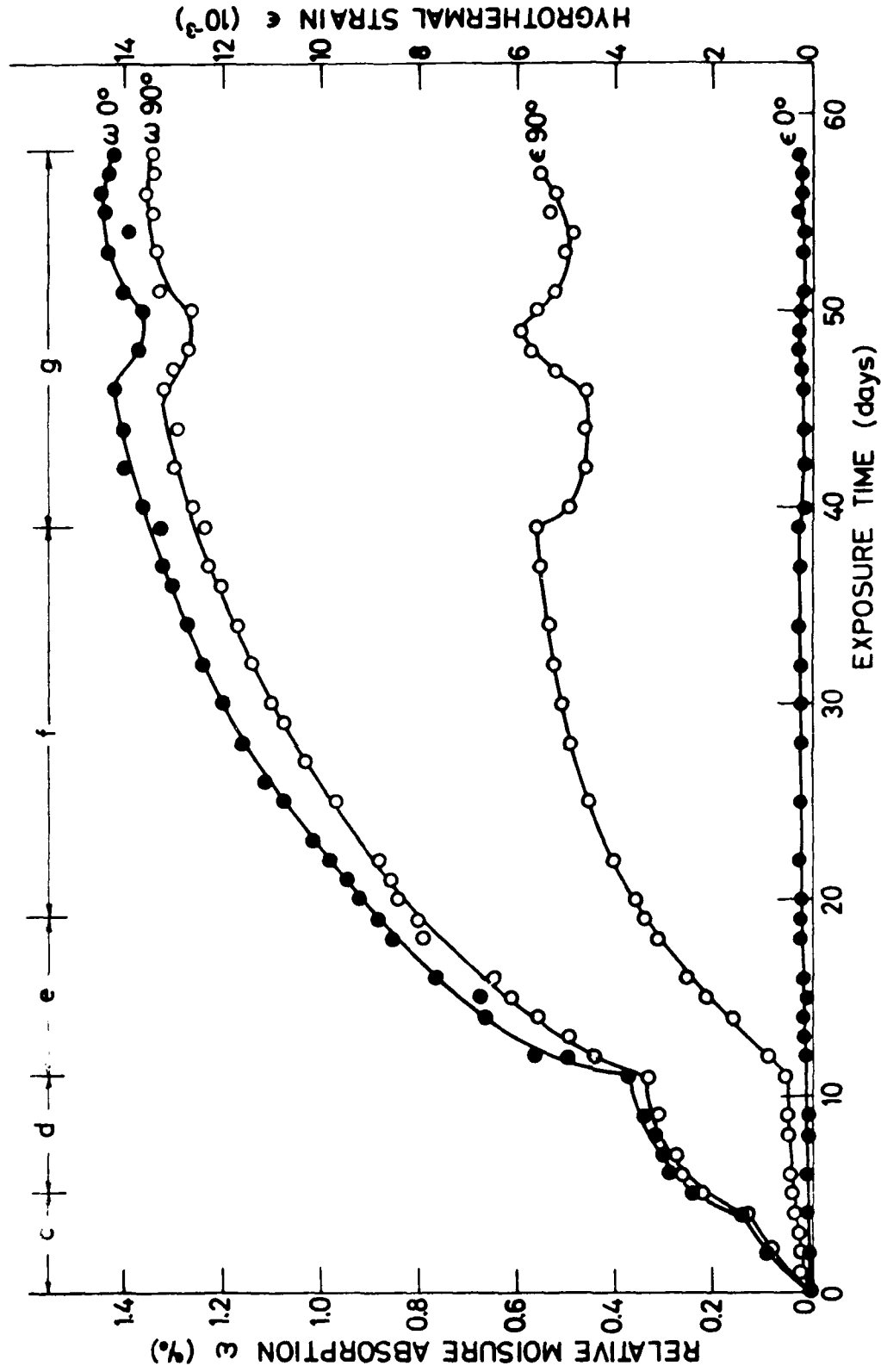


Fig. 8.4 Deformation and weight changes (absorption) vs. time curves for longitudinal and transverse U.D. GFRP specimens exposed to HT conditions during cycle i.

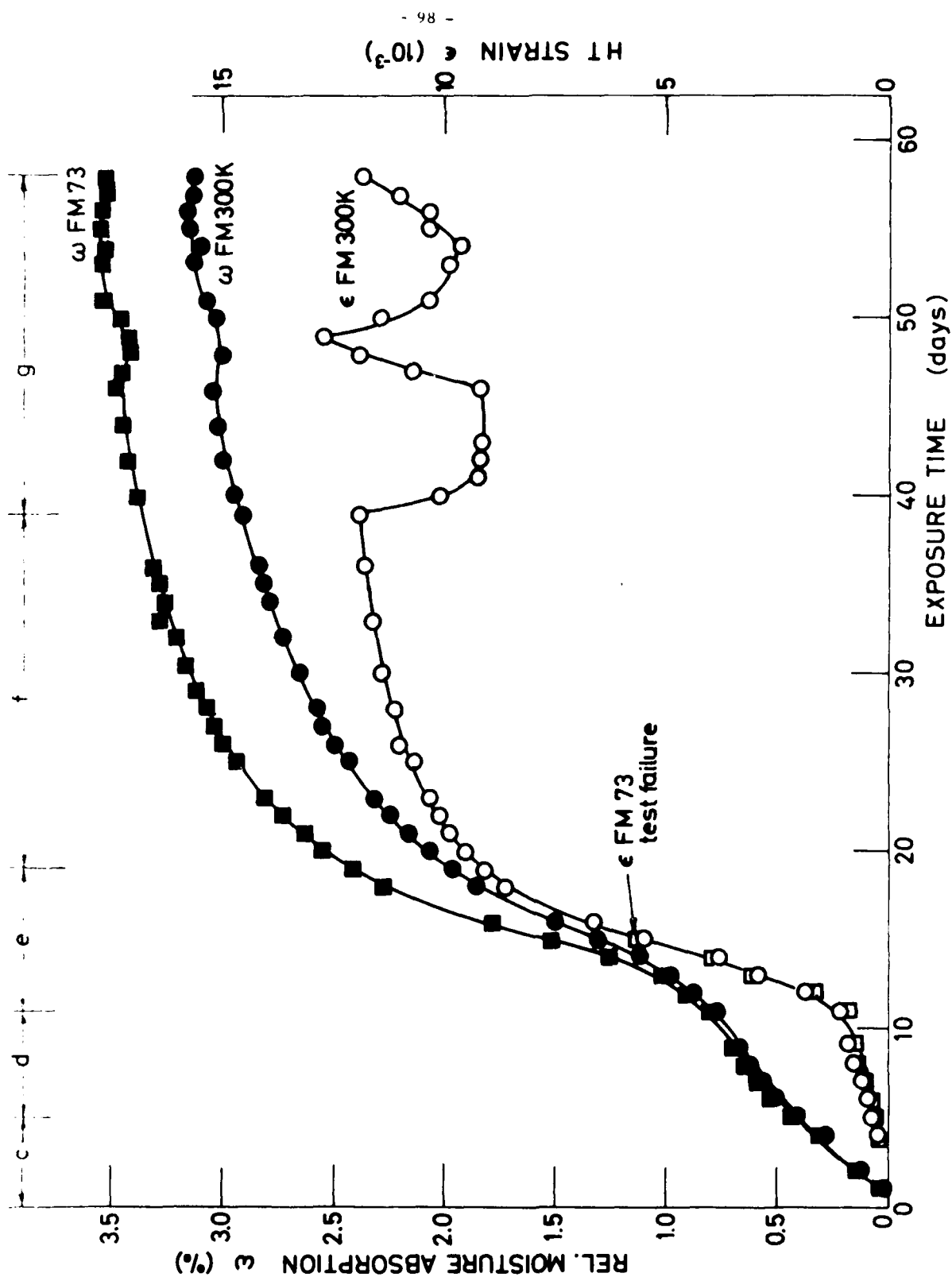


Fig. 8.5 Deformation and weight changes (absorption) vs. time curves for adhesive specimens exposed to HT conditions during cycle 1.

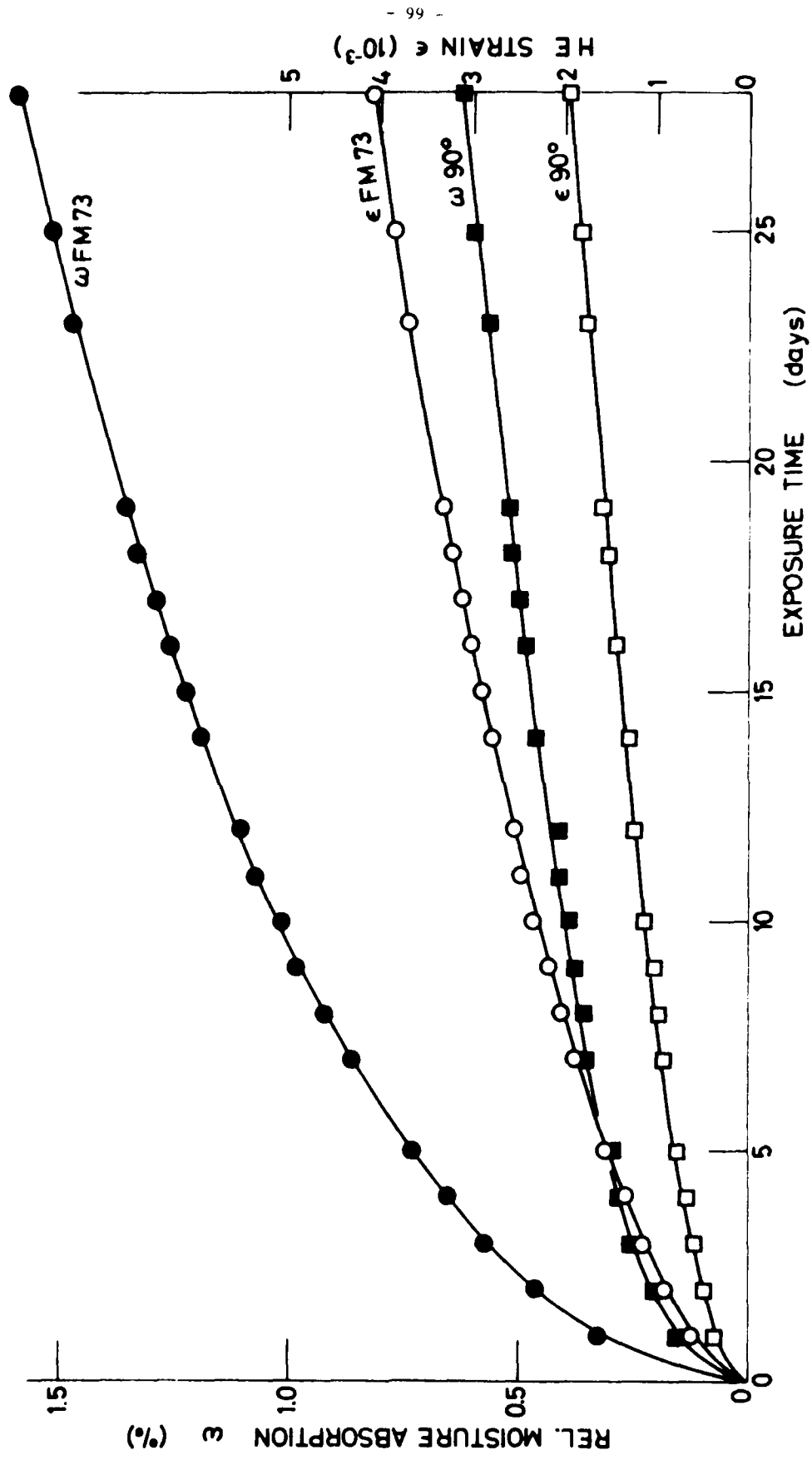


Fig. 8.6 Deformation and absorption vs. time curves for U.D. transverse CFRP and M73 adhesive specimens exposed to warm water (36°C) during cycle II.

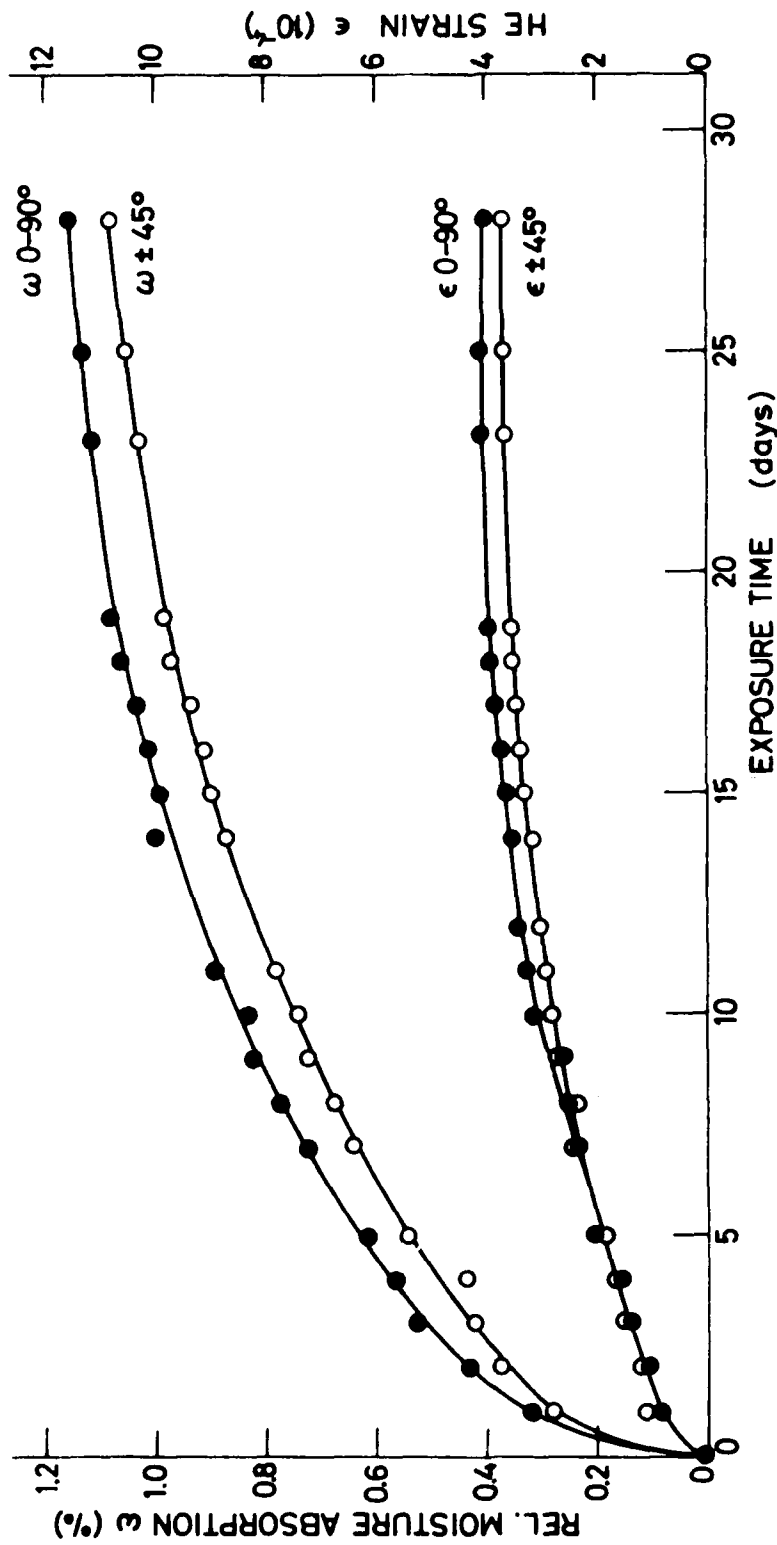


Fig. 8.7 Deformation and absorption vs. time curves for cross-ply and angle-ply CFRP specimens exposed to warm water during cycle 11.

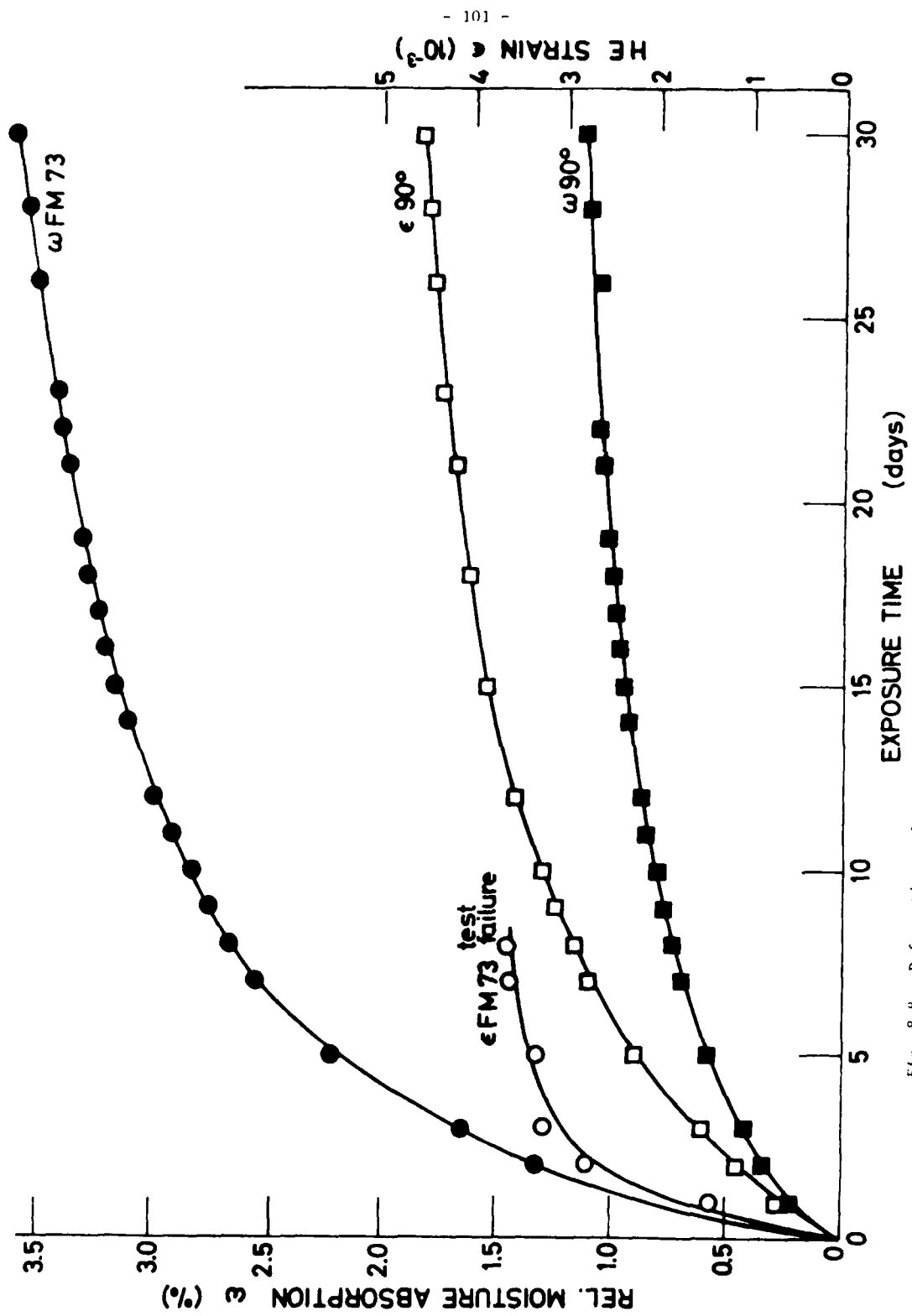


Fig. 8.8 Deformation and absorption vs. time curves for I.D. transverse CFRP and FM73 adhesive specimens exposed to hot-water (70°C) during cycle III.

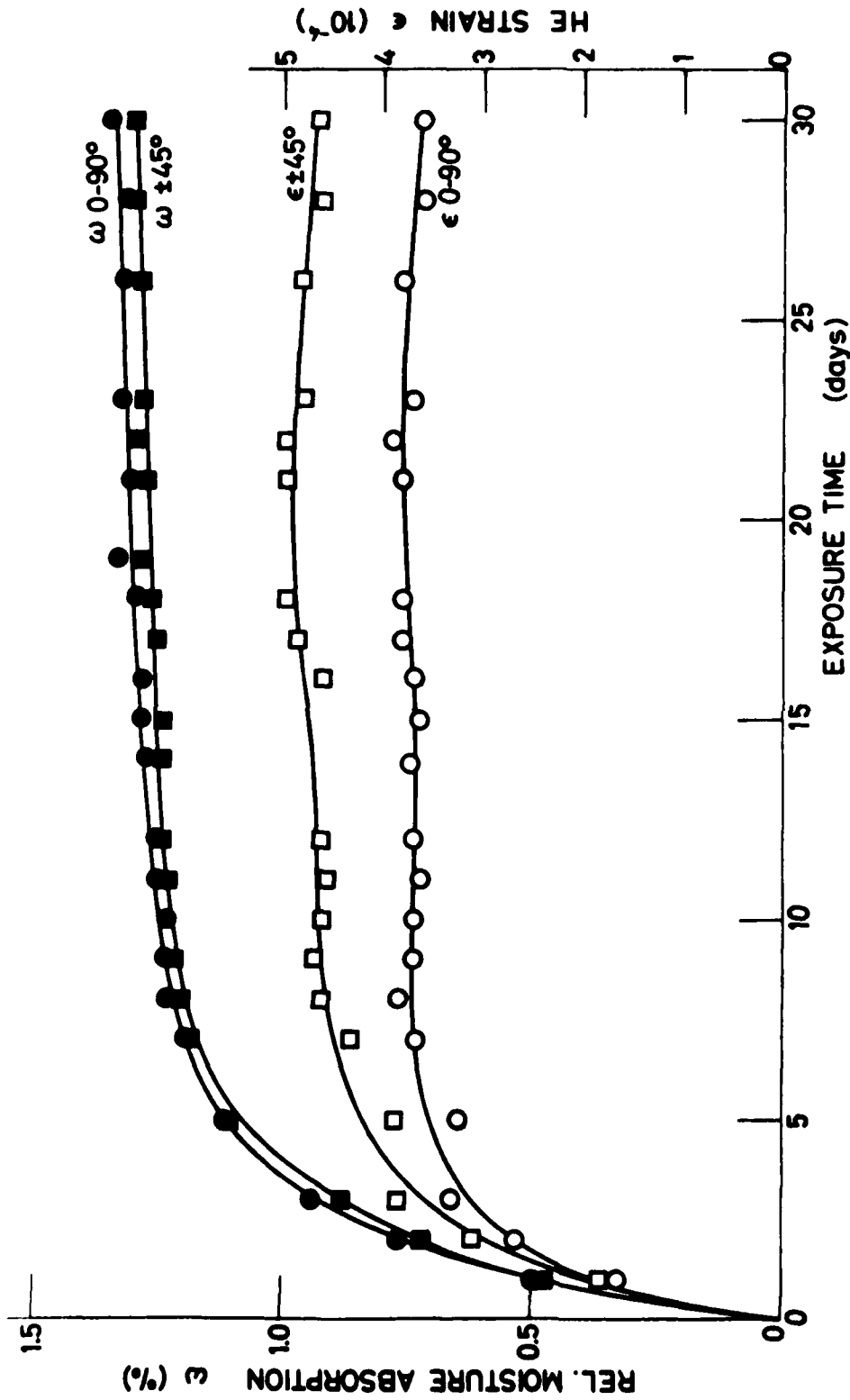


Fig. 8.9 Deformation and absorption vs. time curves for cross-ply and angle-ply CFRP specimens exposed to hot-water during cycle III.

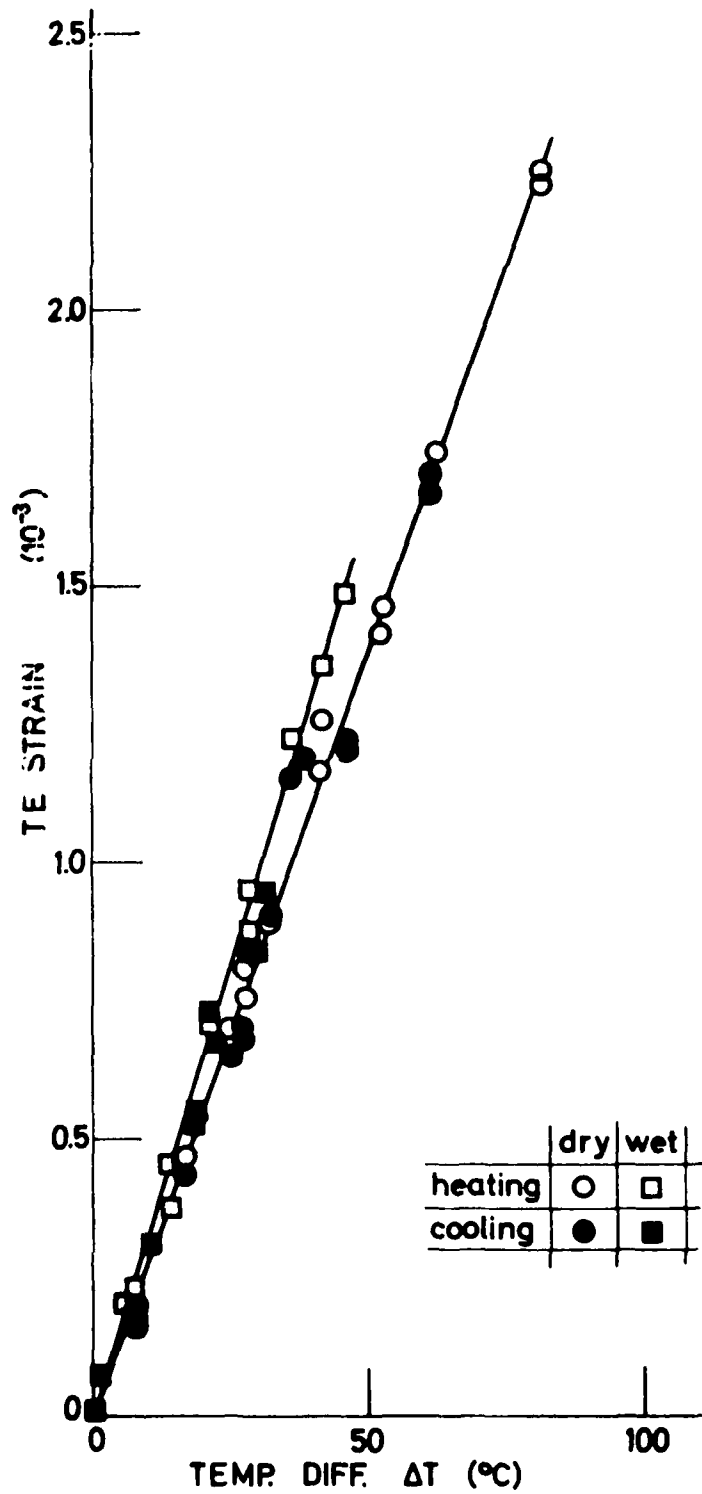


Fig. 8.10 Thermoelastic strain vs. temperature change for determination of CTE of dry and wet transverse CFRP specimens.

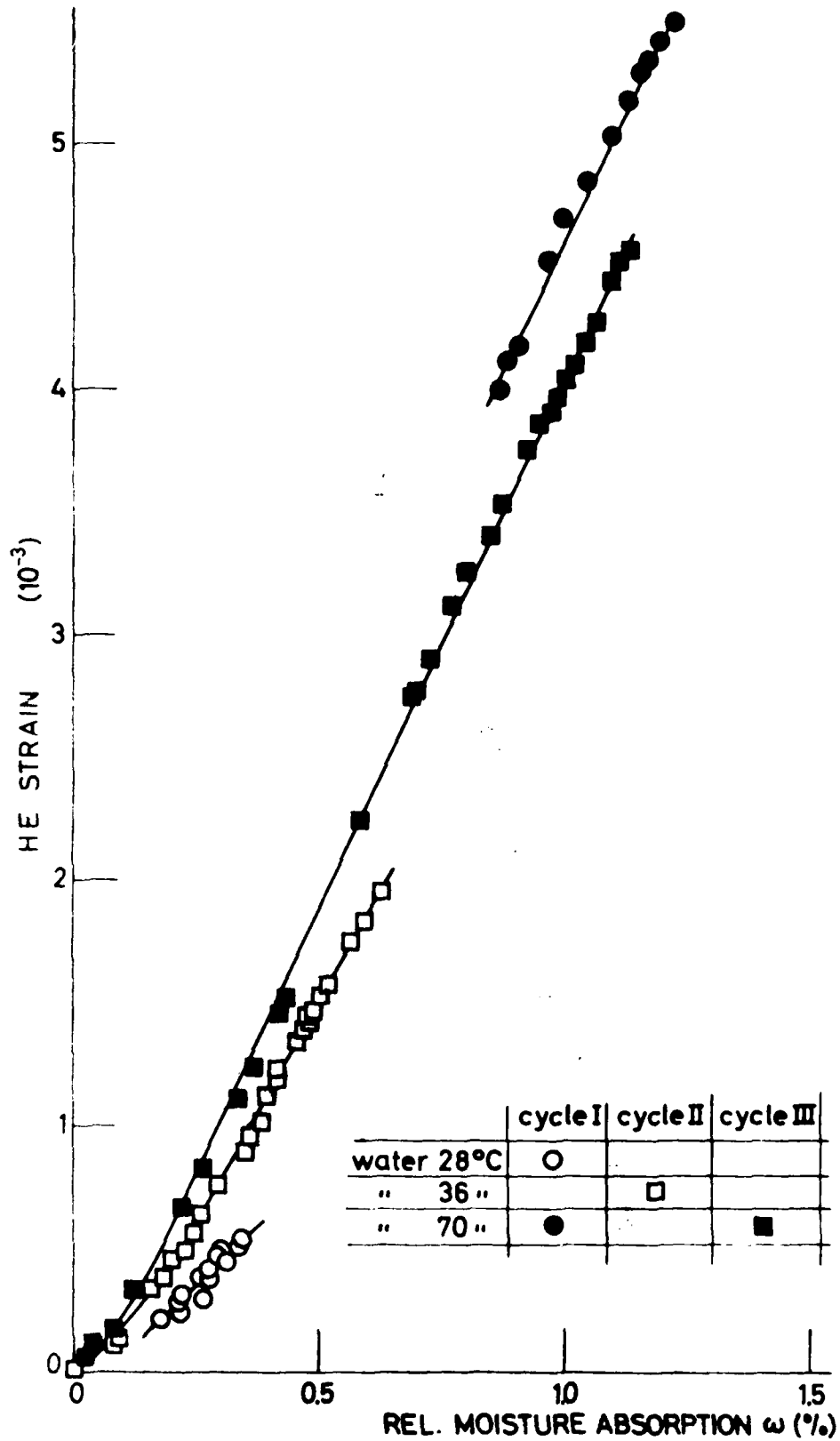


Fig. 8.11 Hygroelastic strains vs. moisture content for the determination of HEC of transverse U.D. CFRP specimens under water exposure at different temperature levels.

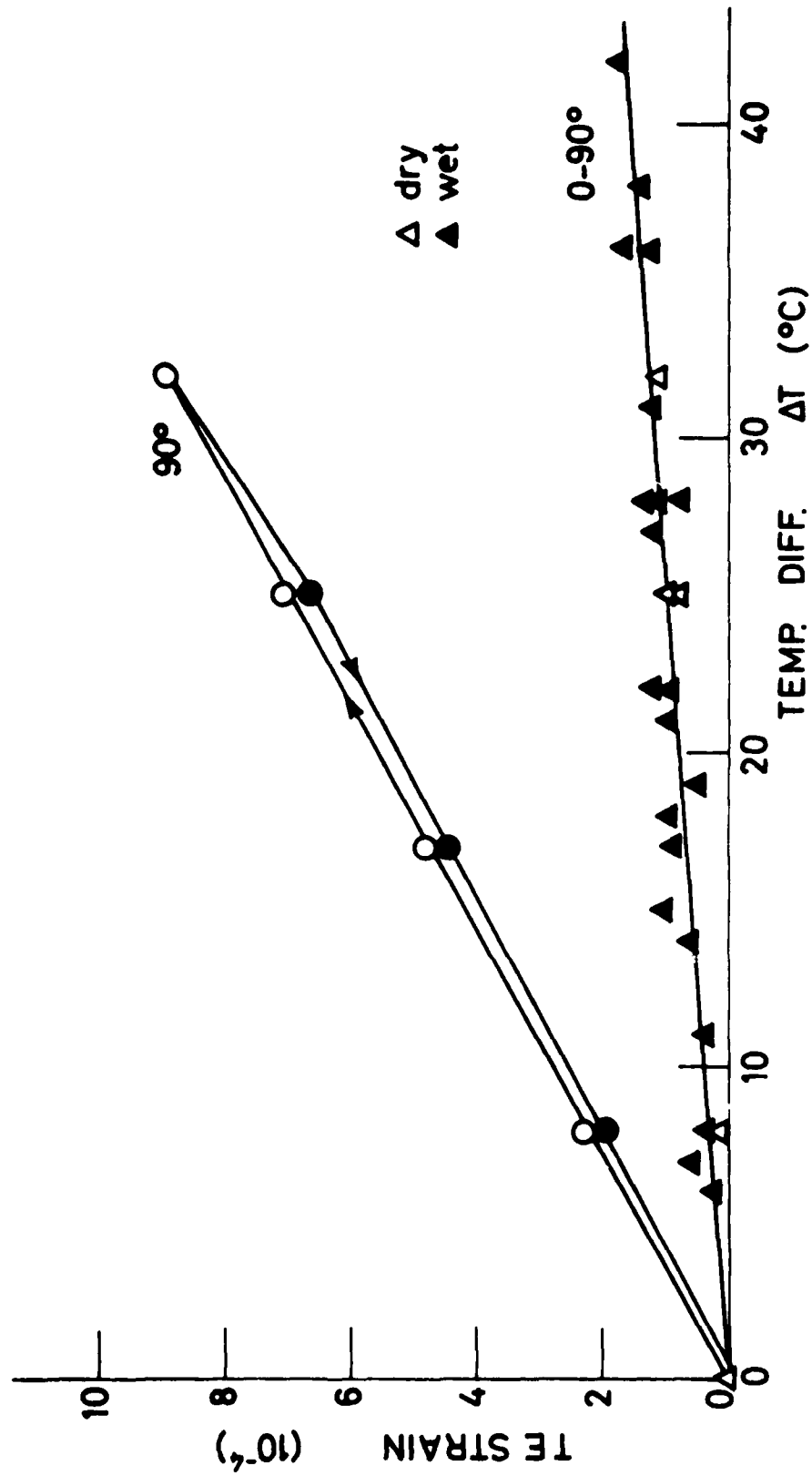


Fig. 8.12 Thermoelastic strain vs. temperature change for the determination of CTE of dry and wet cross-ply CFRP specimens (as compared to U.D. transverse reference).

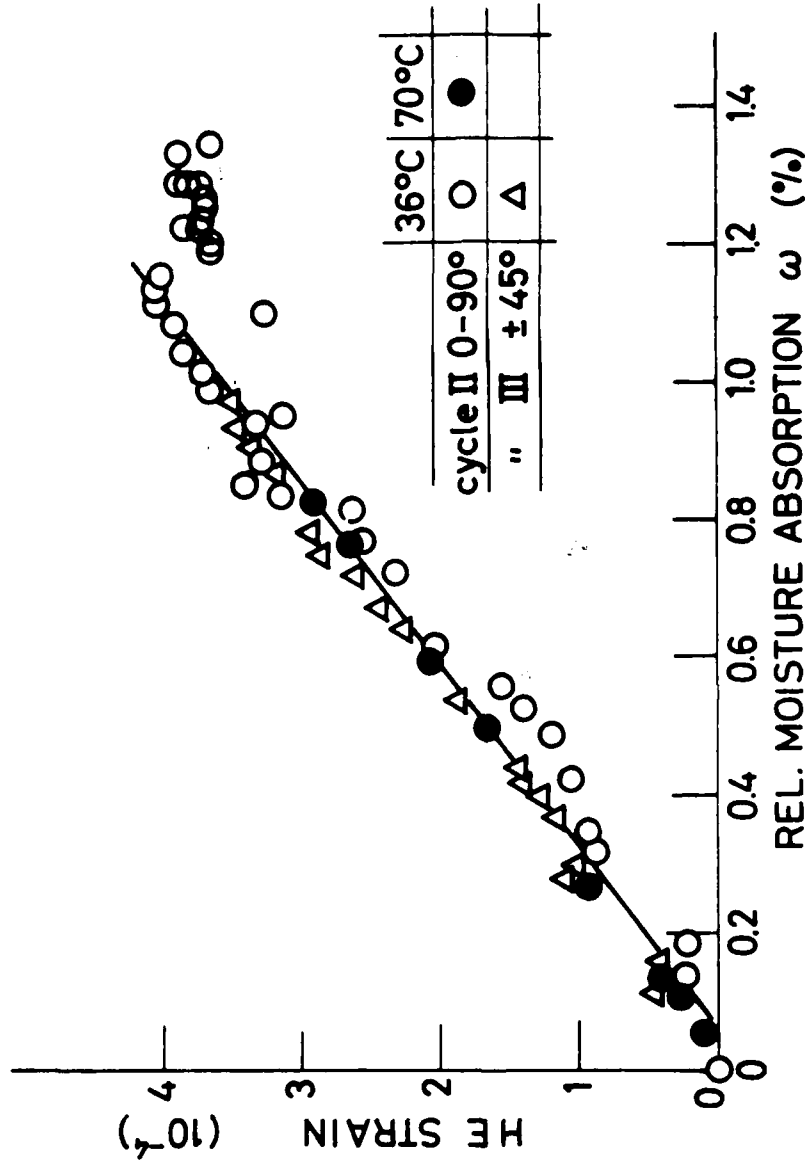


Fig. 8.13 Hygroelastic strains vs. moisture content for the determination of HEC of cross-ply and angle-ply CFRP specimens under water exposure at different temperature levels.

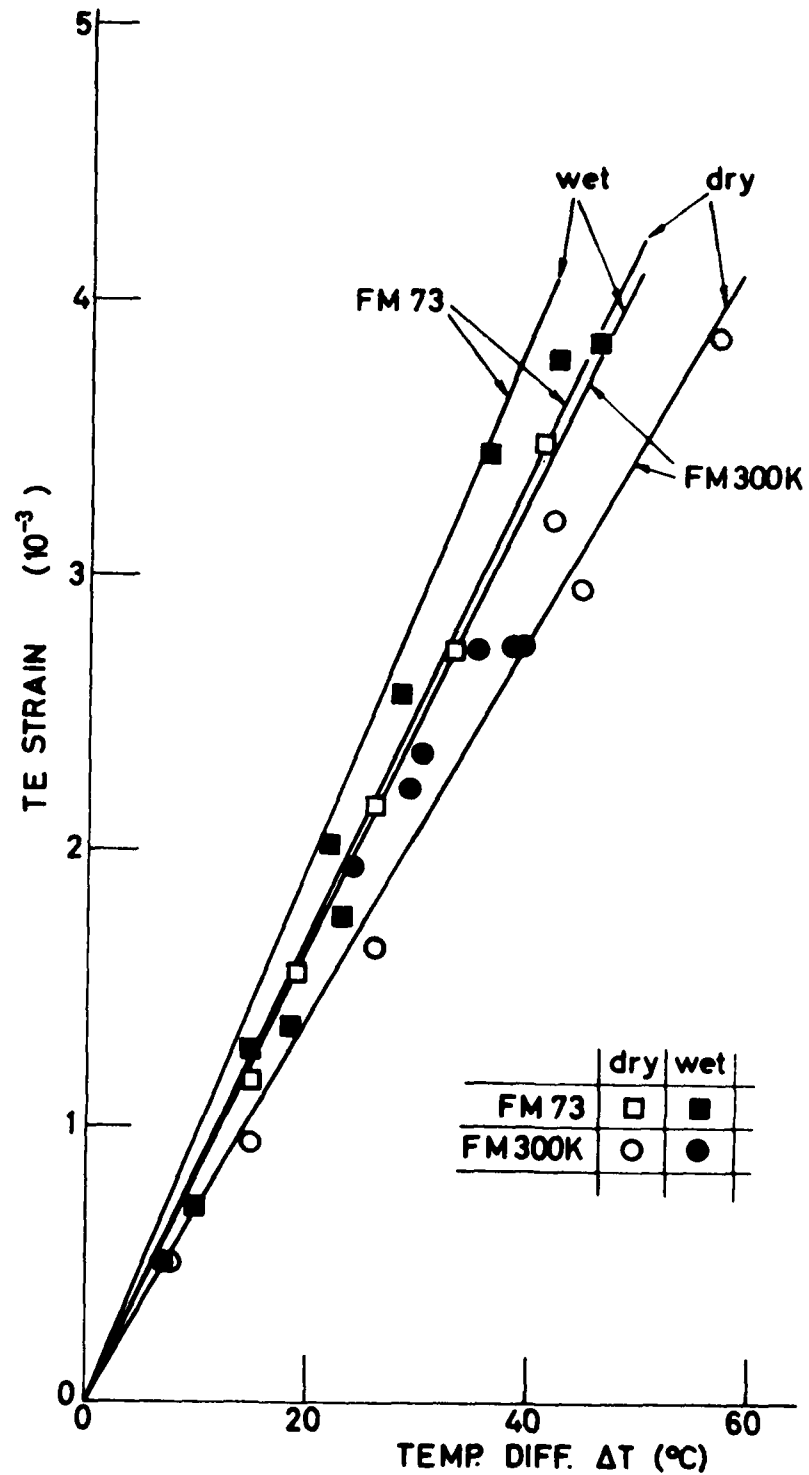


Fig. 8.14 Thermoelastic strain vs. temperature change for the determination of CTE of dry and wet FM73 and FM 300 K adhesive specimens.

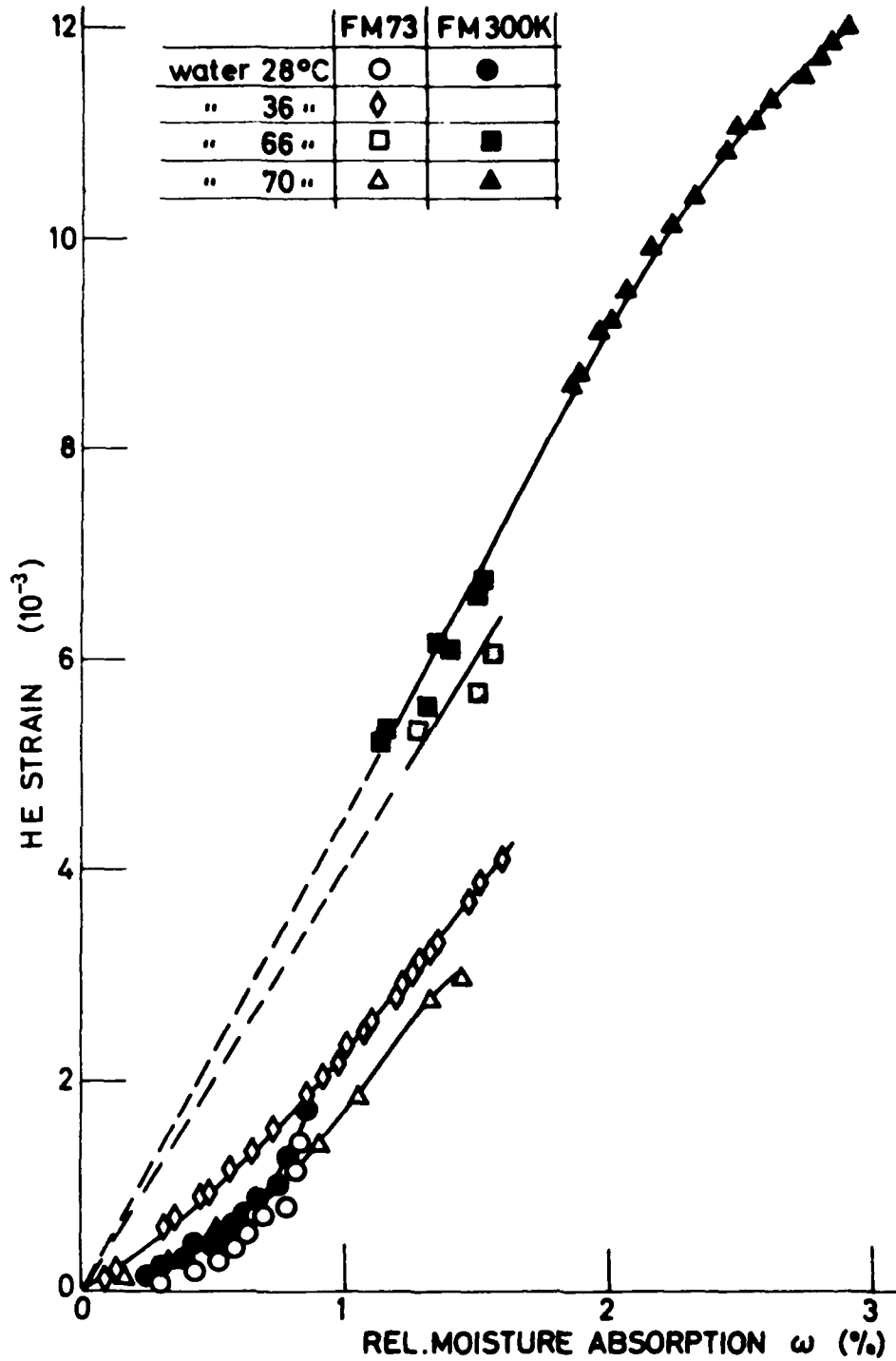


Fig. 8.15 Hydroelastic strains vs. moisture content for the determination of HEC of FM73 and FM 300 K adhesive specimens under water exposure at different temperature levels.

| Parametric Effect | On Adhesive Performance | | Interfacial Failure | FRP Adherend Failure | Bonded Joint Performance | |
|---------------------------------------|-------------------------|----------------------|---------------------|----------------------|--------------------------|-------------------|
| | Interlaminar Stresses | Strength and Failure | | | Static | Long-Term Dynamic |
| Increased Adhesive Thickness | lower | ? | better | better | + | - ? |
| Increased Adhesive Lap Length | lower | ? | better | ? | + | + |
| Increased Adhesive Stiffness | higher | ? | worse | worse | - | + |
| Increased Adhesive Toughness | ? | better | better | ? | + | + |
| Increased Adhesive Creep & Plasticity | lower | better | ? | ? | + | - |
| Tapering Adhesive Edge | lower | ? | better | better | + | + |
| Tapering Adherend Edge | lower | ? | better | better | + | + |
| Fastening Joint Edge | lower (peel) | ? | better | better | + | + |
| Higher Temperature | lower | worse | ? | ? | ? | ? |
| Moisture Penetration | lower | worse | worse | ? | ? | ? |

Table 1.1: Parametric effects on structural performance of adhesively bonded joints.

| ENVIRONMENTAL STAGE | MICROSTRUCTURAL MECHANISMS | EFFECT ON MACROMECHANICAL BEHAVIOUR | |
|--------------------------------------|--|---|--|
| | | INTERNAL STRESSES | STRENGTH AND STIFFNESS |
| | | RESIDUAL STRESSES IN MATRIX AND INTERFACES | |
| 1. DRY-R.T. CONDITION (AFTER CURING) | THERMOELASTIC CONTRACTION OF MATRIX RELATIVE TO FIBERS | | |
| 2. WET-R.T. CONDITIONS | HYGROELASTIC MATRIX SWELLING DUE TO SLOW ABSORPTION RATE | SLIGHT RELIEVE OF CURING STRESSES | SLIGHT CHANGES IN TRANSVERSE AND OFF-AXIS STRENGTH |
| 3. DRY-HOT CONDITION | THERMOELASTIC EXPANSION OF MATRIX RELATIVE TO FIBER. POST CURING OF MATRIX. FIBERS ALIGNMENT IN TENSION. | RELIEVE OF CURING STRESSES. STRESS-RELAXATION | REDUCTION IN TRANSVERSE AND OFF-AXIS PROPERTIES. INCREASE IN LONGITUDINAL STRENGTH |
| 4. WET-HOT CONDITIONS (UN-LOADED) | ACCELERATED HYGROELASTIC PROCESS. MATRIX PLASTIFICATION. INTERFACIAL DEBONDING AND RE-BONDING. | ACCELERATED STRESS RELIEVE AND RELAXATION. | SIGNIFICANT REDUCTION IN TRANSVERSE AND OFF-AXIS STRENGTH AND STIFFNESS |
| 5. WET-HOT CONDITIONS (LOADED) | DEGRADATION OF FIBER SURFACES AND INTERFACES. "STRESS CORROSION" OF FIBERS. INTERFACIAL DEBONDING PROPAGATION. | " | SIGNIFICANT REDUCTION IN TRANSVERSE AND LONGITUDINAL STRENGTH ABOVE CRITICAL LOAD. |

Table 2.1: Modes of behavior during different stages of hygrothermal exposure of FRP laminates.

Table 3.1: Data of coefficient of thermal expansion (CTE) for different U.D. FRP materials, from literature sources.

| Material System | FRP Specification | Fiber volume content V_f | Coefficient of thermal expansion [$10^{-6} \text{ } ^\circ\text{C}^{-1}$] | | Source Reference | Comments |
|--|---|-------------------------------------|---|--|------------------------------|--------------------------|
| | | | Longitudinal α_1 | Transverse α_2 | | |
| CFRP | Celanese 350/A Chemstrand | | 0 0 | 75.0 55.0 | 1970 [58] | |
| CFRP GFRP | HTS-ERLA E glass-epoxy | 0.52 0.55 | 3.0 12.0 | 44.0 37.0 | 1975 [59] | Immersed in boiled water |
| KFRP GFRP CFRP | K49/ERLA S-glass/ERLA HMS/ERLA | | - 4.0 12.0 0.6 | 66 25 33 | 1977 [73] | |
| CFRP CFRP | HTS/ERLA HMS/ERLA | ~ 0.50 ~ 0.50 | - 1.2 - 1.2 | 27.3 27.3 | 1977 [60] | |
| CFRP | T300/Ep 828 | 0.65 | - 0.3 | 33.0 | 1978 [61] | |
| KFRP CFRP | 49/PR-286 HTS | 0.5 0.5 | - 2.1 - 1.2 | 60-80 27-33 | 1979 [62] | |
| CFRP | GY 70/339 | | - 0.7 | 25.2 | 1979 [25] | |
| CFRP CFRP GFRP KFRP | HTS/epoxy HMS/epoxy E glass/epoxy K49 epoxy | | - 0.9 0.0 6.3 0.02 | 35.0 32.0 21.0 57.0 | 1980 [64] | General average data |
| CFRP CFRP CFRP BFRP GFRP KFRP | T300/5208 AS/3501 HMS/3002M B(4)550S E glass/Schotch ply1002 Kevlar 49/epoxy | ~ 0.70 0.48 0.45 | 0.02 - 0.3 - 0.23 6.1 8.6 - 4.0 | 22.5 28.1 33.5 30.3 22.1 79.0 | 1980 [53] 1977 [52] | General average data |

CFRP - Carbon FRP
GFRP - Glass FRP

KFRP - Kevlar FRP
BFRP - Boron FRP

| HT Coefficients | Ambient Conditions | Adhesives | | C F R P | | | |
|---|-----------------------|-----------|--------|---------------------|---------------------|-----------------------|----------------------------------|
| | | FM73 | FM300K | Approximation 0° | Experimental 90° | Experimental 0/90° | Computed Exper. cmptd. 45° |
| α CTE 10 ⁻⁶ /C° | Dry | 85.0 | 70.0 | 0 | 27.5 | 3.51 | 1.84 |
| | Wet | 97.0 | 84.0 | 0 | 30.2 | 3.44 | 2.24 |
| β HEC | 36°C | 0.31 | 0.40 | 0 | 0.30 | 0.042 | 0.023 |
| | 70°C | 0.40 | 0.47 | 0 | 0.43 | 0.035 | 0.033 |

Table 8.1: Coefficient of thermal expansion (CTE) and hygroelastic coefficients (HEC) for FRP and adhesive specimens exposed to different hygrothermal conditions.

Appendix 1: Hygrothermal data evaluation for transverse L.D. CFRP specimen exposed to hot water during cycle III.

| NP | PH | TEMP | DATE | OMEGA | EPSILON TOTAL | DELTAT |
|-----|-----|------|----------|-----------|----------------|--------|
| 000 | IMM | 69 | 050010.7 | +0.000000 | 0 | +00 |
| 001 | IMM | 69 | 050012.0 | +0.000414 | 7.2029846E-05 | +00 |
| 002 | IMM | 69 | 050013.0 | +0.039905 | 1.20049747E-04 | +00 |
| 003 | IMM | 69 | 050014.3 | +0.080094 | 1.73124376E-04 | +00 |
| 004 | IMM | 69 | 050019.5 | +0.119999 | 3.32348250E-04 | +00 |
| 005 | IMM | 70 | 050407.8 | +0.218639 | 6.85714411E-04 | +01 |
| 006 | IMM | 70 | 050414.5 | +0.261442 | 8.22192016E-04 | +01 |
| 007 | IMM | 70 | 050507.8 | +0.335940 | 1.12800296E-03 | +01 |
| 008 | IMM | 70 | 050515.0 | +0.372921 | 1.23794326E-03 | +01 |
| 009 | IMM | 70 | 050607.8 | +0.423335 | 1.46666962E-03 | +01 |
| 010 | IMM | 70 | 050611.5 | +0.429442 | 1.51974424E-03 | +01 |
| 011 | IMM | 72 | 050812.0 | +0.578412 | 2.24164074E-03 | +03 |
| 012 | IMM | 73 | 051007.8 | +0.686056 | 2.74917606E-03 | +04 |
| 013 | IMM | 73 | 051014.9 | +0.707358 | 2.75595915E-03 | +03 |
| 014 | IMM | 72 | 051108.0 | +0.732920 | 2.90001884E-03 | +03 |
| 015 | IMM | 72 | 051208.0 | +0.776944 | 3.11231734E-03 | +03 |
| 016 | IMM | 72 | 051309.0 | +0.803926 | 3.26775010E-03 | +03 |
| 017 | IMM | 72 | 051408.0 | +0.853630 | 3.39411833E-03 | +03 |
| 018 | IMM | 72 | 051508.0 | +0.876776 | 3.53944171E-03 | +03 |
| 019 | IMM | 72 | 051708.0 | +0.921795 | 3.75932231E-03 | +03 |
| 020 | IMM | 72 | 051808.5 | +0.949914 | 3.86799892E-03 | +03 |
| 021 | IMM | 71 | 051908.0 | +0.970789 | 3.90511036E-03 | +02 |
| 022 | IMM | 71 | 052008.0 | +0.986268 | 3.97840389E-03 | +02 |
| 023 | IMM | 71 | 052108.0 | +1.004446 | 4.04158797E-03 | +02 |
| 024 | IMM | 71 | 052209.0 | +1.020493 | 4.10224469E-03 | +02 |
| 025 | IMM | 71 | 052408.0 | +1.042931 | 4.19575713E-03 | +02 |
| 026 | IMM | 71 | 052508.0 | +1.055428 | 4.23745861E-03 | +02 |
| 027 | IMM | 71 | 052608.0 | +1.065227 | 4.34487155E-03 | +02 |
| 028 | IMM | 71 | 052908.5 | +1.095759 | 4.43964766E-03 | +02 |
| 029 | IMM | 71 | 053108.0 | +1.114079 | 4.51167752E-03 | +02 |
| 030 | IMM | 71 | 060208.0 | +1.136232 | 4.57107055E-03 | +02 |

Appendix 2: Hygrothermal data evaluation for cross-ply CFRP specimens exposed to hot water during cycle III.

| NP | PH | TEMP | DATE | OMEGA | EPSILON TOTAL | DELTAT |
|-----|-----|------|----------|-----------|-----------------|--------|
| 000 | IMM | 69 | 050010.7 | +0.000000 | 0 | +00 |
| 001 | IMM | 69 | 050012.0 | +0.069648 | 7.58208092E-06 | +00 |
| 002 | IMM | 69 | 050013.0 | +0.113828 | 2.52736325E-05 | +00 |
| 003 | IMM | 69 | 050014.3 | +0.141896 | 3.91741252E-05 | +00 |
| 004 | IMM | 69 | 050019.5 | +0.273917 | 9.60397947E-05 | +00 |
| 005 | IMM | 70 | 050407.8 | +0.502094 | 1.66663648E-04 | +01 |
| 006 | IMM | 70 | 050414.5 | +0.600850 | 2.04579104E-04 | +01 |
| 007 | IMM | 70 | 050507.8 | +0.767175 | 2.60181089E-04 | +01 |
| 008 | IMM | 70 | 050515.0 | +0.827988 | 2.81663678E-04 | +01 |
| 009 | IMM | 70 | 050607.8 | +0.937139 | 3.28419899E-04 | +01 |
| 010 | IMM | 70 | 050611.5 | +0.955591 | 3.10728354E-04 | +01 |
| 011 | IMM | 72 | 050812.0 | +1.109182 | 3.23090538E-04 | +03 |
| 012 | IMM | 73 | 051007.8 | +1.191305 | 3.63391031E-04 | +04 |
| 013 | IMM | 72 | 051014.9 | +1.204299 | 3.63528354E-04 | +03 |
| 014 | IMM | 72 | 051108.0 | +1.229768 | 3.83747251E-04 | +03 |
| 015 | IMM | 72 | 051208.0 | +1.230287 | 3.68583075E-04 | +03 |
| 016 | IMM | 72 | 051309.0 | +1.223011 | 3.68583075E-04 | +03 |
| 017 | IMM | 72 | 051408.0 | +1.255756 | 3.58473619E-04 | +03 |
| 018 | IMM | 72 | 051508.0 | +1.257315 | 3.67319391E-04 | +03 |
| 019 | IMM | 72 | 051708.0 | +1.269530 | 3.636846759E-04 | +03 |
| 020 | IMM | 72 | 051808.5 | +1.279925 | 3.61000987E-04 | +03 |
| 021 | IMM | 71 | 051908.0 | +1.287722 | 3.67456715E-04 | +02 |
| 022 | IMM | 71 | 052008.0 | +1.282264 | 3.81357208E-04 | +02 |
| 023 | IMM | 71 | 052108.0 | +1.274439 | 3.81357208E-04 | +02 |
| 024 | IMM | 71 | 052209.0 | +1.231102 | 3.82620884E-04 | +02 |
| 025 | IMM | 71 | 052408.0 | +1.238897 | 3.82620884E-04 | +02 |
| 026 | IMM | 71 | 052508.0 | +1.315529 | 3.88939296E-04 | +02 |
| 027 | IMM | 71 | 052608.0 | +1.318128 | 3.72511428E-04 | +02 |
| 028 | IMM | 71 | 052908.5 | +1.320987 | 3.80093524E-04 | +02 |
| 029 | IMM | 71 | 053108.0 | +1.317088 | 3.63655663E-04 | +02 |
| 030 | IMM | 71 | 060208.0 | +1.345416 | 3.53874612E-04 | +02 |

**Appendix 3: Hygrothermal data evaluation for FM73 adhesive specimens
exposed to hot-water during cycle III.**

| NR | RH | TEMP | DATE | OMEGA% | EPSILON TOTAL | DELTAT |
|-----|-----|------|----------|-----------|----------------|--------|
| 000 | IMM | 69 | 050310.7 | +0.000000 | 0 | +00 |
| 001 | IMM | 69 | 050312.0 | +0.163398 | 1.2970215E-04 | +00 |
| 002 | IMM | 69 | 050313.0 | +0.222729 | 1.98156067E-04 | +00 |
| 003 | IMM | 69 | 050314.3 | +0.287179 | 2.93631261E-04 | +00 |
| 004 | IMM | 69 | 050319.5 | +0.514268 | 5.60241247E-04 | +00 |
| 005 | IMM | 70 | 050407.8 | +0.907031 | 1.41889531E-03 | +01 |
| 006 | IMM | 70 | 050414.5 | +1.051663 | 1.84763298E-03 | +01 |
| 007 | IMM | 70 | 050507.8 | +1.325005 | 2.74293813E-03 | +01 |
| 008 | IMM | 70 | 050515.0 | +1.439118 | 2.93568994E-03 | +01 |
| 009 | IMM | 70 | 050607.8 | +1.640239 | 3.23112262E-03 | +01 |
| 010 | IMM | 70 | 050611.5 | +1.668483 | 3.26174673E-03 | +01 |
| 011 | IMM | 72 | 050812.0 | +2.209858 | 3.31634532E-03 | +03 |
| 012 | IMM | 73 | 051007.8 | +2.541015 | 3.6111553E-03 | +04 |
| 013 | IMM | 72 | 051014.9 | +2.583097 | 3.62438793E-03 | +03 |
| 014 | IMM | 72 | 051108.0 | +2.659678 | 3.62799078E-03 | +03 |
| 015 | IMM | 72 | 051208.0 | +2.747632 | 3.63339503E-03 | +03 |
| 016 | IMM | 72 | 051309.0 | +2.826109 | 3.65501205E-03 | +03 |
| 017 | IMM | 72 | 051408.0 | +2.914443 | 3.65501205E-03 | +03 |
| 018 | IMM | 72 | 051508.0 | +2.991403 | 3.65681347E-03 | +03 |
| 019 | IMM | 72 | 051708.0 | +3.100209 | 3.65681347E-03 | +03 |
| 020 | IMM | 72 | 051808.5 | +3.158972 | 3.71445888E-03 | +03 |
| 021 | IMM | 71 | 051908.0 | +3.200106 | 3.68625888E-03 | +02 |
| 022 | IMM | 71 | 052008.0 | +3.232899 | 3.71147874E-03 | +02 |
| 023 | IMM | 71 | 052108.0 | +3.276118 | 3.7078759E-03 | +02 |
| 024 | IMM | 71 | 052209.0 | +3.312513 | 3.7078759E-03 | +02 |
| 025 | IMM | 71 | 052408.0 | +3.358955 | 3.7078759E-03 | +02 |
| 026 | IMM | 71 | 052508.0 | +3.386440 | 3.7078759E-03 | +02 |
| 027 | IMM | 71 | 052608.0 | +3.411083 | 3.75651421E-03 | +02 |
| 028 | IMM | 71 | 052908.5 | +3.487854 | 3.74750711E-03 | +02 |
| 029 | IMM | 71 | 053108.0 | +3.536570 | 3.74750711E-03 | +02 |
| 030 | IMM | 71 | 060208.0 | +3.607843 | 3.74930853E-03 | +02 |

END

DATE
FILMED

3-82

DTIC